FUNCTIONAL CHARACTERIZATION AND CLINICAL RELEVANCE OF UBIQUITIN CONJUGATING ENZYME E2T IN HEPATOCELLULAR CARCINOMA

HO PUI YU

PhD

THE HONG KONG POLYTECHNIC UNIVERSITY

2020

The Hong Kong Polytechnic University
Department of Applied Biology and Chemical Technology

Functional Characterization and Clinical Relevance of Ubiquitin Conjugating Enzyme E2T in Hepatocellular Carcinoma

Ho Pui Yu

A thesis submitted in partial fulfilment of the requirements for the degree of Doctor of Philosophy

June 2019

Certificate of Originality

I hereby declare that this thesis is my own work and that, to the best of my knowledge and belief, it reproduces no material previously published or written, nor material that has been accepted for the award of any other degree or diploma, except where due acknowledgement has been made in the text.

……. (Signed)

Ho Pui Yu

…….....(Name of student)

Abstract

Abstract of thesis entitled
Functional Characterization and Clinical Relevance of Ubiquitin Conjugating Enzyme E2T in Hepatocellular Carcinoma
submitted by
Ho Pui Yu
for the degree of Doctor of Philosophy
at The Hong Kong Polytechnic University
June 2019

Hepatocellular carcinoma (HCC) is one of the common cancers worldwide. Most HCC patients present at an advanced stage when resection or liver transplantation is not feasible. Even after surgery, the long-term prognosis of HCC remains unsatisfactory due to high recurrence rates. Chemotherapy remains the principle alternative for treating unresectable HCC. However, the efficacy is limited due to chemoresistance. Increasing evidence showed the critical role of cancer stem cells (CSCs) on tumor relapse and therapeutic resistance. Since normal stem cells and CSCs share high similarity in genetic profile, we would like to identify the molecules/pathways crucial in liver CSCs by determining what molecules involved in normal liver stem cells during liver regeneration. For this purpose, partial hepatectomy mouse model was employed to analyze the change in genetic profile in regenerating liver. Comparison of expression profiles between early regenerating liver and intact liver revealed the upregulation of DNA Damage Response pathways in self-renewing liver, in which Ubiquitin Conjugating Enzyme E2T (UBE2T) was the most significantly upregulated. This, together with the publicly available dataset (GSE5975) shows upregulation of UBE2T in EpCAM-enriched liver CSC populations, suggest the potential role of UBE2T on regulation of cancer stemness. By qPCR analysis, UBE2T was overexpressed in 91% of the clinical HCC specimens and associated with aggressive phenotype and poorer patients' survival. Significant overexpression of UBE2T in protein level was also confirmed by Western Blot and IHC analyses. By lentiviral based knock-down and ectopic overexpression approaches, we demonstrated the role of UBE2T in regulation of liver CSC properties including self-renewability and expression of CSC markers. Alternation of UBE2T expression level also affected HCC invasiveness and drug resistance. Apart from *in vitro* functional assays, UBE2T also found to regulate *in vivo*

tumorigenicity and CSC frequency. In orthotopic HCC model, UBE2T was found to play pivotal role in lung metastasis *in vivo*.

In order to identify downstream target of UBE2T for regulation of cancer stemness, tandem affinity purification coupled with mass spectrometry (TAP/MS) was employed. Upon analysis, Mule, a E3 ubiquitin ligase, was identified to be the novel protein binding partner of UBE2T. Being the E2 ubiquitination enzyme, UBE2T was found to physically bind and regulate the protein expression of Mule via ubiquitination. Recently, Mule is suggested to further directly degrade protein of β-catenin. Therefore, we further examined the effect of UBE2T on β-catenin expression. Consistently, we found that overexpression of UBE2T increased β-catenin expression via degradation of Mule. Opposite effects were observed when UBE2T expression was suppressed. Furthermore, the effect of UBE2T on β-catenin activity was further confirmed by Immunofluorescence (IF). These effects were offset when E2 activity of UBE2T was impaired by replacing wild-type form of UBE2T with the E2-dead mutant (C86A).

In conclusion, we have uncovered the novel role of UBE2T signaling cascade in regulation liver CSCs. UBE2T regulates liver CSC functions through Mule-mediated β-catenin degradation. Our study not only provides a mechanistic insight for tumor recurrence and drug resistance, but also open a new therapeutic avenue for treatment of HCC.

(494 words)

Publications

1. **Ho PY**, Lee TK. Targeting immune checkpoint proteins as novel strategy for treatment of hepatocellular carcinoma. *Liver: Dis & Transplant* 2016; 5:2. (Impact factor: 0.33)
2. Lau EY, **Ho NP**, Lee TK. Cancer stem cells and their microenvironment: biology and therapeutic implications. *Stem Cell Int* 2017; 2017:3714190 (Impact factor: 3.989)
3. Ma MK, Lau EY, Leung DH, Lo J, **Ho NP**, Cheng LK, Ma S, Lin CH, Copland JA, Lo RC, Ng IO, Lee TK. Stearoyl-CoA desaturase regulates sorafenib resistance via modulation of ER stress induced differentiation. *J Hepatol* 2017; 67(5):979-990. (Impact factor: 15.04)
4. Zhang B, Zhang Y, Zou X, Chan AW, Zhang R, Lee TK, Liu H, Lau EY, **Ho NP**, Lai PB, Cheung YS, To KF, Wong HK, Choy KW, Keng VW, Chow LM, Chan KK, Cheng AS, Ko BC. The CCCTC-binding factor (CTCF)-forkhead box protein M1 axis regulates tumor growth and metastasis in hepatocellular carcinoma. *J Pathol* 2017; 243(4):418-430. (Impact factor: 6.253)
5. Cheng BY, Lau EY, Keung DH, **Ho NP**, Cheng LK, Gurung S, Lin CH, Lo RC, Ma S, Ng IO, Lee TK. IRAK1 augments cancer stemness and drug resistance via the AP-1/AKR1B10 signaling cascade in hepatocellular carcinoma. *Cancer Res* 2018; 78(9):2332-2342 (Impact factor. 9.13)

Acknowledgement

First and foremost, I would like to express my sincere gratitude to my supervisor Dr. Terence Lee for giving me a valuable opportunity to pursue my PhD degree. Dr. Terence Lee is an excellent supervisor with great passion on scientific research. He keens on learning new technique and knowledge and always encourages students to think out of box. Dr. Lee is also a kind and caring mentor. He has patiently taught me the way to design a project and the appropriate attitude to be a reliable and responsible researcher from him. Without his guidance and support, I could not become an independent researcher.

I would also like to thank Dr. Eunice Lau, Dr. Carmen Leung and Dr. Doris Leung for offering me generous support and advice in my project. Their kind advice helped me a lot when I faced problems that I could not solve. I would like to thank my dearest teammates Ms. Katherine Chung, Mr. Etienne Mok, Mr. Kyler Chow, Ms. Martina Lei and Ms. Shilpa Gurung for all the joy we have shared in these 3 years. Problems often happen in scientific research. We encourage and support each other. Our lab is full of laughter every day. I would also like to thank Dr. Stephanie Ma and her research team for all the technical support they have offered. They have given me precious advice and often welcome me with delicious food.

Finally, I am sincerely grateful to my family. Being a PhD student, we must be very hard-working. I have spent all my time in laboratory even during weekends so the time I have spent at home with my family was only little. Still, my family showed understanding and support me as always. They always cheer me up when I feel frustrated for my failure in experiments. Without their support, I would not be able to finish my degree.

I am not good at expressing myself in words. There are so many people I would like to express thanks for all you have done for me. I am really lucky to have you all accompanying me these years. Thank you very much.

Table of Contents

List of Figures

List of Tables

List of Abbreviations

ATM	Ataxia Telangiectasia Mutated
bFGF	Basic fibroblast growth factor
BRCA1	Breast Cancer Type 1 Susceptibility Protein
CHIP	Carboxy Terminus of Hsp70-Interacting Protein
Chk1	Checkpoint kinase 1
Co-IP	Co-Immunoprecipitation
CSC	Cancer stem cell
DDR	DNA damage repair
DMEM	Dulbecco's Modified Eagle Medium
DMSO	Dimethyl sulfoxide
DNA	Deoxyribonucleic Acid
EGF	Epidermal growth factor
EMT	Epithelial mesenchymal transition
EpCAM	Epithelial cell adhesion molecule
FA	Fanconi anemia
FACS	Fluorescence activated cell sorting
FANC	Fanconi anemia complementation group
FBS	Fetal bovine
FDA	Food and Drug Administration
FITC	Fluorescein isothiocyanate
FLT-3	FMS-like tyrosine kinase 3
HBV	Hepatitis B virus
HCC	Hepatocellular carcinoma

HCV	Hepatitis C virus
HNSCC	Head and neck squamous-cell carcinoma
ICL	Interstrand cross link
IF	Immunofluorescence
Ig	Immunoglobin
IHC	Immunohistochemistry
IP	immunoprecipitation
mRNA	Messenger RNA
Mule	Mcl-1 ubiquitin ligase E3
NOD/SCID	Nonobese diabetic/severe combined immune-deficient
NTC	Non-target control
PBS	Phosphate-buffered saline
PE	Phycoerythrin
PI	Propidium iodide
PI3K	Phosphatidylinositol 3-kinase
qPCR	Quantitative polymerase chain reaction
RIPA	Radioimmunoprecipitation assay
RNA	Ribonucleic acid
ROS	Reactive oxygen species
RT	Reverse transcription
SFB	S protein tag, Flag tag, Streptavidin binding peptide
shRNA	Short hairpin RNA
Skp2	S-Phase Kinase Associated Protein 2
STUB1	STIP1 Homology And U-Box Containing Protein 1
TACE	Transarterial chemoembolization

TAP/MS	Tandem affinity purification coupled with mass spectrometry
UBE2T	Ubiquitin conjugating enzyme E2T
VEGF	Vascular endothelial growth factor
VEGFR-2	Vascular endothelial growth factor receptor-2

Chapter 1

Introduction

1.1. Hepatocellular Carcinoma (HCC)

1.1.1. Epidemiology and Etiology of HCC

Liver cancer was the second leading cause of cancer death worldwide in 2012, and hepatocellular carcinoma (HCC) accounts for 90% of liver malignancy [1], [2]. Late diagnosis, frequent relapse and drug resistance are considered the reasons for poor prognosis in HCC patients. Many risk factors are implicated in HCC development. A better understanding of the risks is critical to enable preventive measures.

Sex disparity is present in HCC. Liver cancer is the second leading cause of cancer death in men worldwide and is 2-4 times more likely to occur in men than in women [1], [3]. The prevalence of HCC in men may be attributed to sex-specific exposure to cirrhosis risk factors. Accumulating evidence suggests that sex disparity stems from discrepancies in genomic profiles between males and females [4], [5].

HCC displays geographic variation in incidence around the world. It is more common in less developed countries, especially in Southeast Asia and Africa [1]. The high incidence of HCC in less developed regions is attributed to the prevalence of endemic hepatitis B virus (HBV) and hepatitis C virus (HCV) infection. It has been widely reported that chronic HBV and HCV infection increases susceptibility to liver cirrhosis, which significantly increases the risk of HCC progression [6], [7]. The majority (90%) of HCC cases develop in the cirrhotic liver [7]. In addition, the endemic prevalence of aflatoxins further increases the risk of HCV-induced HCC development [8]. Despite the high incidence of HCC in Southeast Asia, the rate of liver cancer incidence is decreasing in China owing to improved hygiene and HBV vaccination [1], [9]. In contrast, the rate

of liver cancer incidence shows an increasing trend in Western countries such as the United States and United Kingdom, where the HCC incidence rate has been historically low [1], [10]. This increase may be attributed to exposure to other risk factors including excess alcohol intake and obesity.

Alcohol-related liver disease (ARLD), caused by excessive alcohol consumption, increases the susceptibility to chronic liver cirrhosis. Nonalcoholic fatty liver disease (NAFLD) enhances the risk of developing HCC without cirrhosis. The elevated HCC incidence in Western countries has been attributed to the growing number of patients with fatty liver disease [7], [11].

1.1.2. Current Treatment Regimens for HCC

Given that most HCC is preceded by liver cirrhosis, the adoption of treatment modalities for HCC not only depends on the tumor stage but also the underlying cirrhosis. The Barcelona Clinic Liver Cancer (BCLC) staging system, recommended by the American Association for the Study of Liver Diseases, classifies patients based on tumor stage, liver function, performance status and cancer-related symptoms and recommends patients for a specific treatment strategy [12], [13]. The currently available HCC treatments can be classified into 5 categories: (1) surgical therapy; (2) local ablation therapy; (3) chemotherapy; (4) molecular targeted therapy; and (5) immunotherapy.

1.1.2.1. Surgical therapy

Surgical therapy is widely adopted as a curative strategy for early HCC. However, the feasibility of surgical resection can be significantly influenced by the tumor size, the presence of multifocal tumors and a diseased liver state. Hepatic resection and liver transplantation are the

mainstay of surgical therapy for HCC.

1.1.2.1.1. Hepatic Resection

Hepatic resection is the surgical removal of a tumor mass from the liver. Advancements in technologies, especially in medical imaging, and a better understanding of hepatic anatomy have increased the safety and efficacy of resection. Hepatic resection results in better survival benefit than locoregional therapies, but long-term survival remains unsatisfactory because of high tumor recurrence rate [13]. The 5-year probability of HCC recurrence after surgical resection can reach 70% [14]. Given that liver cirrhosis may increase the risk of postoperative liver failure and death, patients with early HCC and minimal cirrhosis are candidates for resection [12]. Surgical resection is effective in patients who do not have hepatic cirrhosis or extrahepatic metastases and whose tumors are unifocal without vascular invasion. However, only 5% of HCC cases develop in noncirrhotic livers, and such cases are often not diagnosed until advanced stage [15], [16]. Preoperative chemotherapy can increase the number of eligible candidates for surgical excision by reducing tumors to a suitable size. Nevertheless, it enhances the risk of postoperative liver failure [17].

1.1.2.1.2. Liver Transplantation

Liver transplantation replaces the diseased liver with a healthy liver and is considered the last resort for curing some end-stage liver diseases such as primary biliary cirrhosis, fulminant hepatic failure and HCC [18]. Patient selection for liver transplantation follows the Milan criteria: a solitary tumor <5 cm or up to 3 nodules ≤3 cm without vascular invasion[19]. Mazzaferro *et al.* [19] demonstrated the curative potential of liver transplantation by a 4-year over survival rate of

75% and a low tumor-recurrence rate of <15%. Because of the low incidence of tumor recurrence, liver allograft transplantation is a better curative approach for HCC patients, especially those with liver cirrhosis, than hepatic resection. Livers for transplantation can be procured from living donors or deceased donors after cardiac death or brain death [20]. Nevertheless, liver transplantation faces severe organ shortage challenge, which limits the availability of liver allografts. In addition, immunosuppressive medications may lead to suboptimal outcomes, including allograft failure, cardiovascular events, infection, malignancy and renal failure [20].

1.1.2.2. Local Ablation Treatment

Local ablation treatment is an important nonsurgical treatment modality for HCC patients who are ineligible for surgical resection. It is minimally invasive and easily repeatable. Two commonly used ablation treatments for early-stage HCC are percutaneous ethanol injection and radiofrequency ablation.

1.1.2.2.1. Percutaneous Ethanol Injection (PEI)

Percutaneous ethanol injection (PEI) utilizes ethanol toxicity to induce tumor necrosis by cellular dehydration and protein denaturation. 95% absolute ethanol is injected directly into lesions under ultrasound guidance to destroy tissues. Multiple studies have shown that PEI can induce complete tumor necrosis in 70-100% of tumors <5 cm [21]. PEI is relatively simple and inexpensive and has very rare treatment-related mortality, contributing to its frequent use in treating HCC [22]. However, the spread of absolute ethanol may be unpredictable due to the restriction by intratumoral septa, limiting the efficacy of the approach [12], [21]. Another limitation of PEI is the high local recurrence rate, which reaches 33% in tumors <3 cm and up to

43% in large tumor lesions ≥3 cm [23].

1.1.2.2.2. Radiofrequency Ablation (RFA)

Radiofrequency ablation (RFA) utilizes electromagnetic energy to induce tumor necrosis through the insertion of electrodes. RFA destroys a larger volume of tissue in one ablation compared to PEI. It has been reported that RFA is significantly superior to PEI with respect to local recurrence and can improve the 5-year overall survival rate by more than 20% [23], [24]. The higher efficacy, lower recurrence rate and better overall survival offered by RFA has led to a shift from PEI to RFA as the standard ablative therapy for unresectable early stage HCC. Nevertheless, the anatomical location of the tumor has a substantial influence on the effectiveness of RFA. Performing RFA near other organs, such as the gastrointestinal tract and bile duct, may cause injury. In addition, the presence of large intrahepatic blood vessels contiguous to the lesion may contribute to incomplete necrosis due to the “heat-sink” effect, increasing the risk of local recurrence.

1.1.2.3. Chemotherapy

1.1.2.3.1. Transarterial Chemoembolization (TACE)

Transarterial chemoembolization (TACE) is the standard treatment for patients with intermediate-stage HCC when ablation therapy is unsuitable. In the TACE procedure, microspheres that adsorb chemotherapeutic agents are administered into supplying arteries to gradually release the drug. A high intratumoral drug concentration and occlusion of blood vessels can be achieved to induce infarction and necrosis. Traditional TACE utilizes lipiodol as a drug carrying agent, while currently developed drug-eluting beads enable slow release of the chemotherapeutic agents over time, minimizing serious side effects [12]. Various

chemotherapeutic agents can be adsorbed on drug-eluting beads, such as doxorubicin, cisplatin and mitomycin c. Drug-eluting beads loaded with doxorubicin (DEBDOX) are widely used in Europe and the U.S.A. [25]. In the study by Lei *et al.* [26], approximately 55% of patients showed complete or partial response to TACE. Despite the better survival benefit offered by TACE, including delayed tumor progression and improved overall survival, the 3-year survival after TACE is approximately 30% only [27]. TACE functions by the insertion of a microcatheter into the tumor feeding artery for embolization. However, the liver parenchyma surrounding the HCC lesion is supplied by both arterial and portal venous circulation. Arterial embolization alone may be insufficient to stop nutrient supply to the tumor. In addition, TACE results in hypoxia that promotes angiogenesis and subsequent tumor growth, contributing to the high local tumor recurrence rate after TACE [23], [25].

1.1.2.4. Molecular Targeted Therapy

1.1.2.4.1. Sorafenib

As mentioned above, HCC cases often present at an advanced stage at which surgical resection and local ablation therapy are unfeasible. Sorafenib is recommended worldwide as the first-line treatment for the system therapy of advanced stage HCC. Sorafenib is a multikinase inhibitor that blocks tumor proliferation by inhibiting Raf-1, B-Raf and kinases in the Ras/Raf/MEK/ERK signaling pathway and receptor tyrosine kinases, including c-Kit, FLT-3, VEGFR-2, VEGFR-3 and PDGFR-β [28].

To date, sorafenib is the only FDA-approved small molecular inhibitor for the systemic therapy of advanced HCC. It has been proposed that patients with TACE resistance or advanced-stage HCC

have residual liver functions. Patients with impaired liver functions are not eligible for sorafenib treatment due to susceptibility to severe adverse effects [29]. Sorafenib offers an overall survival benefit of approximately 3 months over placebo, but the response rate in HCC patients is only 2% [30], [31]. Another drawback of sorafenib is the development of drug resistance. Although the exact mechanism is unclear, it is suggested that the overexpression and activation of EGFR may contribute to sorafenib resistance [30]. Despite the modest survival benefit, sorafenib represents the greatest advancement in treating advanced HCC by far. Its combination with traditional treatments has been widely studied. Combinational therapy of sorafenib with TACE prolongs the 2-year survival of intermediate- and late-stage HCC patients by approximately 30% [32].

1.1.2.5. Immunotherapy

Liver is a lymphoid organ and receives an enormous amount of blood supply from hepatic arteries and the portal vein [33]. Exposure to antigens and microbial products derived from intestinal bacteria contributes to the distinctive immune environment in the liver, where innate lymphocytes are abundant and nonparenchymal hepatic cells function as antigen-presenting cells [34]. As mentioned above, the majority of HCC cases are attributed to HBV or HCV infection-induced liver cirrhosis. Chronic inflammation in the HBV- or HCV-infected liver can promote tumor progression by inducing the production of anti-inflammatory growth factors (EGF and IGF), angiogenic growth factors (VEGF and PDGF) and immunosuppressive cytokines (IL-10 and TGF-β) for the wound-healing process [35]. In addition, the exposure of immunosuppressive immune checkpoint proteins on liver cancer cells to cytotoxic T cells inhibits T-cell activation and promotes T-cell dysfunction due to exhaustion. The clinically relevant immune checkpoints CTLA-4 and PD-1/PD-L1 have been reported in HCC [36]. A highly immunosuppressive intratumoral

environment in advanced HCC has been reported by clinical and preclinical studies [37].

Chimeric antigen receptor-engineered T (CAR-T) cell therapy utilizes a genetic engineering approach to insert antigen-targeted receptors into T cells to generate CAR-T cells for adoptive cell transfer immunotherapy [38]. CAR-T cells specifically target tumor-associated antigens to suppress tumor growth. Transferrin receptor and GPC3 are identified in HCC and may serve as promising tumor-associated antigens for liver cancer [38]. A clinical study of the anti-PD-1 antibody nivolumab showed a response rate of 20% and a 6-month overall survival rate of 72% in HCC patients [39], [40]. The anti-CTLA-4 antibody tremelimumab showed a response rate of 18% in HCC patients with chronic HCV infection with the capacity of reducing viral load in blood [33], [41]. A phase I/II study of tremelimumab immunotherapy combined with TACE or RFA is ongoing (NCT01853618).

1.2. Cancer Stem Cells (CSCs)

1.2.1. Overview of Cancer Models

It has been long established that tumor heterogeneity exists in many cancer types and contributes to the clinical challenge in cancer treatment. Tumor heterogeneity is divided into intertumor and intratumor heterogeneity. The former refers to the heterogeneity between patients with tumors of the same histological type, while the latter refers to the heterogeneity within the tumor cell population in a single patient [42]. Genotypic complexities within tumors limit the efficacy of chemotherapeutic treatments and molecular targeted therapy. Two models have been proposed to explain the acquisition of intratumor heterogeneity: (1) the clonal evolution model and (2) the cancer stem cell model.

1.2.1.1. Clonal Evolution Model

The clonal evolution model is a stochastic model in which every cancer cell has a similar potential to initiate tumors (**Figure 1.1A**). Through a series of genetic mutations, any cancer cell may acquire the abilities of self-renewal, drug resistance and invasiveness, contributing to tumor progression and metastasis. Genetic mutations may originate from intrinsic genomic instability or be induced by an altered tissue microenvironment [43]. It is thought that a complex tissue microenvironment, which offers a proliferative barrier to tumor progression, provides a selection force for adaptative genomic alterations in cancer cells to drive tumorigenesis [44].

1.2.1.2. Cancer Stem Cell Model

In the cancer stem cell model, the heterogeneity of cancer is supported by the tumor hierarchy (**Figure 1.1B**). Therefore, the cancer stem cell model is also termed the hierarchical model. In this

model, cancer cells mirror the hierarchical organization of normal stem cells. A distinct subset of cancer cells called cancer stem cells (CSCs), which possess stem cell-like properties and the abilities of self-renewal and differentiation, is responsible for tumor initiation and gives rise to a heterogeneous cell population. The origin of CSCs remains a controversial topic among scientists. Several hypotheses have been proposed: (1) CSCs are derived from normal tissue progenitor cells with accumulated mutations; (2) CSCs are the transformed form of differentiated somatic cells; and (3) CSCs originate from dedifferentiated tumor cells [45].

Although the clonal evolution model and the cancer stem cell model explain tumor heterogeneity from different perspectives, the 2 models are not mutually exclusive but integrated to support the extensive heterogeneity in tumors (**Figure 1.1C**). CSC populations may acquire genetic changes over time and give rise to differentiated nontumorigenic progenitor cells. These progenitors lose their self-renewal ability but may accumulate mutations to acquire stem cell-like features. Alternatively, tumor cells display plasticity in response to stimuli from the tumor microenvironment. A hypoxic microenvironment has been reported to reprogram cancer non-stem cells to stem-like cells [46].

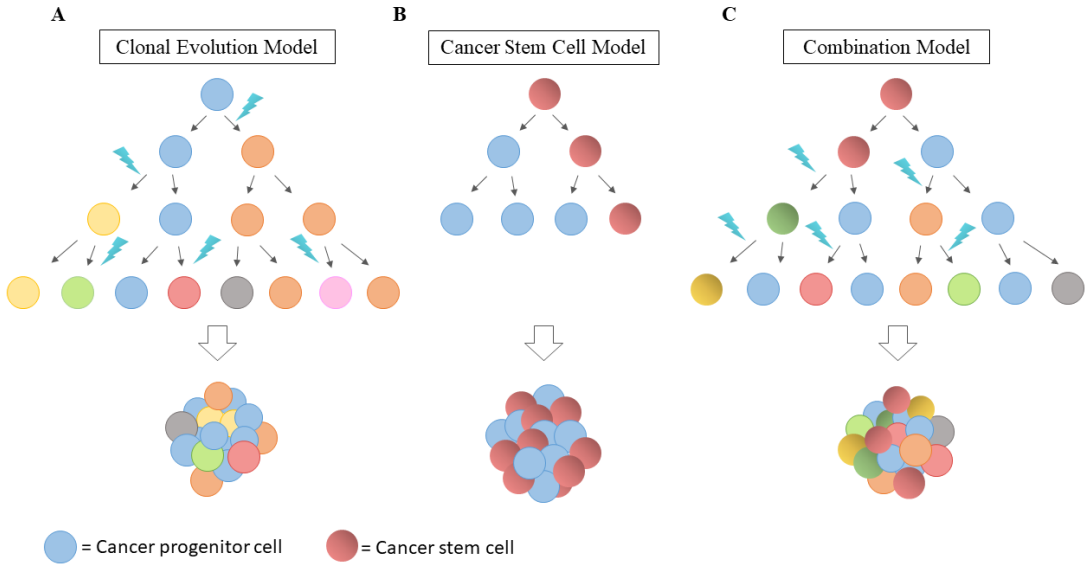

Figure 1.1. Three different models to explain tumor heterogeneity. A. In the clonal evolution, model, every cancer cell has a similar potential to acquire tumorigenic features via the accumulation of mutations. **B.** Cancer heterogeneity is supported by the tumor hierarchy in the cancer stem cell model, in which CSCs are responsible for tumor progression. **C.** The clonal evolution model and cancer stem cell model are integrated to support extensive tumor heterogeneity.

1.2.2. Properties of CSCs

1.2.2.1. Tumorigenicity

CSCs, also termed tumor-initiating cells, are pluripotent and highly tumorigenic. Many stemness-related genes are oncogenic and overexpressed in cancers. The stem cell transcription factor Sox2 is overexpressed in osteosarcoma and responsible for tumor initiation [47]. Knockdown of Nanog impairs the stemness and tumor formation ability of HCC cells [48]. Signaling pathways that maintain stem cell self-renewal are critical in regulating tumorigenicity as well. The regulation of proliferation, development, self-renewal and survival by the Wnt/β-catenin signaling pathway is well known [49], [50]. Cationic Wnt signaling is activated in $EpCAM^+$ CSCs and can drive tumorigenesis in cancers [50], [51]. Notch signaling is another important signaling pathway that maintains stem cell properties. The vital role of Notch signaling in supporting tumor growth has been well established [52]. Upregulation of genes involved in Notch signaling has been reported in CD133+ liver CSCs.

1.2.2.2. Self-renewal

CSCs display the capacity of self-renewal similar to normal stem cells. Asymmetric division ensures that one daughter cell maintains the stem cell features while the other daughter cell becomes committed to differentiation. CSCs with the ability of self-renewal give rise to populations of differentiated tumor cells through asymmetric division. The model that tumor cells originate from population(s) of CSCs can be supported by lineage tracing experiments. Lineage tracing in colorectal cancer shows that $Krt20^+$ cancer cells differentiate from $Lgr5^+$ CSCs [53]. Alternatively, $Notch1^+$ CSCs generate a population of $Notch1^+$ differentiated cancer cells in intestinal tumors [54]. These data fit well with the concept of CSC hierarchy.

1.2.2.3. Metastasis

CSCs are thought to be metastatic precursors. Epithelial-mesenchymal transition (EMT) is an important biological process that supports tumor progression, invasion and metastasis. EMT is a reversible transition process in which epithelial cells lose polarity and acquire mesenchymal features, enhancing the motility of cells. Mesenchymal-epithelial transition (MET), in contrast, induces mesenchymal cells to become epithelial-like for establishment of cell-cell contact. EMT plays a critical role in embryonic development, tissue repair and cancer progression [55]. The correlation of EMT with CSCs has been recently reported [56], [57]. The induction of EMT in nontumorigenic epithelial cells gives rise to $CD44^{+}CD24^{-}$ mesenchymal cells with self-renewal ability. An increase in cancer stemness by EMT has also been demonstrated in a study by Migita *et al.* [58] in which the induction of EMT enhanced expression of the well-studied stemness markers SOX2 and NANOG. Meanwhile, increasing the expression of SOX can promote EMT in esophageal squamous cell carcinoma [59]. Breast $CD44^{+}CD24^{-}$ CSCs are associated with a mesenchymal-like state and are more invasive than bulk breast cancer cells [60]. Since hypoxia and inflammation in the tumor microenvironment can induce EMT in cancer, the induced EMT may facilitate the acquisition of CSC features, which in turn promote the EMT process for microinvasion and metastasis [61].

1.2.2.4. Angiogenesis

Angiogenesis is one of the prominent hallmarks of cancer and promotes new blood vessel formation to supply nutrients for tumor growth [62]. The tumor microenvironment again plays an important role in supporting CSCs. VEGF, an angiogenic factor, promotes tumor stemness by

stimulating CD133 expression and reinforcing the self-renewal ability of CSCs in HCC [63]. An *in vivo* model shows that self-renewal of nestin^{+} brain CSCs is supported by endothelial cells in the tumor capillaries through direct contact [64]. The Notch signaling pathway, one of the important signaling pathways for maintaining cancer stemness, is involved in the regulation of vascular development, indicating that angiogenic signaling may be involved in CSC regulation [65]. It is hypothesized that CSCs may secrete angiogenic factors to stimulate tumor angiogenesis in return [66]. Although this hypothesis has not yet been proven, the fact that VEGF secretion by mesenchymal stem cells can promote the differentiation of epithelial progenitor cells may support the hypothesis to a certain extent [67].

1.2.2.5. Resistance to Radio-/Chemotherapy

CSCs are implicated in tumor recurrence, metastasis and resistance to radio- and chemotherapy [68], [69]. Radiotherapy kills cancer cells by inducing ROS production and radiation-induced DNA damage. Lower ROS levels have been reported in CSCs than in non-CSC cells and are associated with an enhanced free radical scavenger system that gives rise to the overexpression of GSH, a classical antioxidant [70]. Additionally, the hypoxic tumor microenvironment contributes to efficient ROS depletion in CSCs. Hypoxia in many solid tumors leads to oxygen deficiency and thus inhibits the generation of oxygen-dependent ROS, giving rise to radioresistance [71].

At the same time, CSCs are tolerant to DNA damage induced by radiation and chemotherapeutic agents, especially those targeting rapidly dividing cells. CSCs preferentially stay in a quiescent state, in which the CSCs can avoid returning to the cell cycle [72]. The slow-cycling status allows CSCs to become tolerant to dividing cell-targeting chemotherapeutic agents. Moreover, CSCs have

an efficient DNA damage repair system to overcome the DNA damage induced by radiotherapy and chemotherapy. The enhanced DNA repair system in CSCs will be discussed in detail in Section 1.2.4.

1.2.3. Identification of CSCs

CSC surface marker expression is widely studied to identify CSC populations (**Table 1.1**). CD133 is a common surface marker for the detection of CSCs in many solid tumors. It has been reported that isolated CD133+ cancer cells are responsible for tumor initiation, metastasis and drug resistance and possess the abilities of self-renewal and differentiation[73]–[75]. CD133 may potentially play a role in maintaining stem cell-like properties, but the precise mechanism is still unclear[76]. CD44 is another frequently studied CSC surface marker. The subset of cancer cells with enriched CD44 expression is associated with stem cell-like features [75].

However, CSCs display plasticity in the expression of stem cell markers. CSC markers may also be expressed on non-CSCs. CD44, one of the most frequently studied CSC surface markers, is enriched in CSC populations in many solid tumors and co-expressed in most normal epithelial and lymphatic tissues [77]. Lgr5, a well-reported CSC marker, is also a marker of intestinal stem cells [78]. In addition, CSC heterogeneity contributes to diversity in the expression of surface markers in CSC subgroups. Mourao *et al.* [54] discovered the existence of a distinct Notch1^{+} CSC population with a reduced level of Lgr5 in intestinal tumors. This indicates that studying CSC surface markers alone is not sufficiently reliable for the identification of CSC populations.

Apart from CSC surface markers, functional assays are used to identify and study CSC

populations. Since CSCs can escape from anoikis, spheroid formation assay is used to select CSCs with the ability to survive in anchorage-independent serum-free medium. *In vivo* limiting dilution assay (LDA) allows the estimation of tumor-initiating cell frequency in a given cell population that can regenerate xenograft tumors. The serial transplantation assay selects CSCs that can perpetuate xenograft tumors for multiple generations based on the self-renewal and tumorigenic features. LDA combined with serial tumor transplantation assay forms an effective *in vivo* approach to assess the self-renewal property of CSCs.

1.2.4. Enhanced DNA Damage Repair Systems in CSCs

As mentioned above, CSCs contribute to resistance to radio- and chemotherapy and are tolerant to DNA damage, especially that induced by radio-/chemotherapy. Radio-/chemoresistance stems from enhanced DNA damage repair systems in CSCs. DNA replication error is likely to occur during the course of proliferation and self-renewal. To escape DNA damage-induced apoptosis, there are various type-specific DNA repair pathways, including nucleotide excision repair (NER), base excision repair (BER), mismatch repair (MMR), direct repair, and double-strand break (DSB) recombinational repair to overcome DNA lesions. DNA repair systems are active in normal stem cells and CSCs, in which many DNA repair-related effectors, such as Chk1 and Chk2, are upregulated [79]. CD133+ glioblastoma CSCs preferentially activate DNA damage checkpoint proteins including ATM, Chk1 and Chk2 in response to radiation-induced DNA damage to promote radioresistance [80]. Upregulation of the DNA repair protein RAD51 has also been documented in glioblastoma CSCs [81]. Medulloblastoma CSCs can survive radiation by activating the PI3K/Akt pathway to give rise to cell cycle arrest [82]. The involvement of Wnt signaling, one of the important signaling pathways that maintains cancer stemness, during DNA damage repair has

been recently suggested because of its regulation of p53, an important mediator of the DNA repair response [83].

1.2.5. Regulation of CSCs by the Ubiquitin-Proteasome System

Protein quality control (PQC) is a critical system in cells, which maintains proper functioning of proteins and contributes to cellular homeostasis. Protein misfolding can lead to the development of neurodegenerative diseases and cancer [84], [85]. The ubiquitin proteasome system (UPS) is an important PQC system for protein degradation, and its misregulation has been found in many cancer types [86], [87]. The UPS involves 2 processes: ubiquitination and proteasomal degradation. E1-activating enzyme, E2-conjugating enzyme and E3 ligase regulate the ubiquitination of proteins. There are only two E1 enzymes, UBA1 and UBA6, responsible for ubiquitin activation in mammalian cells, whereas approximately 40 E2 enzymes and over 500 E3 ligases have been discovered for conjugating activated ubiquitin to specific substrates [87]. The highly substrate-specific E3 ligase plays a critical role in determining the specificity of the ubiquitination process. Misregulated expression of E2 and E3 enzymes has been reported to support oncogenic signaling in different cancer types [86]. UBE2N is highly expressed in malignant melanoma and displays a suppressive effect on p53, which can be rescued by the UBE2N inhibitor [88], [89]. Overexpression of UBE2C is found in many malignancies, including glioblastoma, breast cancer, colorectal cancer and prostate cancer and is associated with poor prognosis in patients [90]. Aberrant expression of many E3 ligases is found in cancer and is associated with CSC maintenance. Skp2 regulates self-renewal of nasopharyngeal carcinoma CSCs, and its overexpression contributes to the poor prognosis of patients [91]. WWP1 regulates the differentiation of mesenchymal stem cells by promoting the degradation of the transcription factor JunB [92].

Knockdown of STUB1/CHIP impairs the CSC features of breast cancer cells [93]. Fbxw7 promotes the degradation of c-Myc and Notch in hematopoietic and neural stem cells to regulate stem cell properties via the suppression of Wnt and Notch signaling [94]. It is well established that BRCA1 mutations increase the risk of developing breast cancer [95]. BRCA1, an important tumor suppressor and DNA repair protein, is involved in self-renewal and differentiation regulation [96].

Cancer type	Specific CSC surface markers	References
Breast cancer	$CD44^{+}CD24^{-}Lin^{-}$, ALDH, CD133, CD49, CD61	[103]
Colon cancer	CD133, CD44, CD24, CD29, CD26, CD166, CD326	[102]
Glioblastoma	CD133, CD44, CD15, Nestin	[101]
Liver cancer	CD133, EpCAM, CD90, OV6, ALDH	[100]
Lung cancer	CD133, CD44, CD90, CD117, ALDH	[99]
Pancreatic cancer	CD133, CD44, CD24, EpCAM, Nestin, CXCR4, ALDH	[98]
Prostate cancer	CD133, CD44, CD117, EpCAM, CXCR4	[97]

Table 1.1. Specific CSC surface markers in various cancer types.

1.3. Fanconi Anemia DNA Repair Pathway

1.3.1. Overview of Fanconi Anemia DNA Repair Pathway

As mentioned in Section 1.2.4, CSCs have an efficient DNA repair system. The Fanconi anemia (FA) pathway is a DNA repair signaling pathway activated in response to DNA interstrand crosslinks (ICLs). The rare genetic disease Fanconi anemia results from mutations in the FA protein and leads to bone marrow failure due to defective DNA repair. Apart from DNA repair, the association of cancer progression with the FA pathway has been reported.

Physiological biological processes, radiation from radiotherapy and some chemotherapeutic agents, such as cisplatin and mitomycin c, can generate cytotoxic ICLs. Difficulty in repairing ICLs due to detrimental effects on both DNA strands indicates the importance of the FA pathway, which is the major DNA repair pathway responsible for fixing ICLs, in maintaining genomic stability

(

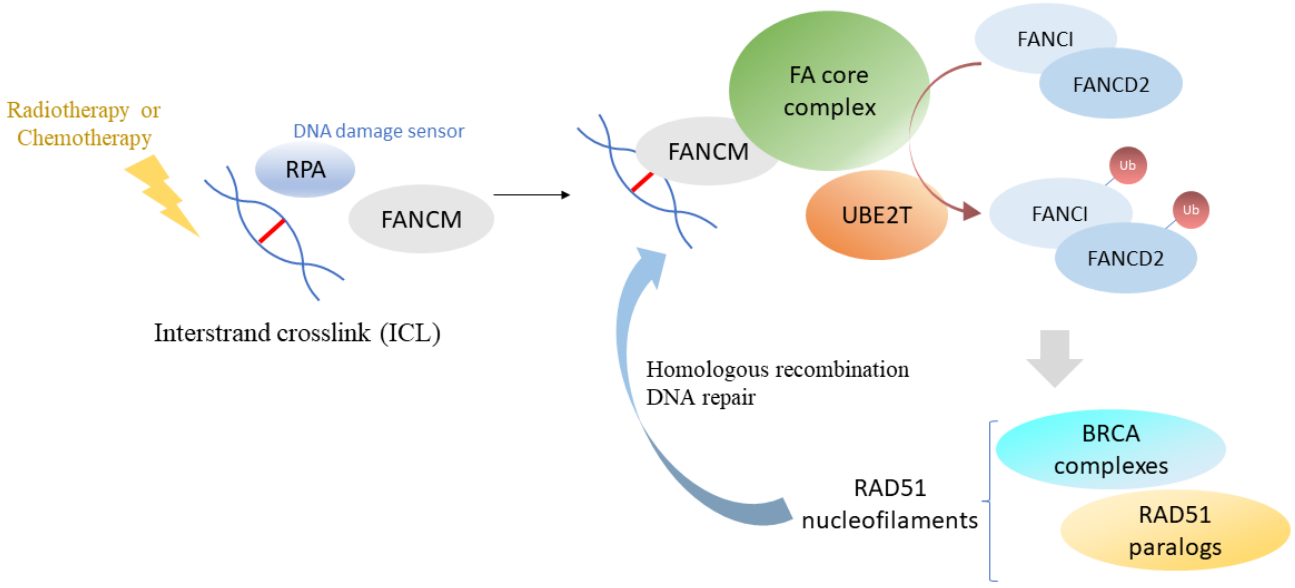

Figure 1.2). ICLs induce stalling of the replication fork and DNA single-strand breaks (SSBs)

that are recognized by the DNA damage sensor RPA to activate DNA damage responses [104], [105]. FANCM, one of the 19 components of the FA pathway, is phosphorylated in an ATR-dependent manner and binds to ICLs together with FAAP24, MHF1 and MHF2 to act as a landing platform for the FA core complex. The FA core complex is a large multisubunit E3 ligase comprising 14 proteins (FANCA, FANCB, FANCC, FANCE, FANCF, FANCG, FANCL, FANCM, FANCT, FAAP100, MHF1, MHF2, FAAP20 and FAAP24). The recruitment of the FA core complex to the ICL site activates two important components, FANCI and FANCD2, by phosphorylation and subsequent monoubiquitination. UBE2T and FANCL in the FA core complex are the E2 and E3 enzymes for monoubiquitination. The activation of FANCI and FANCD2 recruits many downstream repair factors including FANCD1. FANCD1, better known as BRCA2, is an important mediator for homologous recombination (HR) repair. The SSB generated during the course of unhooking the ICL lesions is repaired by nucleotide excision repair (NER)-dependent HR system [104]. FANCD1, together with BRCA1 and RAD51, is well documented for its involvement in HR repair [106].

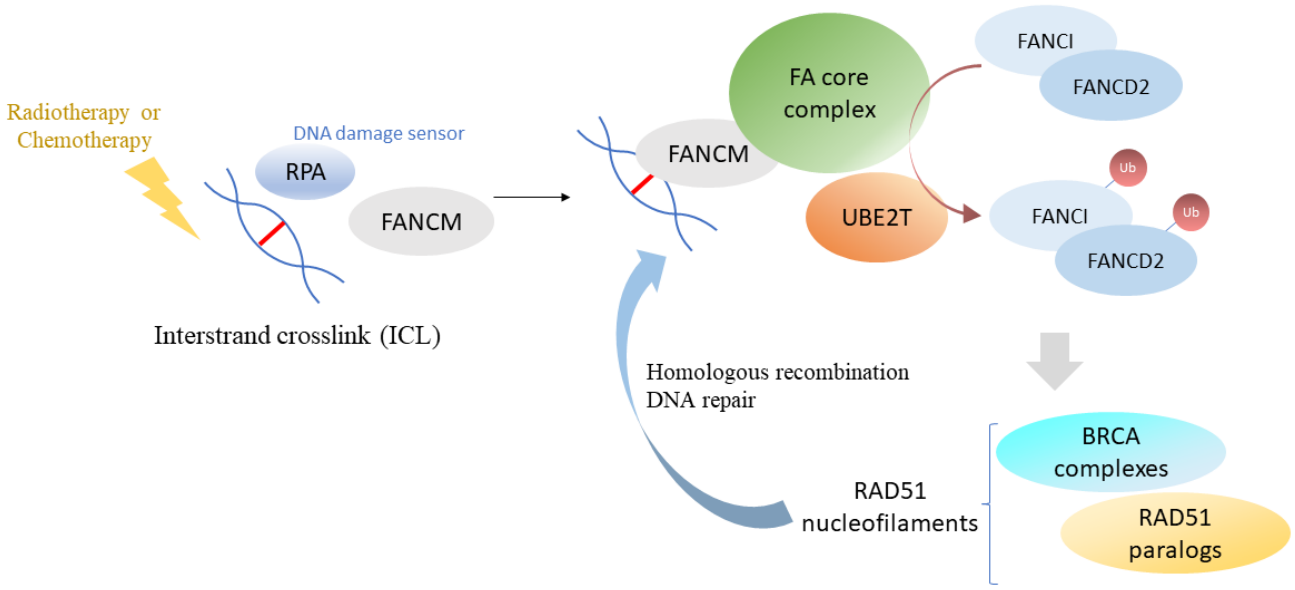

Figure 1.2. Overview of the Fanconi anemia (FA) pathway in DNA interstrand crosslink (ICL) damage repair. Upon the detection of ICL lesions by RPA, FANCM binds to the ICL as a landing platform for the FA core complex. FANCL, a subunit of the FA core complex with E3 ligase activity, and UBE2T activate the FANCI/FANCD2 complex by monoubiquitination. FANCI/FANCD2 monoubiquitination is a critical step in the FA pathway that recruits downstream DNA repair effectors, including BRCA complexes (BRCA1, FANCD1/BRCA2, FANCN/PALB2, FANCJ/BRIP1) and RAD51 paralogs (RAD51, RAD51B, FANCO/RAD51C, XRCC2, XRCC3), for fixing the ICL by HR DNA repair.

1.3.2. The Role of Fanconi Anemia DNA Repair Pathway in Cancer

FA is a rare genetic disorder that is characterized by bone marrow failure and a high propensity for the development of malignancies. Bone marrow failure in FA patients is attributed to hyperactivation of p53/p21 in response to the accumulation of DNA damage impairs hematopoietic stem and progenitor cells [107]. The high risk of carcinogenesis can be explained by genomic instability caused by a defective FA pathway, which fails in repair DNA lesions. Mutations in FA proteins diminish the cellular ability to maintain genome homeostasis, driving tumorigenesis. A high incidence rate of leukemia, liver cancer and head and neck cancer with observed-expected ratios of 785, 386 and 706, respectively, has been reported in FA patients [108]. Alter [109] has attributed the susceptibility to leukemia to FANCD1/BRCA2 mutations, which are found in 50% of leukemia cases among FA patients. Mutations in and epigenetic repression of FA core complex genes FANCM and FANCF in head and neck squamous cell carcinoma (HNSCC) contribute to ICL-induced chromosomal breakage, which is frequently observed in 53% of HNSCC cases [110]. Additionally, depletion of FANCD2 can promote HNSCC invasion through the activation of DNA-Pkcs and Rac1, which are responsible for non-homologous end-joining DNA repair and cell invasion, respectively [111]. A negative correlation of FANCD2 expression with tumor invasion and patient survival has also been demonstrated in breast cancer, but the underlying mechanism is not yet clear [112], [113]. FANCI, the other critical component in the FANCI-FANCD2 complex, also plays a role in regulating tumor growth by inhibiting the phosphorylation of Akt as a tumor suppressor [114]. FANCD1/BRCA2 is an important downstream effector of the FA pathway in DNA repair. Enhanced susceptibility to breast and ovarian cancers caused by FANCD1/BRCA2 mutations has been well documented because of the important role of BRCA proteins in regulating DNA repair, especially through the HR repair system [95], [96], [106], [115], [116].

However, although the FA pathway is generally recognized as a tumor-suppressive signaling pathway, some FA proteins are oncogenic. FANCL and UBE2T are E3 and E2 enzymes for the activation of FANCI-FANCL via monoubiquitination. FANCL promotes β-catenin activity by K11-linked ubiquitination to increase the proliferation of hematopoietic stem cells [117]. Overexpression of UBE2T has been found in many cancer types and is related to poor prognosis of patients. The details will be discussed in detail in the next section.

1.3.3. The Role of E2 Ubiquitin-conjugating Enzyme E2T in Cancer

Ubiquitin-conjugating enzyme E2T (UBE2T), also known as HSPC150, is a ubiquitin-conjugating E2 enzyme. The human E2 enzyme family consists of approximately 35 members, which all share a core ubiquitin conjugation (UBC) domain. UBE2T was first reported as an E2 enzyme in the FA pathway by Machida *et al.* in 2006 [118]. Although mutations in UBE2T can lead to FA, the risk of cancer development posed by UBE2T mutations remains unknown [119]–[121]. Nevertheless, upregulation of UBE2T has been reported in many cancer types, including lung cancer [122], [123], breast cancer [123], [124], HCC [125], bladder cancer [126], gastric cancer [127], [128], prostate cancer [129], myeloma [130], osteosarcoma [131] and nasopharyngeal cancer [132]. The contribution of UBE2T overexpression to poor prognosis and patient survival has also been well documented. UBE2T promotes cell proliferation and tumor invasion via the negative regulation of cell cycle arrest and apoptosis through Akt-related signaling pathways [126], [131], [132]. Due to the important role of the FA pathway in DNA repair, the relationship between UBE2T and p53, a well-studied tumor suppressor for the mediation of DNA repair, was studied. Proteasomal degradation of p53 by UBE2T has been observed in HCC,

showing the role of UBE2T in supporting tumor progression and development of drug resistance [125]. Despite many studies reporting the overexpression of UBE2T in cancer and its contribution to poor prognosis, the knowledge of the mechanism of UBE2T underlying the promotion of tumorigenesis is limited.

1.4. Hypothesis/Aim of Study

HCC is a prevalent fatal disease worldwide and accounts for a vast number of patient deaths. Currently, surgical resection is generally proposed as a treatment strategy for early-stage HCC. However, tumor relapse frequently occurs after surgery. TACE and chemotherapy are common therapeutic modalities for moderate- to advanced-stage HCC. Doxorubicin and sorafenib are commonly used chemotherapeutic agents in TACE and systemic chemotherapy to cause genomic instability and multikinase inhibition, respectively. Despite the diverse mechanism of action of anticancer drugs, the development of chemoresistance is frequently observed in HCC patients. HCC cells are tolerant to different types of chemotherapeutic agents. Tumor recurrence, drug resistance, metastasis and poor survival have been attributed to CSCs in HCC patients.

The cancer stem cell model has been considered an important model to explain tumor heterogeneity and cancer origin. CSCs are a subpopulation of cancer cells resembling normal stem cells and possess the ability to self-renew and differentiate. CSCs contribute to cancer progression via the promotion of tumorigenicity, metastasis and angiogenesis. Efficient DNA damage repair systems in CSCs allow malignant cells to escape apoptosis caused by radiation-induced or chemotherapy-induced DNA damage. Despite extensive studies on CSCs, eradicating CSCs remains a challenge. Discovering new therapeutic targets against CSCs is urgently needed to prolong patient survival.

Based on integrative comparative genomic analyses showing molecular similarities between liver CSCs and normal liver stem cells, we tried to identify critical molecules/pathways involved in the maintenance of liver CSCs by determining the molecules/pathways involved in normal stem

cells during the process of liver regeneration. For this purpose, we employed a mouse model of severe partial hepatectomy to activate normal liver stem cells. Using a cDNA microarray, we compared the expression profiles between the early regenerating liver and the intact liver, which differ in their capacity for self-renewal. This analysis showed that Ubiquitin Conjugating Enzyme E2 T (UBE2T) was drastically upregulated in the self-renewing liver, among other genes being activated in DNA damage response (DDR) pathways. Further analysis showed that UBE2T had a remarkably high expression in the self-renewing liver cells, indicating the role of UBE2T in liver CSCs.

The FA pathway is an important DNA repair signaling pathway for the specific repair of ICLs. It is generally recognized as a tumor suppressor pathway since mutations in different FA proteins, such as FANCD1 (also better known as BRCA2), have been reported to increase susceptibility to cancer development. However, UBE2T, which is the critical E2 enzyme for the monoubiquitination of FANCI-FANCD2 in the FA pathway, is upregulated in many malignancies. Although the underlying mechanism is not fully understood, UBE2T has been found to be positively correlated with proliferation, EMT and tumor invasion through Akt-related signaling pathways. Based on the well-studied relationship between CSCs and EMT, UBE2T may be involved in the regulation of cancer stemness [56], [133]. Nevertheless, there are no studies on the role of UBE2T in CSCs at present.

In view of the significant upregulation of UBE2T in the self-renewing liver in the partial hepatectomy mouse model, it is hypothesized that UBE2T may act as a molecular regulator for cancer stemness and drug resistance in HCC and bear clinical significance. Targeting UBE2T may

be a promising therapeutic target to improve the prognosis of HCC patients.

The objectives of this study include the following:

1. To evaluate the clinical relevance of UBE2T expression in human HCC
2. To functionally characterize the role of UBE2T in the regulation of liver CSCs
3. To elucidate the molecular mechanism by which UBE2T functionally contributes to tumor initiation, self-renewal, and drug resistance

Chapter 2

Materials and Methods

2.1. Materials

Table 2.1. Cell lines

Cell line	Characteristics	Source/Vendor
Bel7402	HCC	Shanghai Institute of Biological Sciences, Chinese Academy of Sciences
Hep3B	HCC	Shanghai Institute of Biological Sciences, Chinese Academy of Sciences
HepG2	HCC	ATCC (Manassas, VA)
Huh7	HCC	Japanese Cancer Research Bank (JCRB0403)
MIHA	Immortalized liver cells	Gift from Dr. J.R. Chowdhury, Albert Einstein College of Medicine
MHCC-97L	HCC	Liver Cancer Institute, Fudan University
PLC/PRF/5	HCC	Japanese Cancer Research Bank (JCRB0406)
SMMC-7721	HCC	Shanghai Institute of Biological Sciences, Chinese Academy of Sciences
293FT	Human embryonic kidney cells	Invitrogen™, Thermo Fisher Scientific (Waltham, MA)

Table 2.2. Primers for qPCR

Gene	Forward primer (5'-3')	Reverse primer (3'-5')
UBE2T	TTAGGTGGAGCCAACACACC	GAGGGATGGTCTCCAAGCAC
Mule	AGCGCCTCATTTCCATCTTCA	TGCAGGGGTACCTTGGAAGT
Actin	GTGGGGCGCCCCAGGCACCA	CTCCTTAATGTCACGCACGATTTC
GAPDH	CCTCCTGGCGTCGTGATTAGTG	CAGAGGGCTACAATGTGATGG

Table 2.3. shRNA sequences

Genes	shRNA sequence (5'-3')
Non-target control (NTC)	CCGGTTGTGCTCTTCATCTTGTTGCCGGCAACAAGATGAAGAGCACCAATTTTTG
shUBE2T_89	CCGGGTCCTGGTTCATCTTAGTTAACTCGAGTTAACTAAGATGAACCAGGACTTTTT
shUBE2T_60	CCGGTGAGGAAGAGATGCTTGATAACTCGAGTTATCAAGCATCTCTTCCTCATTTTTTG
shMule_04	CCGGCCACACTTTCACAGATACTATCTCGAGATAGTATCTGTGAAAGTGTGGTTTTTG
shMule_06	CCGGCGACGAGAACTAGCACAGAATCTCGAGATTCTGTGCTAGTTCTCGTCGTTTTTG

Table 2.4. Antibodies

Antibody	Purpose	Conditions	Vendor
UBE2T	Western Blot	1:1000	Proteintech (Rosemont, IL)
	Immunofluorescence	1:100	
	Immunoprecipitation	5 µg/mg	
Mule	Western Blot	1: 1000	Abcam (Cambridge, UK)
	Immunofluorescence	1:100	
	Immunoprecipitation	10 µg/mg	Bethyl Laboratories (Montgomery, TX)
β-catenin	Western Blot	1: 1000	Cell Signaling Technology (Danvers, MA)
	Immunofluorescence	1:100	BD Biosciences
HA	Western Blot	1:1000	Proteintech
β-Actin	Western Blot	1:1000	MilliporeSigma (St. Louis, MO)
α-Tubulin	Western Blot	1:1000	MilliporeSigma
DDK (Flag)	Western Blot	1:1000	OriGene (Rockville, MD)
HRP-linked rabbit IgG	Western Blot	1:5000	GE Healthcare (Chicago, IL)
HRP-linked mouse IgG	Western Blot	1:5000	GE Healthcare
Normal rabbit IgG	Immunoprecipitation	3-10 µg/mg	Invitrogen, Thermo Fisher Scientific

PE mouse anti-human CD47	Flow cytometry	5 µL/test	BD Biosciences (San Jose, CA)
PE mouse anti-human CD90	Flow cytometry	5 µL/test	BD Biosciences
PE mouse IgG1, κ isotype control	Flow cytometry	5 µL/test	BD Biosciences

Table 2.5. Plasmids

Plasmid	Vendor
pCMV6-Entry	OriGene
Myc-DDK-tagged UBE2t	OriGene
pSuper8XTOPflash	A gift from Dr. Moon R, University of Washington, USA
pSuper8XFOPflash	A gift from Dr. Moon R
pRL-CMV construct	Promega (Madison, WI)

Table 2.6. Other chemicals

Chemicals	Vendor
Dimethyl sulfoxide (DMSO)	MilliporeSigma
Doxorubicin	EBEWE Pharma (Unterach, Austria)
Puromycin	MilliporeSigma
Lipofectamine™ 2000 transfection reagent	Invitrogen, Thermo Fisher Scientific
Annexin V-FITC reagent	BioVision (Milpitas, CA)

10X Annexin V binding buffer	BD Biosciences
Methyl cellulose	MilliporeSigma
Matrigel™ Matrix	Corning (Corning, NY)
Polybrene	MilliporeSigma
G418	GoldBio (St Louis, MO)
MG132	Merck Millipore
Insulin	MilliporeSigma
B27™	Gibco™, Thermo Fisher Scientific
EGF	MilliporeSigma
bFGF	MilliporeSigma
PolyHEMA	MilliporeSigma
TRIzol® Reagent	Invitrogen, Thermo Fisher Scientific
PhosSTOP™	Roche (Basel, Switzerland)
cOmplete™ EDTA-free protease inhibitor cocktail	Roche
Bovine serum albumin (BSA)	MilliporeSigma
Crystal violet	MilliporeSigma
BrightGreen 2X qPCR MasterMix-ROX	Abm (Vancouver, Canada)
Streptavidin Sepharose High Performance	GE Healthcare

Protein A agarose	Cell Signaling Technology
Amersham™ ECL™ Western Blotting Detection Reagents	GE Healthcare

2.2. Methods

2.2.1. *In Vitro* Studies

2.2.1.1. Collection of Clinical Specimens

Paired patient's HCC and adjacent non-cancerous liver tissue specimens were collected at the time of surgical resection with informed consent of patients at Queen Mary Hospital, Hong Kong, from 1992 to 2013 with informed consent of patients. After collection from surgical resection, all samples were immediately snap-frozen in liquid nitrogen before storage at −80°C, with Institutional Review Board (IRB) approval of the University of Hong Kong/Hospital Authority Hong Kong West Cluster.

2.2.1.2. Gene Expression Profiling Analysis of UBE2T in HCC Clinical Samples

Gene expression profiling was performed by analyzing the expression of UBE2T transcripts available in publicly available (GEO accession number GSE5975 and GSE25097), and Liver Hepatocellular Carcinoma (LIHC) of the TCGA Research Network and analyzed using UCSC Xena Browser.

2.2.1.3. Cell Culture

The cell lines used in this study were listed in **Table 2.1**. The cells were maintained in Dulbecco's Modified Eagle Medium (DMEM) with high glucose and L-glutamine (Gibco™, Thermo Fisher Scientific) with supplementation of 10% heat-inactivated fetal bovine serum (FBS) (Gibco™, Thermo Fisher Scientific), 50 U/mL Penicillin G, and 50 mg/mL streptomycin (Gibco™, Thermo Fisher Scientific) unless stated otherwise. All cell lines were kept in a humidified chamber at 37°C with 5% CO_2 and the culture medium was refreshed every 2 days. Cells were passaged

once met 80% confluency or when necessary. Trypsinization was conducted Trypsin-EDTA (Gibco™, Thermo Fisher Scientific) at 37°C to detach the cells from culture plates. The trypsin was inactivated with equal volume of serum-containing medium and the cell suspension was centrifuged at 1,200 rpm for 3 min. The cell pellet was resuspended in fresh culture medium and split at a ratio between 1/5 to 1/10 depending on cell lines and needs.

2.2.1.4. Cell Counting

Cells were counted with hematocytometer. Cell suspension was mixed with 0.4% trypan blue solution (Gibco™, Thermo Fisher Scientific) at 1:1 ratio and 10 μL of the mixture was loaded to the hematocytometer. The number of transparent viable cells was counted under light microscope. The cell concentration of the original cell suspension was calculated according to the following equation:

Number of cells / mL = Total number of viable cells in a set of 16 corner squares $\times 2 \times 10^4$

2.2.1.5. RNA Extraction

Total RNA in HCC cells was extracted using TRIzol® Reagent (Invitrogen, Thermo Fisher Scientific). HCC cells were lysed by 1mL of TRIzol® to solubilize biological materials and denature proteins. 200 μL chloroform was added to isolate the RNA by phase separation. The mixture was centrifuged at 13,000 rpm for 15 min at 4ºC for separation of phases. RNA in the aqueous phase was saved with extra care to prevent contamination with DNA and proteins from the other phases. RNA was precipitated by incubation with 500 μL isopropanol for 10 min at room temperature. The RNA precipitate was collected by centrifuge at 13,000 rpm for 15 min at 4ºC and was washed by 75% ethanol. The purified RNA precipitate was left to air dry before complete

resuspension in RNase-free UltraPure™ Distilled Water (Invitrogen, Thermo Fisher Scientific). The RNA obtained was stored at -80ºC prior to usage.

2.2.1.6. cDNA Synthesis

RNA concentration was measured by NanoDrop™ One Spectrometer (Thermo Fisher Scientific). 1 µg of RNA was subjected to reverse transcription for cDNA synthesis using PrimeScript™ RT Reagent Kit (Takara, Shiga, Japan). 1 µg of RNA diluted in 6.5 µL of UltraPure™ Distilled Water was mixed with 2 µL of 5X PrimeScript Buffer containing dNTP mixture and Mg^{2+}, 0.5 µL of 50 µM Oligo dT Primer and 0.5 µL of 100 µM Random 6 mers. 0.5 µL of PrimeScript RT Enzyme Mix I was finally added to the reaction mixture before incubation in Thermal Cycler. The reaction mixture in total volume of 10 µL was incubated at 37ºC for 15 min, followed by 85ºC for 5 seconds for generation of cDNA by reverse transcription. The cDNA synthesized was diluted with UltraPure™ Distilled Water to make a 5-fold dilution and was stored at -20ºC prior to usage.

2.2.1.7. Quantitative PCR (qPCR) Analysis

Gene expression was studied by quantitative PCR (qPCR) analysis using primers listed in **Table 2.2**. 5µL of BrightGreen 2X qPCR MasterMix (abm) was mixed with 2 µL of 10 µM forward primer and 2 µL of 10µM reverse primer and topped up to 10µL with UltraPure™ Distilled Water. 2 µL of 5-fold diluted cDNA was added to the reaction mixture before incubation in accordance with amplification protocol at 94°C for 15 seconds, 63°C for 30 seconds, and 72°C for 60 seconds. The qPCR was monitored in real time by QuantStudio 7 Flex Real-time PCR system (Applied Biosystems, Thermo Fisher Scientific).

2.2.1.8. Protein Extraction

Total proteins in HCC cells was extracted by cell lysis with 1X RIPA (20 mM Tris-HCl (pH 7.5), 150 mM NaCl, 1 mM Na_2EDTA, 1 mM EGTA, 1% NP-40, 1% sodium deoxycholate, 2.5 mM sodium pyrophosphate, 1mM β-glycerophosphate, 1mM Na_2VO_4, 1 μg/mL leupeptin) (Cell Signaling Technology) or NETN (0.5% NP-40, 20 mM Tris-HCl, pH 8, 100 mM NaCl, 1 mM EDTA) lysis buffer for 10 min on ice. cOmplete™ EDTA-free protease inhibitor cocktail (Roche) and PhosSTOP™ phosphatase inhibitor (Roche) was freshly added to the lysis buffer before protein extraction. Cell lysate was centrifuged at 13,000 rpm for 10 min at 4ºC to remove cell debris. Supernatant was collected as protein lysate. The concentration of total proteins was determined by Bradford assay. 2 μL of protein lysate was added to 1 mL of 1X Bradford reagent (Bio-Rad Laboratories) and the absorbance at 595 nm was measured. Protein concentration was calculated according to standard curve plotted by measuring absorbance of BSA solution at concentrations ranged from 0 to 100 μg/mL. After determination of protein concentration, the protein lysate was subjected to protein denaturation by mixing with 6X SDS loading buffer (0.35M Tris-HCl pH 6.8, 30% glycerol, 21.4% β-mercaptoethanol, 10% SDS and 0.05% bromophenol blue) to final concentration of 1X. The protein lysate was then boiled at 100ºC for 5 min to denature the protein. The denatured proteins were stored at -20ºC prior to Western Blot analysis.

2.2.1.9. Western Blot Analysis

The denatured proteins were resolved by 5% or 10% SDS-PAGE at constant voltage of 80 V for 20 min for stacking layer and 120 V for 80 min for separating layer. The proteins were transferred from polyacrylamide gel to PVDF membrane (Merck Millipore) at constant voltage of 100V for

90 min. The PVDF membrane blocked with 5% skimmed milk or 5% BSA (MilliporeSigma) in TBS-T (20 mM Tris-HCl, 137 mM NaCl, 0.1% Tween 20) for 30 min and incubated with primary antibody at 4ºC overnight. After washing, the membrane was incubated with HRP-linked rabbit IgG Ab (GE Healthcare) or HRP-linked mouse IgG Ab (GE Healthcare) for 1 hour. The chemiluminescence signal was detected using X-ray film (Fujifilm, Tokyo, Japan) after applying Amersham™ ECL™ Western Blotting Detection Reagents (GE Healthcare). The antibodies used for Western Blot analysis and their working dilution conditions were listed in **Table 2.4**.

2.2.1.10. Lentiviral-based Knockdown of Genes

shRNA knock-down clones were established through lentiviral-based approach in **Table 2.3**. 293FT cells were seeded in 60mm culture dish and transfected with packaging mix and lentiviral vectors containing the shRNA sequences when 90% cell confluency was reached. The transfection medium was replaced by fresh culture medium supplemented with 20% FBS after 24 hours. The lentivirus-containing medium was collected 48 hours after the transfection and was centrifuged at 3,000 rpm for 5 min at 4ºC prior to infection. HCC cells were infected by directly adding the lentivirus-containing medium to the culture medium of HCC cells together with polybrene (MilliporeSigma) at final concentration of 8 μg/mL. The infected HCC cells were selected by 1 to 2 μg/mL of puromycin (MilliporeSigma) depending on cell lines. The knockdown efficiency was confirmed by Western Blot analysis and qPCR analysis.

2.2.1.11. Overexpression of Genes

SFB-UBE2T plasmid construct was generated by Gateway system and its control vector pMH-SFB was gifted from Dr. Michael Huen, The University of Hong Kong. Myc-DDK-UBE2T

plasmid construct and its control vector pCMV6-Entry were purchased from OriGene. 293T cells or HCC cells were seeded in 6-well plate one to two days prior to transient transfection. When 80% cell confluency was reached, 2 µg of the plasmid construct or its control vector was transiently transfected into the cells by mixing with 5 µL of Lipofectamine 2000 before addition. Stable cells were selected by treatment of puromycin or G418 according to the drug resistance gene on the transfected plasmid. Stable single cell clone was established by dilution of cells in 96-well plate to allow only one cell to grow in the well before drug selection. The stable single cell clone selected was then expanded for subsequent analysis.

2.2.1.12. Site-directed Mutagenesis

To produce UBE2T enzyme-dead mutant, the 86th cysteine residue was substituted with alanine. Myc-DDK-UBE2T plasmid construct was subjected to site-directed mutagenesis by GenScript (Nanjing, China) for generation of Myc-DDK-UBE2T C86A plasmid construct.

2.2.1.13. Spheroid Formation Assay

HCC cells were counted and seeded onto 24-well plate pre-coated with 1% polyHEMA (MilliporeSigma) at 200-300 cells per well. Each well contained 300 µL of 0.25% methyl cellulose (MilliporeSigma) in DMEM/F12 medium (Gibco™, Thermo Fisher Scientific) supplemented with 4 µg/mL insulin (MilliporeSigma) and B27™ (Gibco™, Thermo Fisher Scientific). Supplement of 20 ng/mL EGF (MilliporeSigma) and 20 ng/mL bFGF (MilliporeSigma) was applied to Huh7 and MHCC-97L HCC cells at the same time. 100 µL of the supplemented medium was added per well every other day for approximately 10 days. The spheroids formed were counted and photographed under a light microscope.

2.2.1.14. Migration and Invasion Assays

Migration and invasion abilities of HCC cells were investigated using transwell inserts with 6.5 mm polycarbonate membranes of 8 μm pore size (Merck Millipore). The transwell inserts were pre-coated with Matrigel (Corning) for invasion assay. HCC cells were seeded in the upper chamber of the transwell in serum-free culture medium while the lower chamber contained medium with 10% FBS. The cells were incubated for 24 hours and then fixed by 2% PFA in PBS. The migrated cells were stained by crystal violet and randomly photographed under a light microscope for counting the numbers of the migrated cells. The experiments were repeated independently three times.

2.2.1.15. Analysis of CSC Surface Markers

1 x 10^5 HCC cells were stained by PE mouse anti-human CD47 antibody (BD Biosciences), PE mouse anti-human CD90 antibody (BD Biosciences) or PE mouse IgG1, κ isotype control (BD Biosciences) in 100 μL of PBS containing 2% FBS with incubation at 4°C for 30-60 min. The samples were washed by PBS prior to analysis with BD Accuri™ C6 flow cytometer (BD Biosciences).

2.2.1.16. Annexin V Assay/Propidium iodide (PI) Apoptosis Assay

Apoptosis of HCC cells after drug treatment was investigated by staining the cells with 1 μL/test of Annexin V-FITC reagent (BioVision) and 10 μL/test of PI in 100 μL of Annexin V binding buffer (BD Biosciences) for 15 min in room temperature without exposure to light. 300-400 μL of Annexin V binding buffer was added to the stained cells after the 15 min incubation. The cells

were analyzed by BD Accuri™ C6 flow cytometer.

2.2.1.17. Immunohistochemistry (IHC) Analysis

Immunohistochemical (IHC) staining for UBE2T were performed on formalin-fixed, paraffin-embedded sections of 4 μm using labeled horseradish peroxidase (HRP) method. The sections of HCC clinical specimen mounted on glass slide were de-waxed by xylene and rehydrated stepwise from absolute ethanol to 70% ethanol and finally distilled water. Heat antigen retrieval was performed with 1 mM Tris-EDTA buffer. Endogenous peroxidase activities were quenched by 3% H_2O_2. The sections were then immersed in serum free-protein blocking solution (Dako) for 30 min and incubated with UBE2T antibody in dilution ratio of 1:500 at 4°C overnight. The sections were thoroughly washed and incubated with Envision™ HRP-conjugated secondary antibody (Dako). Positive signals were visualized using 3,3′-diaminobenzidine (Dako) and the nuclei were counterstained with hematoxylin. The sections were then examined under a light microscope.

2.2.1.18. Immunofluorescent (IF) Analysis

HCC cells were seeded on coverslips and were fixed in 4% PFA/PBS for 15 min in room temperature. After washing by PBS, the cells were permeabilized with 0.1% Triton-X100 in PCS for 15 min and blocked with 5% BSA for 1 hour in room temperature. The cells were stained with primary antibody at 4°C overnight, followed by incubation with FITC and TexaRed (Invitrogen, Thermo Fisher Scientific) as the fluorochrome-conjugated secondary antibodies at room temperature for 1 hour together with DAPI (MilliporeSigma) for nucleus staining. The samples were also stained with the fluorochrome-conjugated secondary antibodies only to serve as controls. All images were captured using Leica TCS SPE Confocal Microscope (Leica, Wentzler, Germany).

The antibodies used for IF analysis and their working dilutions were listed in **Table 2.4**.

2.2.1.19. Tandem Affinity Purification Coupled with Mass Spectrometry (TAP/MS)

UBE2T ORF (NM_014176.3) was cloned into pMH-SFB vector (a gift from Dr. Michael Huen from University of Hong Kong) using Gateway system. The pMH-SFB-UBE2T generated was transfected into 293T cells using Lipofectamine® 2000. Puromycin was used to select stable 293T cells expressing UBE2T with N-terminal SFB fusion tag (S protein tag, Flag tag, Streptavidin binding peptide). The expression of SFB-UBE2T was verified by Western Blot and IF analysis. NETN buffer (0.5% NP-40, 20 mM Tris-HCl, pH 8, 100 mM NaCl, 1 mM EDTA) was used to lyse the stable 293T cells for the harvest of SFB-UBE2T proteins. The SFB-UBE2T was pulled down by Streptavidin Sepharose High Performance bead slurry (GE Healthcare) and was eluted from the bead by incubation with NETN containing 2 mg/mL biotin. The SFB-UBE2T and its binding partners were further purified by incubating the biotin-eluate with S-protein agarose and were eluted by heating at 95ºC for 5min. The eluate was sent to Taplin Mass Spectrometry Facility at Harvard Medical School for LC/MS/MS mass spectrometry analysis.

2.2.1.20. Co-immunoprecipitation (Co-IP) Assay

HCC cells were transfected with pCMV6-Entry, Myc-DDK-tagged UBE2T or its C86A mutant construct using Lipofectamine® 2000. The cells were lysed by NETN buffer with the addition of protease and phosphatase inhibitors. The protein concentration in lysate was measured by Bradford protein assay. Lysate was precleared by incubation with Protein A agarose (Cell Signaling Technology) at 4ºC for 30min. The precleared lysate was immunoprecipitated with UBE2T antibody (15 μg/mg) or Mule antibody (10 μg/mg) together with normal rabbit IgG in equal

concentration with incubation of 15 μL Protein A agarose at 4ºC overnight. The agarose beads were washed by NETN buffer and were boiled for 5 min with the addition of 2X SDS loading buffer to eluate the proteins. The pull-down purified proteins were then subjected to Western Blot analysis.

2.2.1.21. Ubiquitination Assay

HCC cells were transfected with HA-Ubiquitin together with pCMV6-Entry, Myc-DDK-tagged UBE2T or its C86A mutant construct using Lipofectamine® 2000. After 24 hours, the transfected cells were treated with 20 μM MG132 for 7 hours. The cells were directly lysed by NETN buffer with protease inhibitor cocktail and phosphatase inhibitors. The protein concentration was measured by Bradford protein assay. 1 mg of cell lysate was incubated with Mule antibody (Abcam) at concentration of 3 μg/mg and Protein A agarose (Cell Signaling Technology) at 4ºC overnight. The agarose beads were washed by NETN buffer and were boiled for 5 min with the addition of 2X SDS loading buffer to eluate the proteins. The pull-down purified proteins were then subjected to Western Blot analysis. HA antibody (Proteintech) was used for detection of ubiquitinated Mule.

2.2.2. *In Vivo* Studies

2.2.2.1. *In Vivo* Tumorigenicity Assay

In vivo evaluation of tumorigenicity of HCC cells was performed by subcutaneous inoculation of tumor xenograft in NOD-SCID mice. The HCC cells were suspended in 100 μL of serum-free culture medium mixed with Matrigel (BD Biosciences) in 1:1 ratio and subcutaneously injected into the flanks of NOD-SCID mice. The mice were under observation for tumor growth and sacrificed at the end of experiment. Tumors were harvested for documentation. T-IC frequency

was calculated using Extreme Limiting Dilution Analysis (ELDA) software [134] with 95% CI.

2.2.2.2. *In Vivo* Orthotropic Implantation

Luciferase-labeled MHCC-97L cells were suspended in 20 μL of Matrigel and injected into the left lobes of livers of BALB/c nude mice. Six weeks after implantation, mice were administered with 100 mg/kg D-luciferin via intraperitoneal injection prior to bioluminescent imaging using IVIS Lumina Series III Pre-clinical In Vivo Animal Imaging Systems (Perkin-Elmer, Waltham, MA) under anesthesia. The mice were then sacrificed, and the lungs and livers were harvested for *ex vivo* imaging.

2.2.3. Statistical Analysis

Statistical significance of the quantitative results obtained from qPCR, spheroid formation assays, flow cytometry analysis, migration and invasion assays and β-catenin TCF binding assay was determined by Student's t-test using Microsoft Office Excel software (Microsoft Corporation, Redmond, WA). The displayed results showed the means and the standard deviations, and those with p-values less than 0.05 were considered statistically significant (* $p<0.05$, ** $p<0.01$, *** $p<0.001$). Kaplan-Meier survival analysis was used to analyze disease-free survival and the statistical significance was calculated by log-rank test; these analyses were carried out using SPSS 20 software (IBM, Armonk, NY).

Chapter 3

Clinical Relevance of UBE2T Overexpression in HCC

3.1. Introduction

HCC is one of the deadly diseases and the second leading cause of cancer death worldwide in 2012. The current common treatment modalities for HCC include surgical resection for the early-stage malignancy; TACE with chemotherapeutic agents for the moderate-stage; and sorafenib chemotherapy for the advanced-stage. However, each treatment modality has its own limitations and drawbacks. For example, 5-year probability of tumor recurrence after surgical resection is 70% [14]. TACE and sorafenib treatments may select highly tumorigenic drug-resistant cancer cells, leading to development of chemoresistance and tumor recurrence. Sorafenib is the first-line therapeutic agent for advanced-stage HCC to date but it prolongs the survival of HCC patients by approximately 3 months only with a low response rate of 2% [30], [31]. It is suggested that the drug resistance, metastasis and poor survival of HCC patients are attributed to the liver CSCs.

CSCs are currently recognized as the origin of cancers and play a critical role in promoting tumor progression. CSCs are a subset of malignant cells with the ability of self-renewal and differentiation. Many studies have reported the active involvement of CSCs in tumorigenicity, metastasis, angiogenesis, and development of radio-/chemoresistance, contributing to the escape of tumor cells from cell death caused by conventional therapies. Therefore, identifying potent therapeutic target against CSCs is in urgent need.

Since tumor progression requires extensive cell proliferation for tumor growth, DNA replication errors are prone to occur during cell division. CSCs have efficient DNA damage response (DDR) system to repair the DNA lesions, contributing to the development of radio-/chemoresistance. Therefore, it may be a good starting point to look for potential therapeutic

target by investigating the DDR system in liver CSCs.

CSCs resembles normal adult stem cells to have the ability of self-renewal and differentiation. It is suggested that CSCs may originate from normal stem cells which acquire tumorigenicity by accumulation of mutations [135]. CSCs and normal stem cells share many similarities. Some CSC markers such as CD44 are also the markers of normal stem cells [77]. Hedgehog signaling is active in CSCs and normal stems cells [136]. Hence, investigating the DDR systems in the normal stem cells may give a clue to the potential therapeutic target against liver CSCs.

In this chapter, we looked for the potential therapeutic target by investigating the DDR-related genes actively involved in hepatic stem cell. The expression status and clinical relevance of the potential therapeutic target were then examined in several clinical cohorts to demonstrate the clinical significance of the potential target.

3.2. Experimental Scheme

In this chapter, the potential therapeutic target against liver CSCs was identified by studying the gene expression profile in liver regeneration model. The expression and clinical relevance of the potential target were then studied in different clinical cohorts. The experimental outline is summarized in the following diagram. The methods used in this chapter are mentioned in Chapter 2: Materials and Methods in further detail.

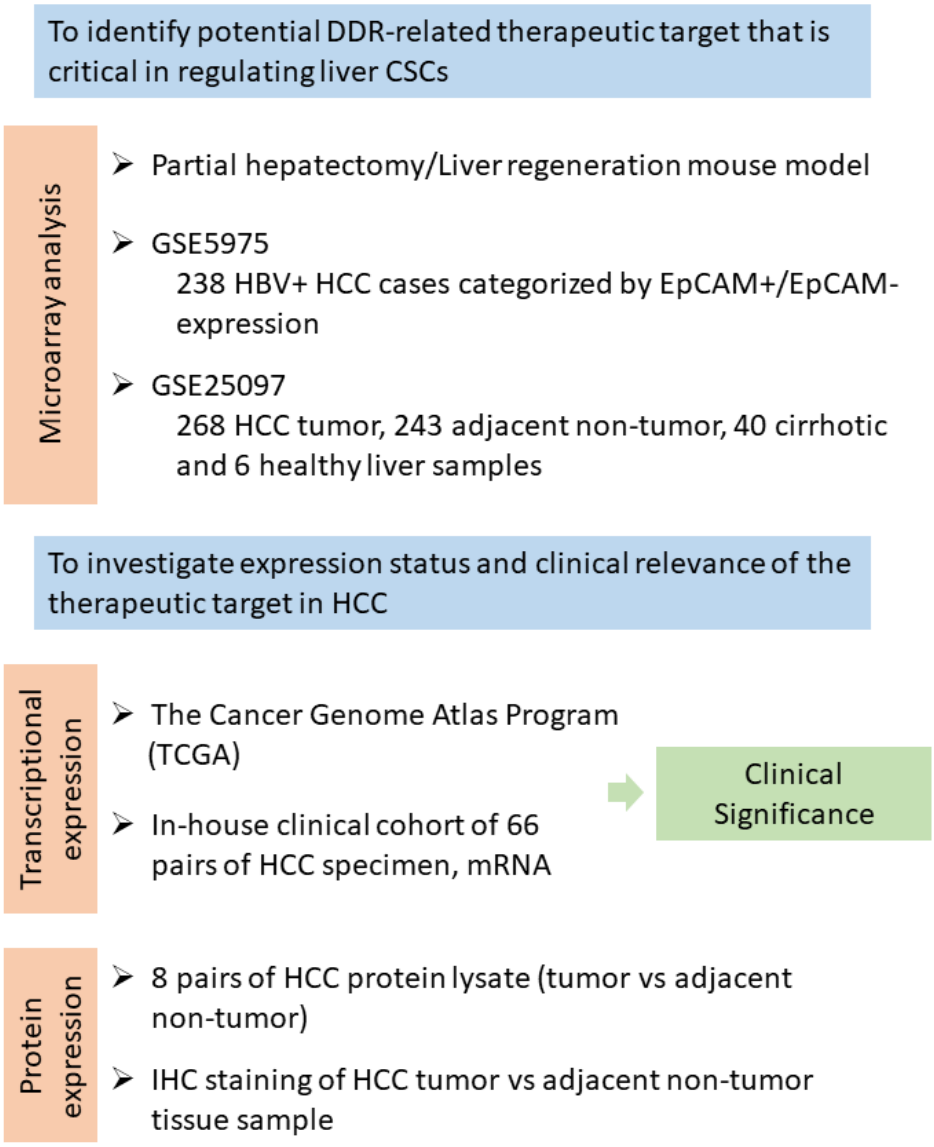

Figure 3.1. Experimental scheme of identifying potential potent therapeutic target against liver CSCs.

3.3. Results

3.3.1. UBE2T was significantly upregulated during liver regeneration

Severe partial hepatectomy was performed in nude mice in which 70% of the livers were excised under anesthetic condition (**Figure 3.2A**). The mouse liver entered liver regeneration after the excision of liver. 2 mice were sacrificed at different time points (Day 0, Day 3 and Day 7 after the surgery) each for harvest of the livers. The liver at Day 3 is generally considered the early regenerating liver because of the high cell proliferation rate while the liver at Day 7 was considered the late regenerating liver because of the slower cell proliferation [137]. Total mRNA was extracted from the harvested livers and cDNA was synthesized by reverse transcription for the subsequent cDNA microarray analysis. Expressions of various DNA damage response (DDR)-related genes were investigated by comparing the expression profile of the early regenerating livers to that of the intact liver (Day 0). The analysis discovered that UBE2T was one of the most upregulated DDR-related genes with significant upregulation by 11 folds (**Table 3.1**). Surprisingly, it is found that the expression of UBE2T dropped drastically on Day 7, the time of late liver regeneration (**Figure 3.2B**). The high expression of UBE2T in the regenerating liver indicates its potential important role in regulating hepatic stem cells.

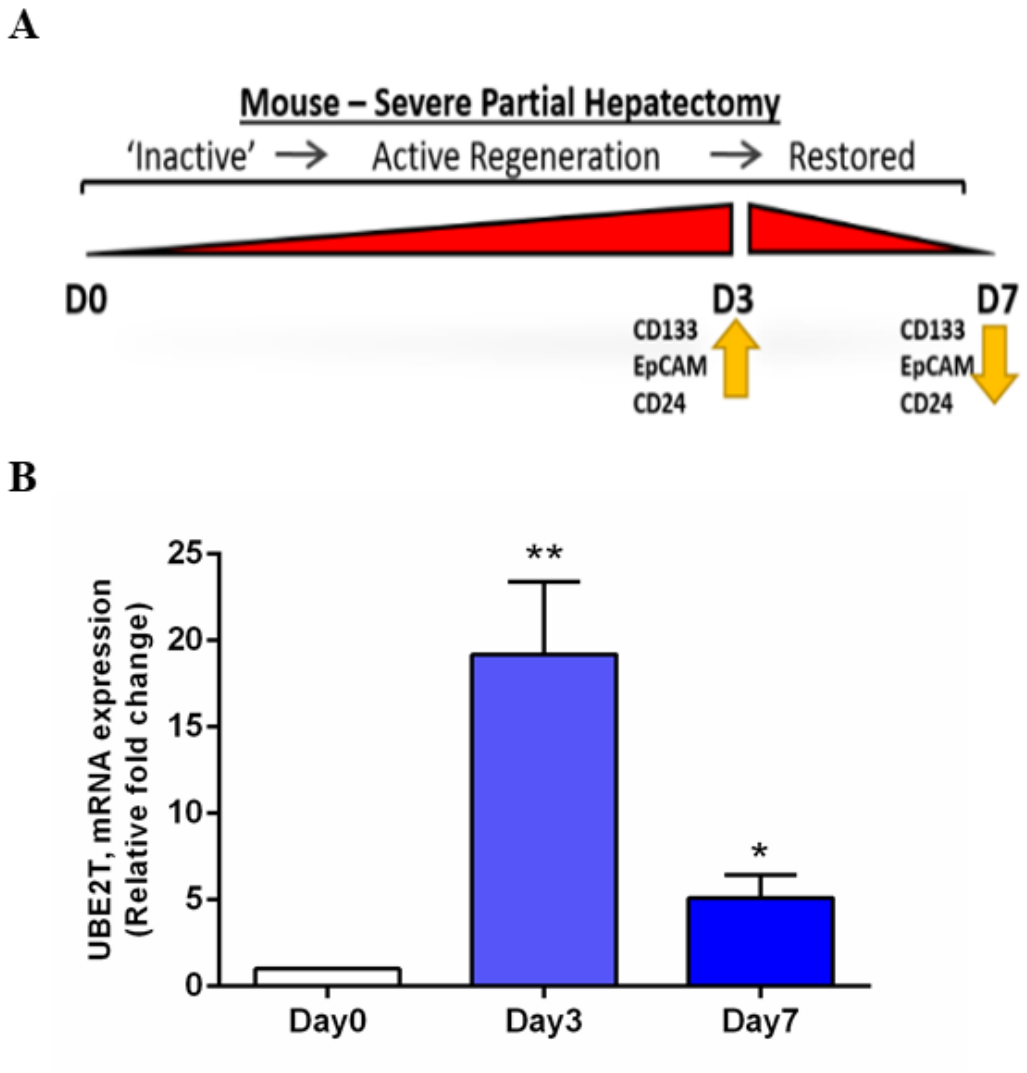

Figure 3.2. Significant upregulation of UBE2T was found in early regenerating liver but drastically dropped in late regenerating liver. (A) Partial hepatectomy mouse model was employed for study of gene expression profile in regenerating liver. 70% of mouse liver was excised at Day 0. The regenerating liver was harvest for subsequent microarry profiling at Day 3 and Day 7 as early regenerating liver and late regenerating liver respectively. (B) UBE2T, one of the DDR-related genes examined, significantly increased the mRNA expression in the early regenerating liver but the expression dropped drastically in the late regenerating liver (Day 7). (**$p<0.01$, *t* test)

Gene	Fold change (Regenerating liver (Day3) / Intact (Day0))
UBE2T	**11.54**
BRCA1	11.54
PTTG1	7.59
FOXM1	4.714
CDCA5	4.3
FEN1	2.9
MDM2	2.82
HLTF	2.26
CDH1L	2.115
NUCKS1	2.11

Table 3.1. Upregulation of DDR-related genes was observed in early regenerating liver. Microarray data of early regenerating liver (Day 3) was compared to that of intact liver (Day 0). Various DDR-related genes were found to be upregulated in the regenerating liver.

3.3.2. Elevated expression of UBE2T was associated with cancer stemness and HCC development

The potential role of UBE2T in cancer stemness was further explored in another clinical cohort (GEO accession number: GSE5975), in which 238 HBV^+ HCC cases are involved. The HCC samples were categorized according to the expression of EpCAM, a liver CSC marker. Higher mRNA level of UBE2T was observed in the $EpCAM^+$ group of HCC tumors, indicating the association of UBE2T expression with cancer stemness in HCC (**Figure 3.3**).

The relationship of UBE2T and CSCs was investigated by microarray analysis of another publicly available dataset (GEO accession number: GSE25097). The mRNA level of UBE2T has

been increased in stepwise manner during HCC development (**Figure 3.4**). The median of UBE2T expression increased by approximately 2.5 folds in cirrhotic liver compared to the healthy liver. A 6-fold sharp rise in UBE2T mRNA level was found when cirrhotic liver developed into HCC tumor. Significance Analysis of Microarrays (SAM) highlighted significant upregulation of UBE2T in HCC samples. Among 577 genes with over 2-fold overexpression, UBE2T was the 15th most upregulated (**Table 3.2**). Expressions of 17 DDR-related genes were further examined to study the correlation of DDR with CSCs in HCC. UBE2T was found to be the second most upregulated DDR-related gene in the dataset (**Table 3.3**).

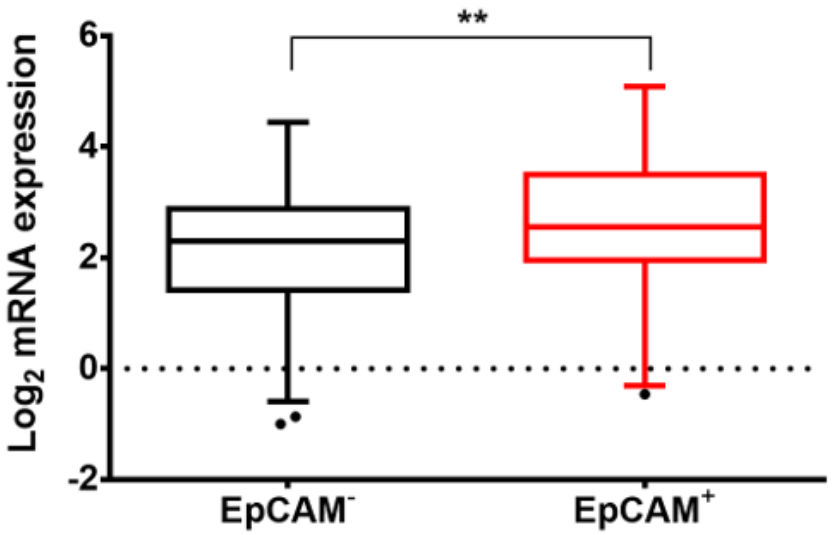

Figure 3.3. Higher UBE2T mRNA level is correlated with expression of liver CSC marker EpCAM. Microarray data of a publicly available clinical dataset GSE5975 was analyzed. 238 cases of Chinese HBV^{+} HCC patients were categorized according to the EpCAM expression. 1.36-fold higher UBE2T mRNA level was found to be related to the EpCAM^{+} group (**p<0.01, *t* test).

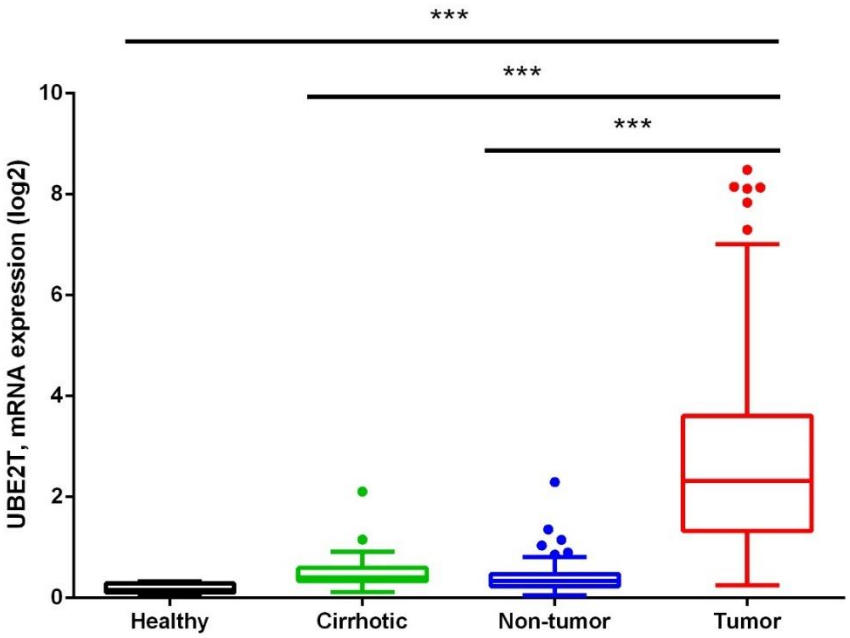

Figure 3.4. UBE2T mRNA expression increased in stepwise manner during HCC development. Microarray analysis of GSE25097 revealed the stepwise increase in UBE2T expression during development of HCC from liver cirrhosis. (***p<0.001, *t* test)

Rank	d(i)	Fold-change	Gene
1	25.65	2.23	RACGAP1
2	25.27	98.55	PSMB4
3	24.30	2.52	KLHL12
4	23.15	7.7	ITGA6
5	22.64	3.72	SNRPC
6	22.36	6.71	FAM189B
7	21.69	5.39	PIGC
8	21.33	2.46	SNX27
9	21.20	133666	GPC3
10	21.20	14.21	LARP1
11	21.06	7.33	CASC3
12	21.05	9.85	PTTG1
13	20.67	4.87	REPIN1
14	20.46	6.52	PYGO2
15	**20.38**	**4.94**	**UBE2T**
16	20.31	4.42	TOP2A
17	20.22	2.05	PPOX
18	20.21	5.38	RRM2
19	20.19	2.97	CASC5
20	19.96	7.64	NUSAP1

Table 3.2. UBE2T is the 15th most upregulated genes in HCC tumor samples in GSE25097. SAM analysis revealed that UBE2T is the 15th most upregulated gene in the clinical dataset

GSE25097.

Rank	d(i)	Fold-change	Gene
1	21.05	9.85	PTTG1
2	**20.38**	**4.94**	**UBE2T**
3	19.79	6.26	AURKA
4	18.03	2.26	CDCA5
5	17.27	3.14	FEN1
6	17.10	2.56	FOXM1
7	16.68	3.83	NPLOC4
8	16.48	3.99	HLTF
9	16.36	2.1	RNASEH2A
10	15.70	3.02	NCOA6
11	15.13	3.18	NSMCE2
12	14.20	4.73	CHD1L
13	12.28	3.45	GRB2
14	10.61	3.36	TCEA1
15	9.29	11.95	NDRG1
16	8.66	2.89	NUCKS1
17	-13.64	0.082	GADD45A

Table 3.3. UBE2T is the second most upregulated DDR-related gene in HCC tumor samples in GSE25097. Expressions of DDR-related genes were investigated by SAM analysis. UBE2T was found to be the second most upregulated DDR-related gene in GSE25097.

3.3.3. UBE2T overexpression promoted poor prognosis of HCC patients

The above preliminary data indicates the overexpression of UBE2T in HCC and its relationship to liver CSCs. Clinical relevance of UBE2T was then examined in our in-house clinical cohort. The expression status of UBE2T in 82 pairs of HCC tumors and the adjacent non-tumor liver tissues was investigated by qPCR analysis. 91% of the cases showed over 2-fold upregulation of UBE2T mRNA level (**Figure 3.5**). More than half of the cases (55%) showed over 8-fold UBE2T overexpression. Elevated expression of UBE2T in HCC in protein level was confirmed by 8 pairs of protein lysates obtained from HCC tumors and the adjacent non-tumor liver tissues. Significant upregulation of UBE2T in tumor was detected in 7 pairs of samples (**Figure 3.6**). IHC staining also highlighted distinct upregulation of UBE2T in HCC tumor compared to adjacent non-tumor tissue (**Figure 3.7**).

After confirming the overexpression of UBE2T in HCC, the clinical relevance was examined by looking into the clinico-pathological data of 66 HCC cases from our in-house cohort. The HCC cases were divided into 2 groups according to the UBE2T mRNA level. It is found that high expression of UBE2T (T:N≥8) is positively correlated to tumor size (p=0.023) (**Table 3.4**). UBE2T upregulation is also related to absence of tumor encapsulation and advanced tumor stages with p-values of 0.053 and 0.074 respectively. Although statistical significance has not been reached, Kaplan-Meier analysis shows that high expression of UBE2T contributed to poorer 3-year disease-free survival of HCC patients (**Figure 3.8**).

The clinical relevance of UBE2T was further studied in The Cancer Genome Atlas (TCGA), which is a large publicly available clinical cohort involving 442 cases of human HCC. UBE2T

mRNA upregulation (z-score >2) was found in 17% of the HCC cases and higher UBE2T mRNA level was associated with advanced tumor stages (**Figure 3.9A**) and poorer survival of HCC patients (**Figure 3.9B**).

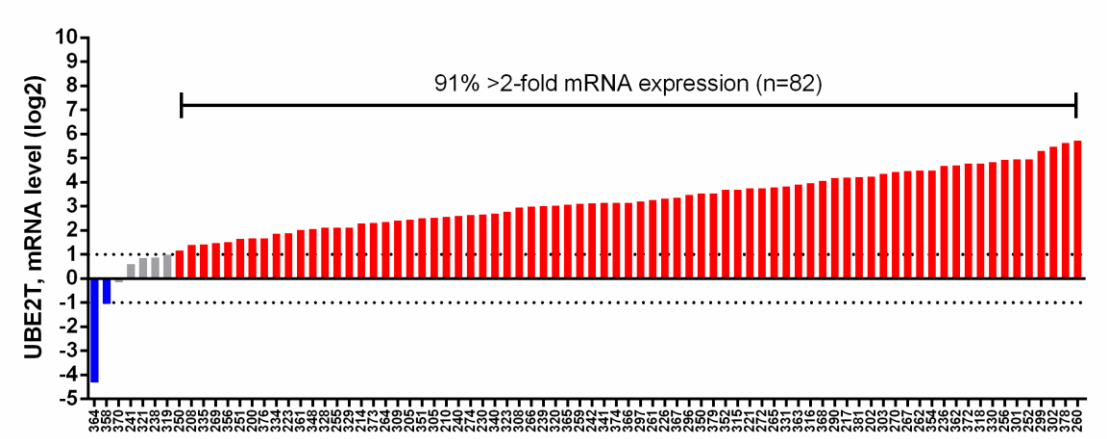

Figure 3.5. Overexpression of UBE2T was found in over 90% of HCC cases. UBE2T mRNA level was examined in 82 cases of our in-house clinical cohort. 91% of the HCC cases showed over 2-fold UBE2T upregulation and 55% showed over 8-fold upregulation.

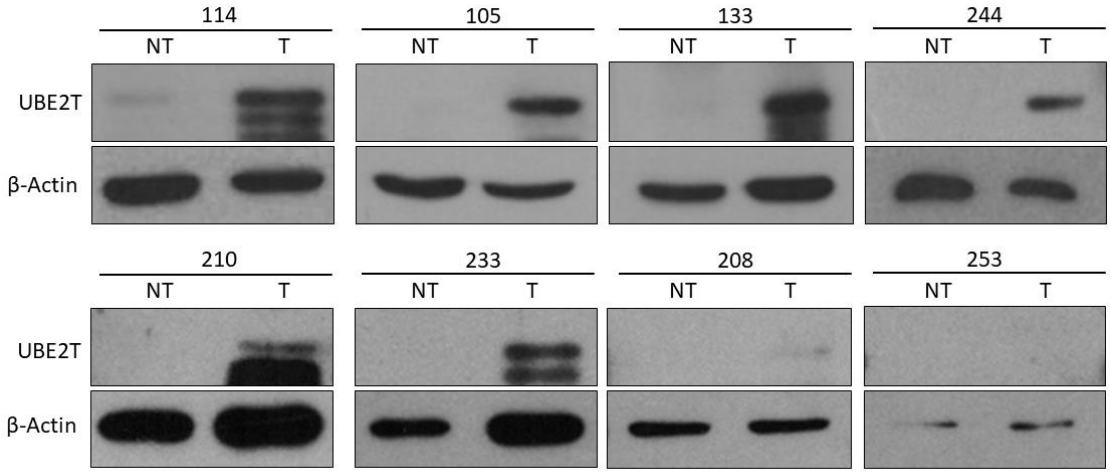

Figure 3.6. Overexpression of UBE2T was found in 87% of HCC tumors. 8 pairs of protein samples obtained from HCC tumors and the adjacent non-tumor liver tissues. UBE2T overexpression was found in 87% (7/8) of the HCC cases by Western Blot analysis.

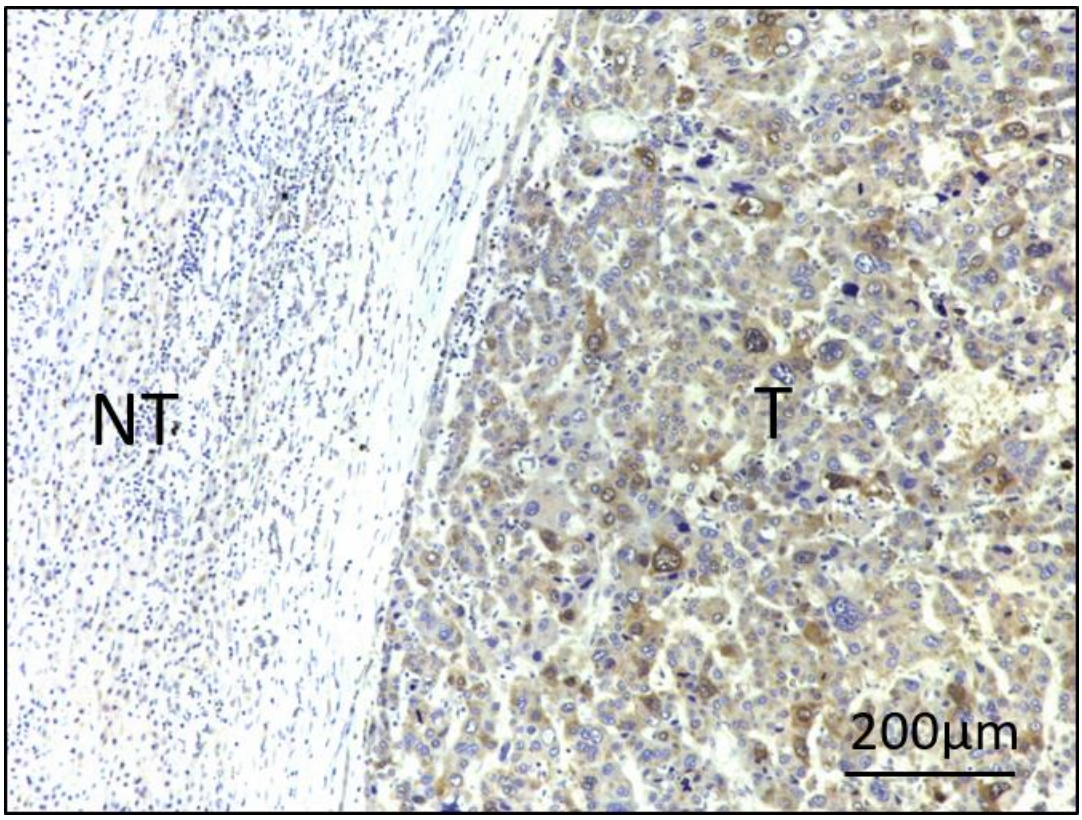

Figure 3.7. UBE2T has a higher expression in tumor compared to the adjacent non-tumor liver tissue. IHC staining of HCC clinical specimen showed higher expression of UBE2T in HCC tumor compared to the non-tumor tissue.

Clinico-pathological features	UBE2T, mRNA		p value (Fisher-exact test)
	T:NT < 8	T:NT ≥ 8	
Gender			
Male	20 (74.0%)	29 (74.4%)	1.000
Female	7 (25.9%)	10 (25.6%)	
Venous invasion			
Absent	14 (60.9%)	14 (37.8%)	0.112
Present	9 (39.1%)	23 (62.2%)	
Tumor encapsulation			
Absent	11 (47.8%)	26 (74.3%)	0.053
Present	12 (52.2%)	9 (25.7%)	
Tumor microsatellite formation			
Absent	12 (52.2%)	13 (35.1%)	0.282
Present	11 (47.8%)	24 (64.9%)	
Cellular differentiation by Edmondson grading			
I – II	13 (56.5%)	12 (32.4%)	0.105
III – IV	10 (43.5%)	25 (67.6%)	
Tumor size			
≤5 cm	11 (47.8%)	7 (18.9%)	**0.023***
>5 cm	12 (52.2%)	30 (81.0%)	
Cirrhotic liver			
Normal and chronic hepatitis	9 (39.1%)	24 (64.9%)	0.065
cirrhosis	14 (60.9%)	13 (35.1%)	
Tumor stage			
I/II	15 (55.6%)	12 (30.8%)	0.074
III/IV	12 (44.4%)	27 (69.2%)	

Table 3.4. UBE2T upregulation is associated with aggressive HCC features. Clinical relevance of UBE2T was studied by analyzing clinico-pathological data of 66 cases of HCC patients. High expression of UBE2T (T:NT≥8) was correlated to larger tumor size (*p=0.023) and was related to

absence of tumor encapsulation (p=0.053) and advanced tumor stage (p=0.074). (*p<0.05, Fisher-exact test)

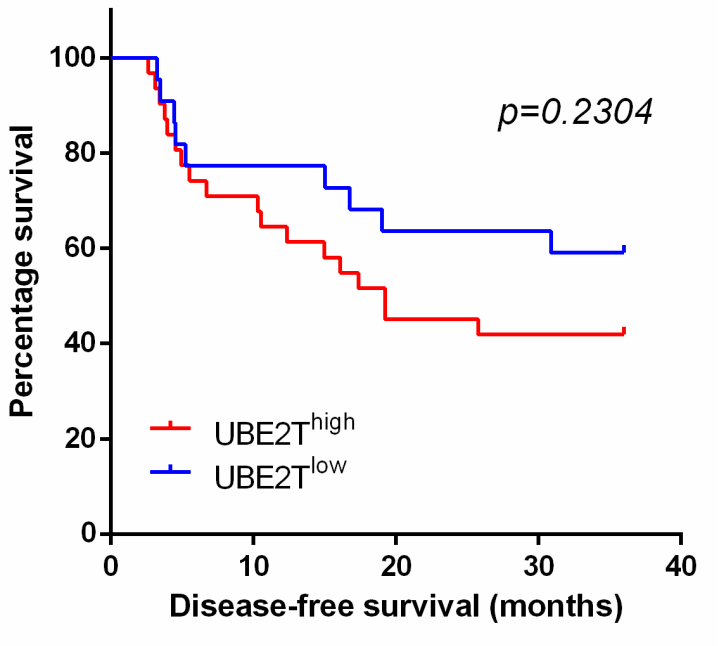

Figure 3.8. High UBE2T expression contributed to poor 3-year disease-free survival of HCC patients. Kaplan-Meier analysis of 66 HCC cases showed that high expression of UBE2T (T:NT≥8) contributed to poorer 3-year disease-free survival of HCC patients (p=0.2304, Logrank test).

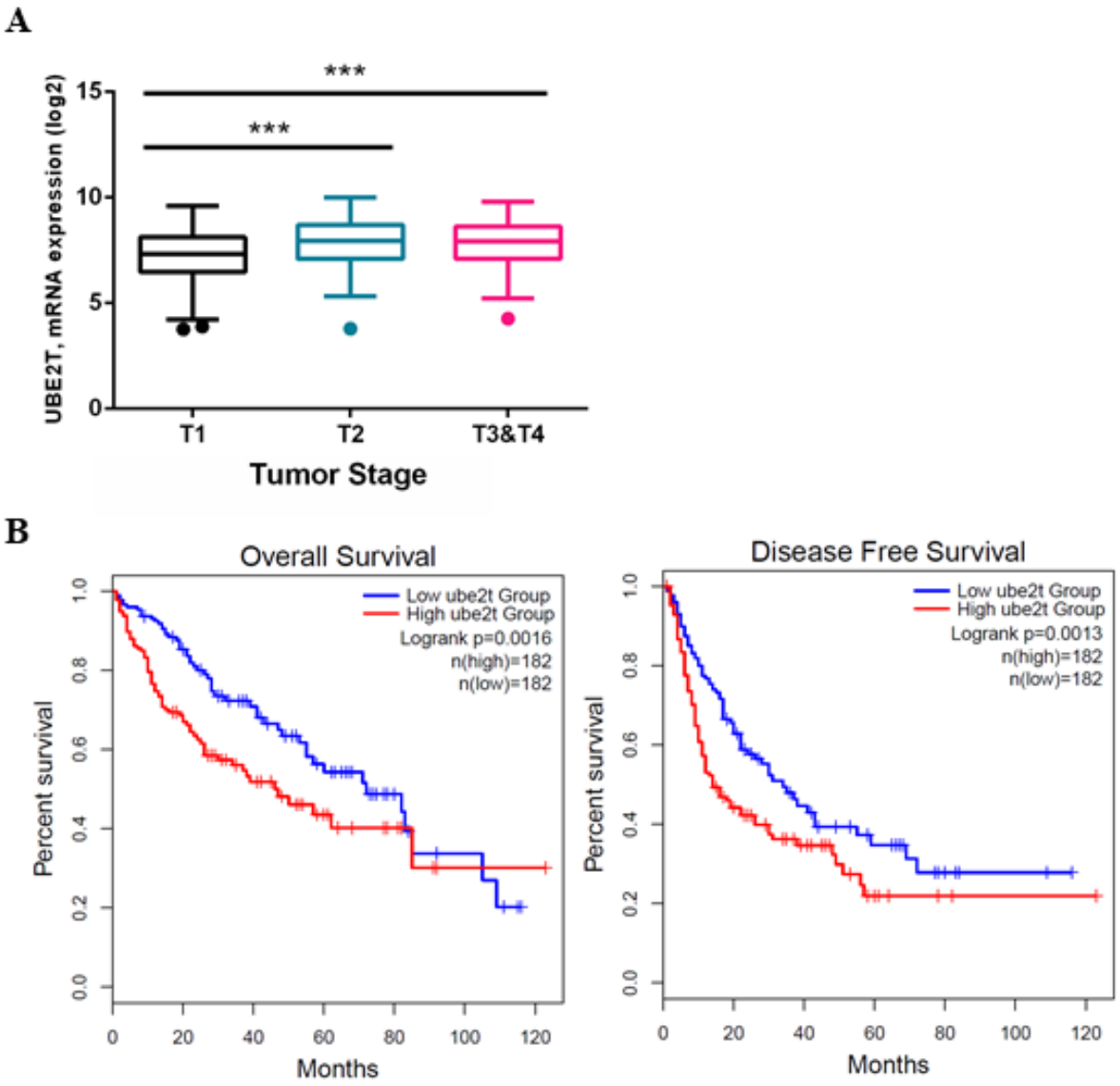

Figure 3.9. UBE2T mRNA upregulation was related to poor prognosis of HCC patients in TCGA cohort. (A) Elevated UBE2T mRNA level was found in 17% of the HCC cases (n=442) in TCGA cohort. (***p<0.001, *t* test) (B) UBE2T mRNA level is positively correlated with advanced tumor stages of HCC patients. (C) UBE2T mRNA upregulation was associated with poor overall survival (left) and disease-free survival (right). (**p<0.01, Logrank test)

3.4. Discussion

CSCs resemble normal stem cell having the ability of self-renewal and differentiation. The genes that play an important role in regulating normal stem cells may be involved in the maintenance of CSCs as well. Therefore, partial hepatectomy was performed to identify the potential therapeutic target for liver CSC regulation. Partial hepatectomy is a widely used mouse model for study of liver regeneration, which is a unique capacity of mammalian liver. After acute injury or resection, the remaining uninjured liver lobes can grow to compensate the original mass. Liver regeneration requires extensive cell proliferation and differentiation for compensation of the lost tissue. Hepatic oval cells, which are a heterogenous population of progenitor cells with the ability to proliferate and differentiate, are actively involved in the regenerative process and are recognized as a subgroup of stem cells [138], [139]. Besides, excision of liver leads to mobilization of stem cells to the liver lobe remained to promote liver regeneration [140]–[142]. Hence, partial hepatectomy is a good start point to investigate the genes that are critical in hepatic stem cells. In the mouse liver regeneration model, 70% of the rodent liver was resected and the whole liver regeneration can be completed in 7 days in rodents [138]. Day 3 is commonly regarded as early liver regeneration because of significant upregulation of cell proliferation rate at around Day 3 after surgery of partial hepatectomy [137]. Cell proliferation slows down at around Day 7 so Day 7 is commonly regarded as late liver regeneration [137]. The livers were harvested in different time points to compare the expression profiles in intact, early and late regenerating livers at Day 0, Day 3 and Day7 respectively. As discussed previously, CSCs have efficient DDR system to overcome the DNA replication errors that are probably occur during extensive proliferation. The microarray analysis highlighted the significant upregulation of UBE2T in the early regenerating liver. The expression of UBE2T was enhanced to the same extent as BRCA1, which is well-studied for its

substantial functions in DNA repair, cell cycle regulation, cell division and maintenance of CSCs [96], [115], [143], [144]. The remarkable increase in UBE2T expression suggests its potential importance in the regenerative process. Additionally, the mRNA expression of UBE2T drastically dropped by approximately 4 folds from the early regenerating liver to the late regenerating liver. Similar expression pattern has been found in CSC marker CD133, which displayed great increase in mRNA level in the early regenerating liver but exhibited a significant drop in expression in the late regenerating liver [145]. Therefore, the microarray data from the liver regeneration model suggests that UBE2T may have an important undiscovered role in the regulation of liver CSCs.

Meanwhile, microarray analysis revealed the correlation of UBE2T and liver CSC marker EpCAM, which supports the hypothesis that UBE2T is associated with liver CSCs. Stepwise increase in UBE2T expression during HCC development has been discovered as well. On the one hand, the significant high expression of UBE2T in HCC tumor highlights the substantial role of UBE2T in tumor progression. On the other hand, the elevated expression of UBE2T in cirrhotic liver compared to healthy liver suggests that UBE2T may be critical in the stem cell-mediated cell proliferation. Majority of HCC develops in cirrhotic liver, which is the result of repeated wound healing for damages caused by chronic liver diseases such as hepatitis virus infection, fatty liver disease and alcoholic liver disease. Different to acute liver injury which gives rise to liver regeneration, chronic liver diseases lead to fibrosis, which may eventually develop into cirrhosis [146]. Repeated wound healing requires extensive cell proliferation and differentiation for compensation of the injured cells. It has been reported that expressions of liver stem cell markers such as EpCAM and CD133 were enhanced in cirrhosis [147]. Numbers of stem cell-like hepatic oval cells were found to be elevated in response to progressive fibrosis [148]. Therefore, the

upregulation of UBE2T in cirrhotic liver may indirectly indicates the potential role of UBE2T in regulating hepatic stem cells.

In this chapter, the expression status of UBE2T in HCC was explored in different clinical cohorts. Remarkable overexpression of UBE2T has been found in all the 4 cohorts we have examined. Apart from the general upregulation of UBE2T in HCC, our study found that higher expression of UBE2T is positively correlated with tumor size. Although statistical significance has not been reached, UBE2T mRNA upregulation was related to absence of tumor encapsulation and advanced tumor stages. Without encapsulation, tumors are more invasive, leading to higher incidence rate of direct liver invasion and poorer survival of HCC patients [21]. Hence, elevated expression of UBE2T contributes to tumor growth and invasiveness in HCC. Kaplan-Meier analysis showed that the HCC patients with UBE2T upregulation had poorer disease-free survival as well. Significant upregulation of UBE2T in protein level and mRNA level has been reported in many cancers including lung, breast, prostate and HCC cancers and is related to poor survival of the patients [122], [124], [125], [129]. Nevertheless, the clinical importance of UBE2T has been discussed in detail in limited studies only. Prostate tumor tissue obtained from patients with distant metastasis exhibited higher expression of UBE2T [129]. UBE2T upregulation was associated with advanced stages in T classification in nasopharyngeal carcinoma and gastric cancer, indicating the promotion of UBE2T on tumor growth [128], [132]. UBE2T was found to support metastasis in nasopharyngeal carcinoma and HCC as well [125], [132]. In our study, UBE2T overexpression is found to be correlated with advanced tumor stage and tumor invasion in HCC. Our finding is consistent with the previous studies.

In summary, we discovered UBE2T as the potential therapeutic target against liver CSCs. It is remarkably overexpressed in HCC and may play an important role in regulating stem cell functions. Elevated expression of UBE2T is found to promote tumor progression and invasiveness. Meanwhile, our study reported the potential correlation of UBE2T and liver CSCs. To date, there has been no studies investigating the role of UBE2T in the maintenance of CSCs. It is hypothesized that UBE2T may regulate liver CSCs to promote tumorigenesis and lead to poor prognosis of patients. Further investigations on the role of UBE2T in CSCs were performed in the next chapter.

Chapter 4

Functional Characterization of UBE2T in Regulation of Liver CSCs

4.1. Introduction

In Chapter 3, we found overexpression of UBE2T in various cohorts of HCC patients. UBE2T overexpression contributes to poor clinical outcomes including larger tumor size, advanced tumor stage, risk of metastasis and poorer survival of HCC patients. Despite the common overexpression of UBE2T in a wide range of cancers, only limited studies have investigated the functional role of UBE2T in tumorigenesis.

The elevated expression of UBE2T was first reported in lung cancer, in which over 60% of the lung cancer specimens showed upregulation of UBE2T, in 2008 [122]. One year later, the first study investigating the role of UBE2T in tumorigenesis in breast cancer was published. Ueki et al [124] identified the upregulation of UBE2T in breast cancer by microarray analysis and discovered the proteasomal degradation of BRCA1 by UBE2T. More studies reporting the clinical significance of UBE2T in cancers have been released afterwards. Enhancement in cell proliferation and cell migration and invasion upon UBE2T overexpression has been reported in various cancer types such as prostate cancer [129], stomach cancer [127], [128] and nasopharyngeal carcinoma [132]. In concordance, suppression of cell proliferation by UBE2T knockdown has been revealed in cancers of liver [125], bladder [126] and osteosarcoma [131]. These studies provide compelling evidence for the critical role of UBE2T in tumorigenesis through promotion of cell proliferation and invasion. UBE2T is suggested to enhance cell proliferation via regulation of cell cycle. Downregulation of UBE2T resulted in cell cycle arrest [126]–[128]. Meanwhile, UBE2T enhances EMT process by activation of Akt-dependent signaling pathways to promote tumor invasiveness [127], [128], [131], [132].

UBE2T was first identified in $CD34^+$ hematopoietic stem cells, suggestive of its regulatory role in stemness properties of these cells [149]. Although this finding suggests a potential role of UBE2T in regulating stemness, the molecular mechanism by which UBE2T regulates stemness properties is poorly understood. Whether UBE2T regulates CSCs also remains unexplored. In Chapter 3, we found that UBE2T was found to be most significantly upregulated in self-renewal liver in the severe partial hepatectomy model. This, together with the publicly available dataset showing that UBE2T was significantly upregulated in the enriched liver CSC populations, has prompted us to investigate the role of UBE2T in regulation of liver CSCs. In this chapter, functional characterization of UBE2T in HCC was performed especially in the respect of cancer stemness to reveal the previously undefined biological role of UBE2T in regulation of the liver CSCs.

4.2. Experimental Scheme

In this chapter, the functional role of UBE2T on regulation of cancer stemness in HCC was investigated. UBE2T knockdown and overexpression clones were generated and various functional assays were performed to examine both the *in vitro* and *in vivo* CSC properties of the HCC cells. The experimental outline is summarized in the following diagram. The methods used in this chapter are mentioned in Chapter 2: Materials and Methods in further detail.

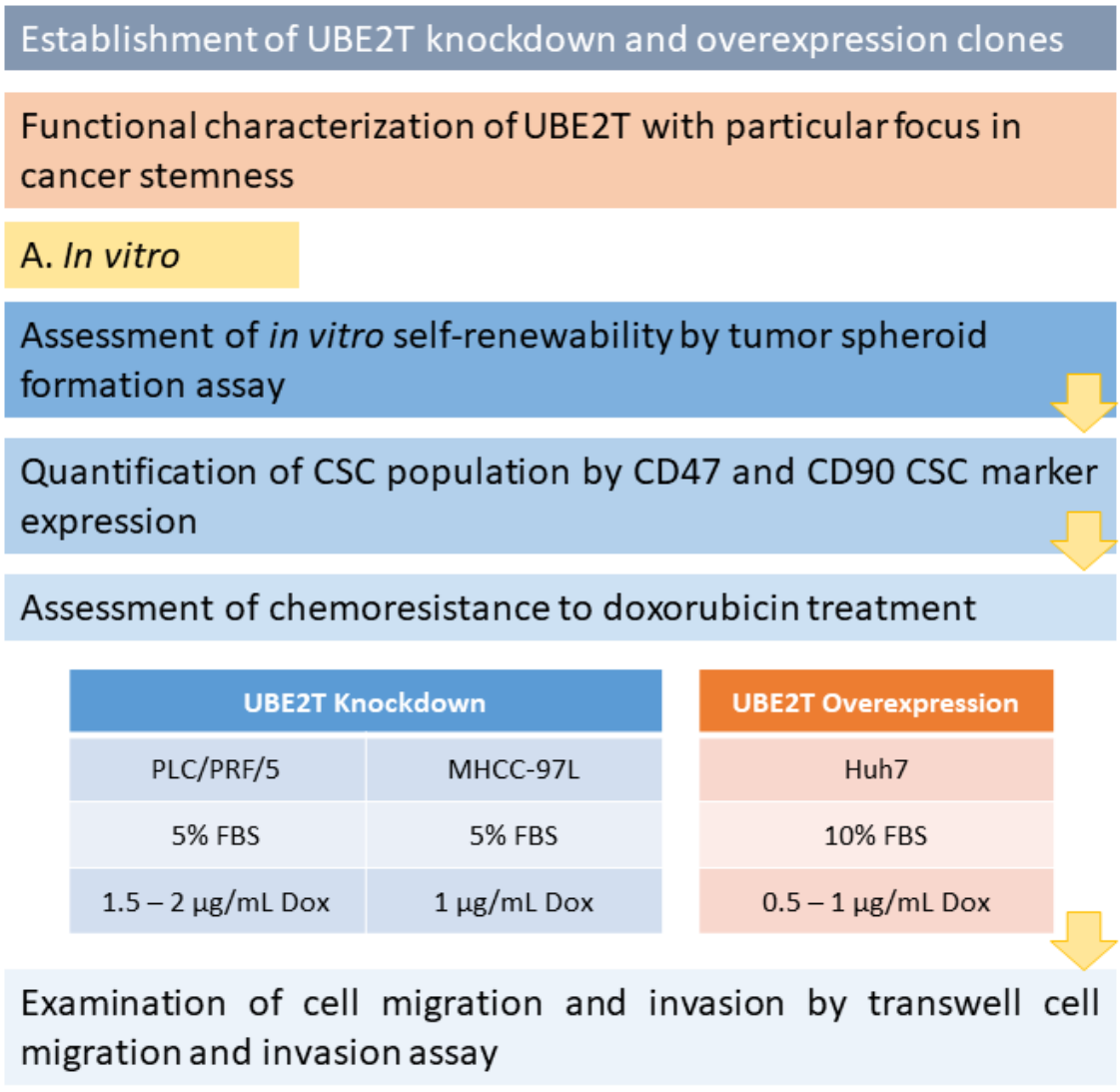

(Continued on the next page)

B. *In vivo*

Study of *in vivo* tumorigenicity and self-renewability by limited dilution assay

UBE2T Knockdown		UBE2T Overexpression
PLC/PRF/5	MHCC-97L	Huh7
1000 cells/injection	500 cells/injection	1000 cells/injection
10000 cells/injection	1000 cells/injection	5000 cells/injection
50000 cells/injection	10000 cells/injection	10000 cells/injection

Study of *in vivo* tumorigenicity and metastasis by orthotopic xenograft implantation model

Figure 4.1. Experimental scheme of investigation of functional role of UBE2T on regulating cancer stemness in HCC.

4.3. Results

4.3.1. Establishment of UBE2T knockdown and overexpression clones

In order to characterize the functional role of UBE2T in regulating cancer stemness in HCC, UBE2T knockdown and overexpression clones were established in HCC cell lines. The HCC cell line suitable for UBE2T knockdown or overexpression was determined based on the endogenous protein expression level of UBE2T, which was assessed across a panel of HCC cell lines by Western Blot analysis with β-actin as the loading control. UBE2T expression was found to be the highest in PLC/PRF/5 and MHCC-97L and the lowest in Huh7 and MIHA, a human immortalized normal liver cell line (**Figure 4.2A**). Therefore, UBE2T expression was repressed in PLC/PRF/5 and MHCC-97L while it was overexpressed in Huh7. Lentiviral-based knockdown approach was employed to establish UBE2T knockdown clones (shUBE2T(89) and shUBE2T(60)) with significantly reduced endogenous UBE2T protein levels in PLC/PRF/5 and MHCC-97L (**Figure 4.2B**). UBE2T was overexpressed in Huh7 by ectopic transfection of MYC-DDK-UBE2T plasmid. Stable clone with UBE2T overexpression was selected by G418 treatment for 2 weeks. Western Blot analysis showed that Myc-DDK-tagged UBE2T was approximately 10 kDa larger than the endogenous UBE2T (23 kDa) (**Figure 4.2C**). It is noted that a small portion of the endogenous UBE2T is conjugated with ubiquitin to form a larger protein at size of 32 kDa [118], [124]. Similarly, Myc-DDK-tagged UBE2T is monoubiquitinated to form a larger protein at size of about 40 kDa.

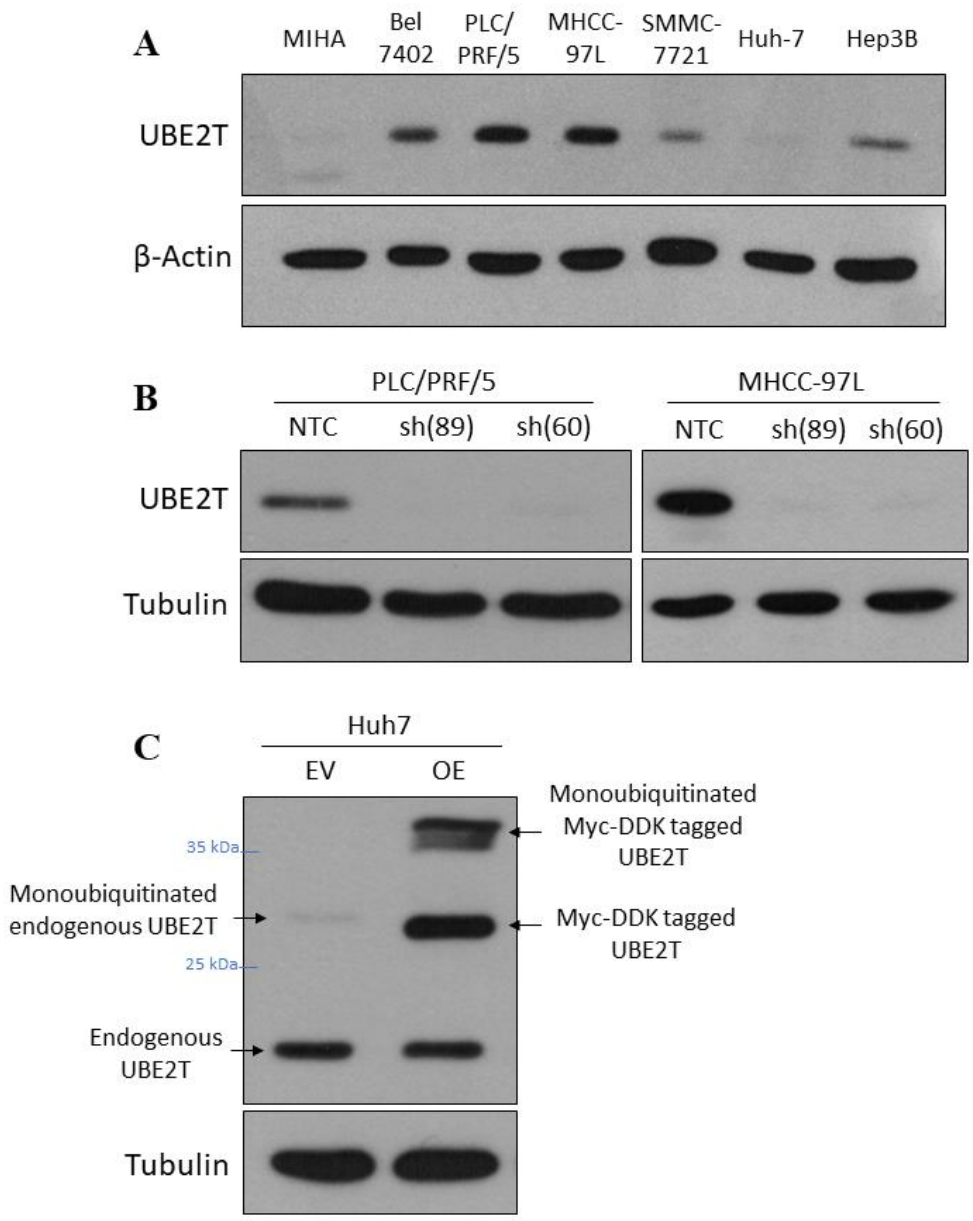

Figure 4.2. Establishment of UBE2T knockdown and overexpression clones. (A) The endogenous UBE2T protein levels was assessed in a panel of HCC cell lines, in which UBE2T has the highest expression in PLC/PRF/5 and MHCC-97L and the lowest expression in Huh7 and MIHA. (B) UBE2T expression was repressed by lentiviral-based approach in PLC/PRF/5 and MHCC-97L. (C) Myc-DDK-tagged UBE2T was overexpressed in Huh7.

4.3.2. UBE2T regulated tumor spheroid formation ability of HCC cells.

The role of UBE2T in regulating CSC properties in HCC was first examined in respect of the *in vitro* self-renewal ability. The *in vitro* self-renewal ability of the UBE2T knockdown cells and UBE2T overexpressing cells were determined by tumor spheroid formation assay. Knockdown of UBE2T significantly suppressed the tumor spheroid formation ability of HCC cells with remarkable reduction in size and number of the spheroids formed (**Figure 4.3A&B**). The number of spheroids formed was significantly reduced by half in PLC/PRF/5 shUBE2T(89) and shUBE2T(60) cells when compared to non-target control (NTC) cells. In MHCC-97L, shUBE2T(89) and shUBE2T(60) led to decrease in the number of spheroids formed by more than 5 folds. In both PLC/PRF/5 and MHCC-97L, smaller spheroids were formed in the UBE2T knockdown cells with size reduction to about one half. In concordance, overexpression of UBE2T promoted the spheroid formation ability of Huh7 cells (**Figure 4.3C**). UBE2T overexpressing cells displayed 1.23-fold increase in the number of spheroids formed with remarkable enlargement in size.

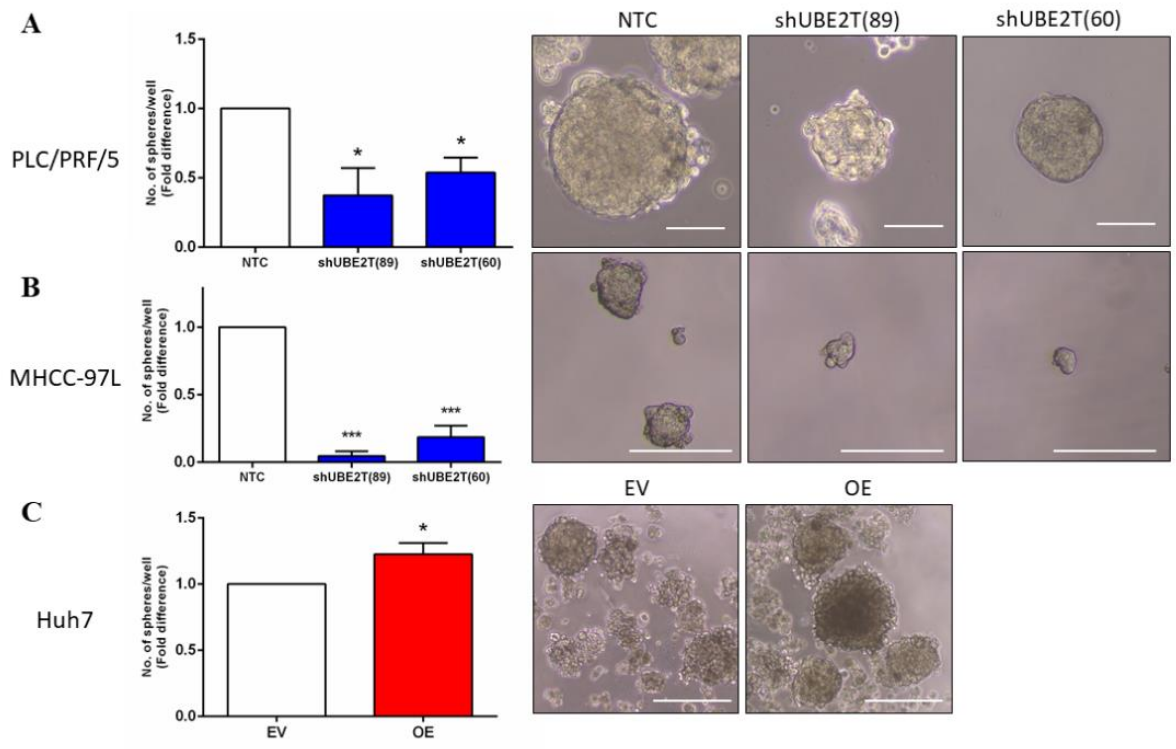

Figure 4.3. UBE2T promoted self-renewal ability of HCC cells. Tumor spheroid formation assay was performed to assess the self-renewal abilities of the UBE2T knockdown clones derived from PLC/PRF/5 and MHCC-97L cells and the UBE2T overexpressing Huh7 cells. Knockdown of UBE2T led to significant reduction in spheroid size and number in (A) PLC/PRF/5 and (B) MHCC-97L. (C) UBE2T overexpression enhanced the spheroid formation ability of Huh7 in term of size and number. (Scale bar: 100 μm) (*p<0.05, ***p<0.001, *t* test).

4.3.3. UBE2T enhanced expression of CSC markers

The link of UBE2T and cancer stemness was further investigated by examining the effect of UBE2T expression on the expression of liver CSC markers. The expression of CD47 and CD90 in UBE2T knockdown cells and UBE2T overexpressing cells were examined by flow cytometry analysis (**Figure 4.4**). UBE2T knockdown exhibited significant inhibition in CD47 expression in both PLC/PRF/5 and MHCC-97L. shUBE2T(89) and shUBE2T(60) led to reduce in CD47 expression level by half in both the PLC/PRF/5 and MHCC-97L cells. In respect to CD90, shUBE2T(89) displayed 1.4-fold decrease in the expression while shUBE2T(60) displayed 1.7-

fold decrease in PLC/PRF/5. In MHCC-97L, shUBE2T(89) and shUBE2T(60) suppressed the CD90 expression to approximately 0.5-fold. Consistently, overexpression of UBE2T promoted expression of CD47 and CD90 expression in Huh7 cells. UBE2T overexpressing Huh7 exhibited about 1.2-fold increase in expression of CD47 and CD90.

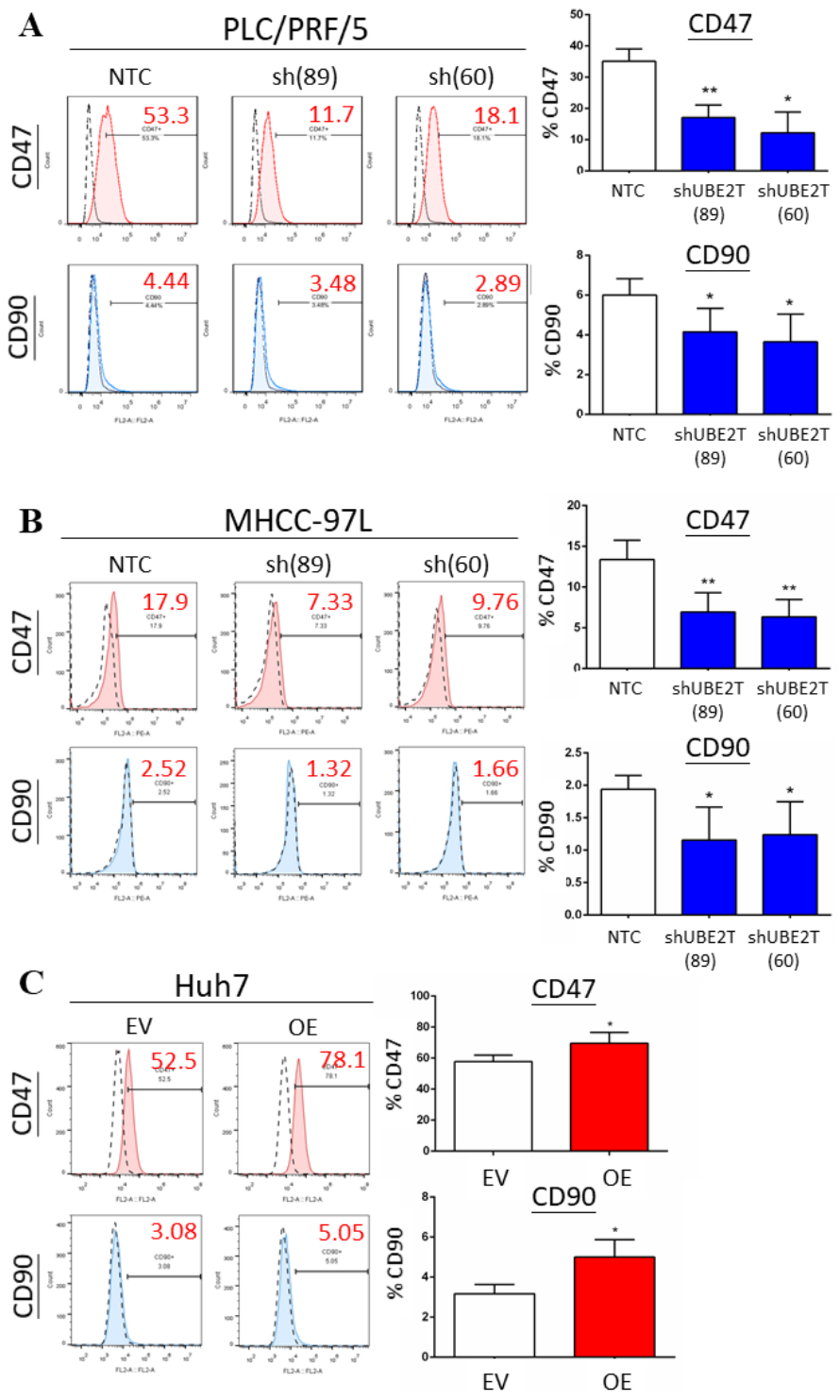

Figure 4.4. UBE2T enhanced CSC marker expression in HCC cells. Flow cytometry analysis showed downregulation of CD47 and CD90 in UBE2T knockdown cells in PLC/PRF/5 and MHCC-97L and upregulation of CD47 and CD90 in UBE2T overexpressing Huh7 cells. (*p<0.05, **p<0.01, *t* test).

4.3.4. UBE2T regulated sensitivity of HCC cells to doxorubicin

CSCs confer development of drug resistance. If UBE2T promotes CSC properties, increase in sensitivity to chemotherapeutic agents would be observed upon UBE2T knockdown. In addition, UBE2T is critical in FA DNA repair pathway. Ablation of UBE2T would sensitize the HCC cells particularly to DNA damage-inducing agents. Upon UBE2T knockdown and overexpression, HCC cells were treated with doxorubicin for 24 hours to assess the drug sensitivity. Annexin V assay showed that knockdown of UBE2T elevated the sensitivity of HCC cells to doxorubicin (**Figure 4.5**). Compared to the NTC cells, shUBE2T (89) and shUBE2T(60) enhanced the percentage of apoptotic cells by approximately 1.2 folds at 2 μg /mL doxorubicin in PLC/PRF/5. In MHCC-97L, shUBE2T(89) showed 1.8-fold higher doxorubicin sensitivity while shUBE2T(60) showed 1.4-fold higher. In line with the elevated sensitivity to doxorubicin upon UBE2T knockdown, increased resistance to doxorubicin was observed in UBE2T overexpressing Huh7 cells. The overexpression of UBE2T reduced the percentage of apoptotic cells to 0.57-fold at 1 μg/mL doxorubicin respectively.

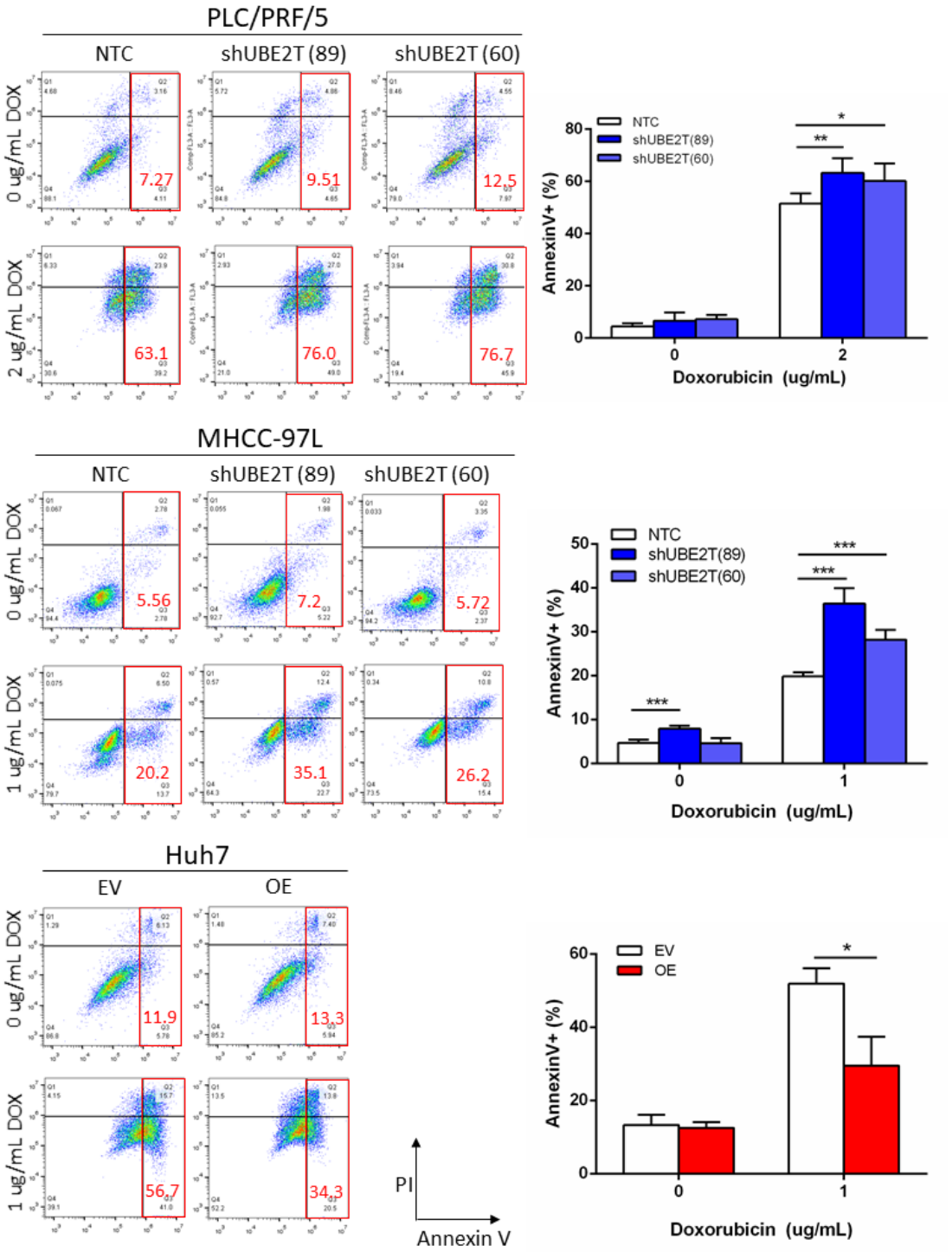

Figure 4.5. UBE2T regulated sensitivity of HCC cells to doxorubicin. Annexin V assay showed the percentage of apoptotic cells when the UBE2T knockdown PLC/PRF/5 and MHCC-97L cells and UBE2T overexpressing Huh7 cells were subjected to doxorubicin treatment for 24 hours. (*p<0.05, **p<0.01, ***p<0.001, *t* test).

4.3.5. UBE2T promoted migration and invasion of HCC cells

CSCs are considered as metastatic precursor because they promote EMT process [56], [57]. Since UBE2T was found to regulate liver CSCs, we hypothesize that UBE2T pose an effect on the migration and invasion abilities of the cancer cells upon manipulation of its expression level. The effect of UBE2T on the invasiveness of HCC cells was evaluated by cell migration and invasion assays. Cell migration and invasion were significantly suppressed upon knockdown of UBE2T in PLC/PRF/5 and MHCC-97L. shUBE2T(89) and shUBE2T(60) resulted in 0.47- and 0.29-fold differences in cell migration respectively when compared to the control cells in PLC/PRF/5 (**Figure 4.6A**). Cell invasion of PLC/PRF/5 was reduced to 0.75- and 0.33-fold in shUBE2T(89) and shUBE2T(60) knockdown clones respectively. For MHCC-97L, the cell migration was reduced by half in both shUBE2T(89) and shUBE2T(60) while the cell invasion was reduced to 0.44- and 0.37-fold respectively in shUBE2T(89) and shUBE2T(60) (**Figure 4.6B**). On the contrary, UBE2T overexpression promoted migration and invasion of Huh7 cells, leading to approximately 1.5-fold increase in the number of migrated and invaded cells (**Figure 4.6C**).

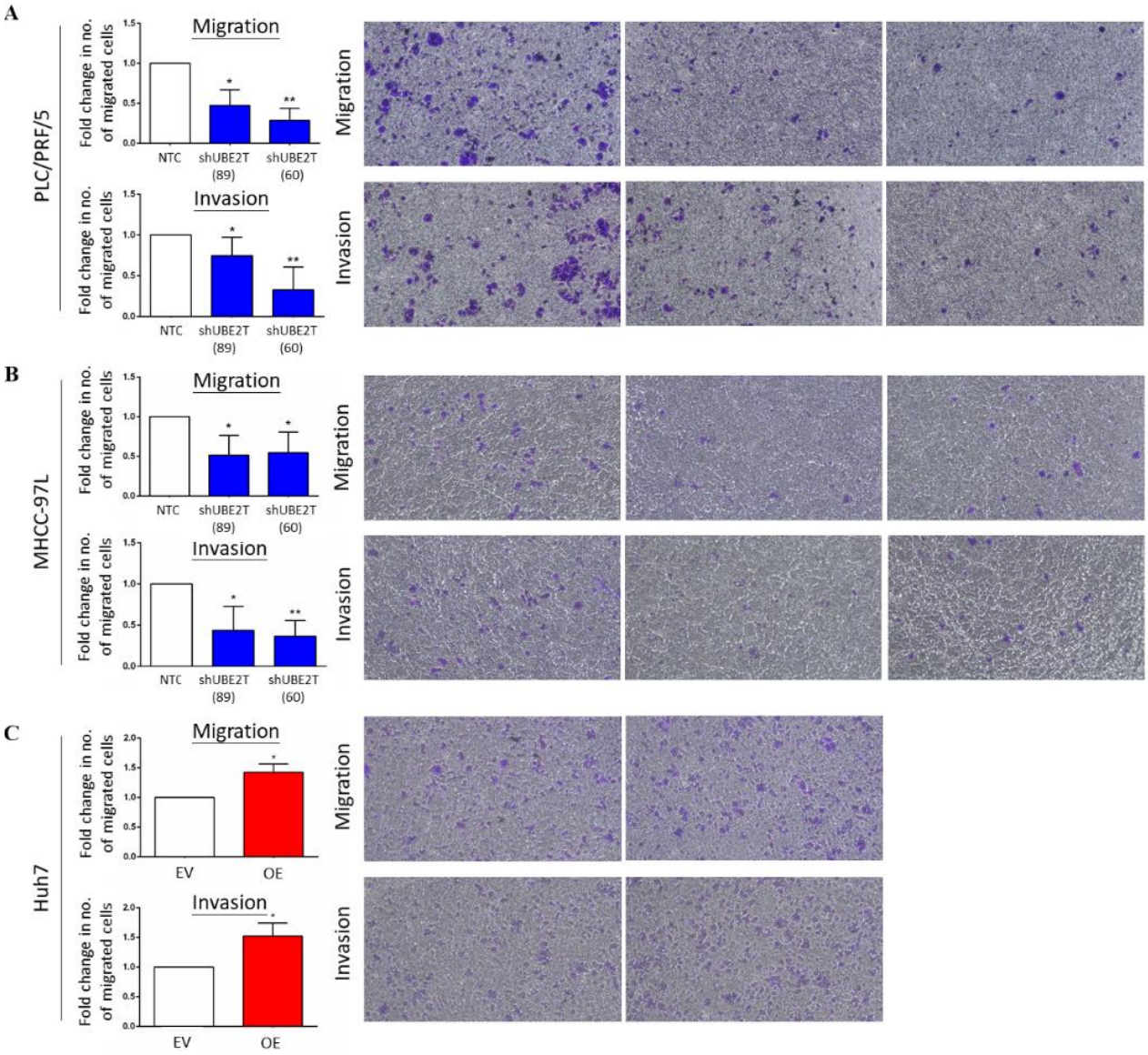

Figure 4.6. UBE2T enhanced migration and invasion of HCC cells. Migration and invasion of HCC cells were assessed upon UBE2T knockdown in (A) PLC/PRF/5 and (B) MHCC-97L and (C) UBE2T overexpression in Huh7. (*p<0.05, **p<0.01, *t* test).

4.3.6. UBE2T promoted *in vivo* tumorigenicity of HCC cells

The role of UBE2T in regulating liver CSC properties has been examined in various *in vitro* assays. Next, *in vivo* tumorigenicity assay was performed to study the effect of UBE2T alterations on the tumorigenicity of HCC cells. UBE2T knockdown and UBE2T overexpressing cells were subcutaneously injected to the flanks of NOD/SCID mice at different cell numbers to perform limiting dilution assay to determine the CSC frequency. In both PLC/PRF/5 and MHCC-97L, UBE2T knockdown resulted in decline in size and number of the tumors formed (**Figure 4.7A&B**). By calculating the tumor incidence rate, CSC frequency was estimated by Extreme Limiting Dilution Analysis (**Table 4.1**). shUBE2T(89) and shUBE2T(60) led to 5.13- and 7.81-fold decrease in stem cell frequency respectively in PLC/PRF/5. The effect of UBE2T was more dramatic in MHCC-97L, in which shUBE2T(89) and shUBE2T(60) significantly reduced the stem cell frequency by 13.71 and 14.45 folds respectively. Consistently, the tumorigenicity of Huh7 cells was elevated upon UBE2T overexpression (**Figure 4.7C**). The overexpression of UBE2T led to 5.6-fold increase in the stem cell frequency. It is noted that UBE2T overexpression remarkably enhanced the tumor size by approximately 3 folds when 10,000 UBE2T overexpressing Huh7 cells were inoculated into the NOD/SCID mice.

A PLC/PRF/5

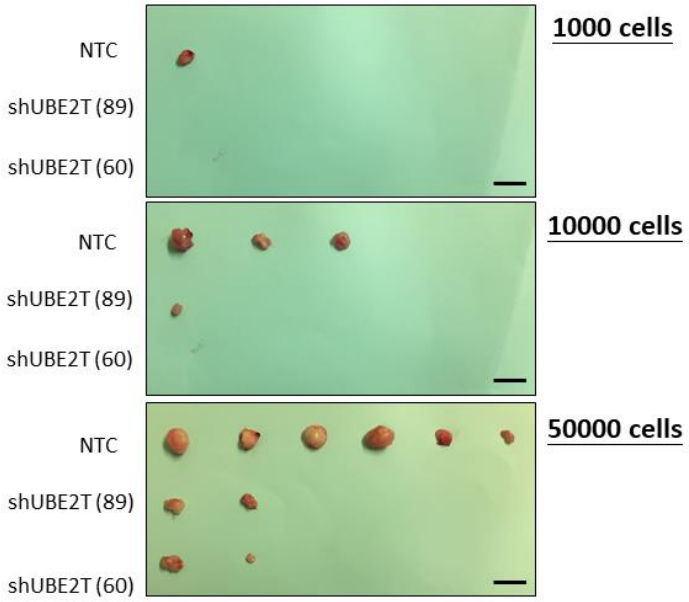

B MHCC-97L

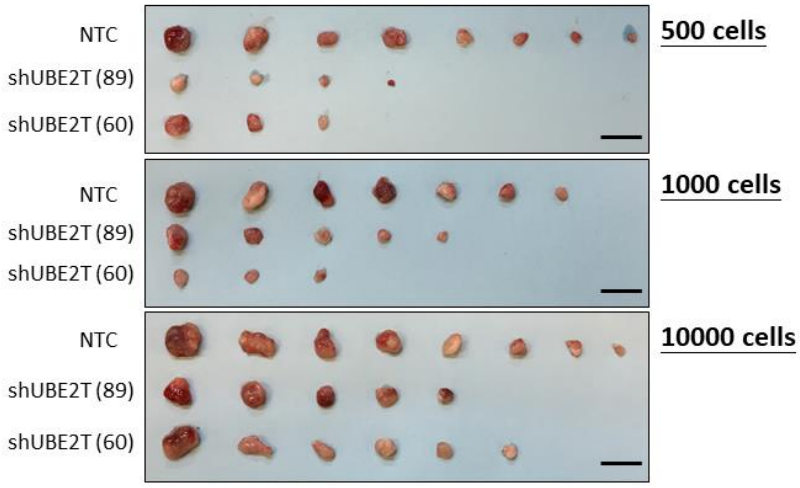

C Huh7

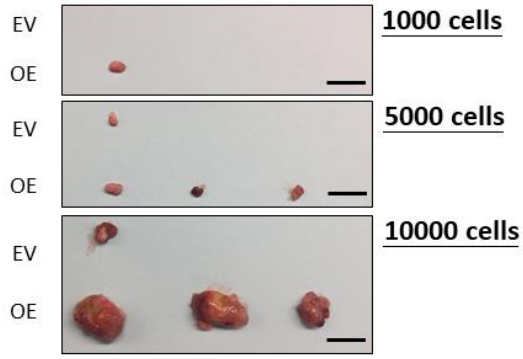

Figure 4.7. UBE2T promoted *in vivo* tumorigenicity of HCC cells. The effect of UBE2T on *in vivo* tumorigenicity of HCC cells was examined by subcutaneous inoculation of UBE2T knockdown (A) PLC/PRF/5 and (B) MHCC-97L and (C) UBE2T overexpressing Huh7 cells to the flanks of NOD/SCID mice. The sizes and numbers of the tumors formed were recorded. Tumor incidence rate was calculated for subsequent estimation of stem cell frequency by Extreme Limiting Dilution Analysis [134]. (Scale bar: 1 cm)

PLC/PRF/5	**Tumor incidence rate**			**Estimated CSC frequency**	**95% CI**	**P-value**
	1000 cells	10000 cells	50000 cells			
NTC	1/8	3/8	6/8	1/27903	1/56286-1/13834	
shUBE2T(89)	0/8	1/8	2/8	1/143347	1/450782-1/45584	0.0073**
shUBE2T(60)	0/8	0/8	2/8	1/218045	1/863707-1/55047	0.0021**
MHCC-97L	**Tumor incidence rate**			**Estimated CSC frequency**	**95% CI**	**P-value**
	500 cells	1000 cells	10000 cells			
NTC	8/8	7/8	8/8	1/279	1/556-1/140	
shUBE2T(89)	4/8	5/8	5/8	1/3825	1/7969-1/1836	<0.0001***
shUBE2T(60)	3/8	3/8	6/8	1/4032	1/8380-1/1940	<0.0001***
Huh7	**Tumor incidence rate**			**Estimated CSC frequency**	**95% CI**	**P-value**
	1000 cells	5000 cells	10000 cells			
EV	0/4	1/4	1/4	1/28065	1/113104-1/6964	
OE	1/4	3/4	3/4	1/5010	1/11509-1/2181	0.0195*

Table 4.1. UBE2T regulated CSC frequency and *in vivo* tumorigenicity. UBE2T knockdown PLC/PRF/5 and MHCC-97L cells and UBE2T overexpressing Huh7 cells were subcutaneously

injected to NON/SCID mice. Tumor incidence rate was calculated for estimation of stem cell frequency by Extreme Limiting Dilution Analysis [134]. (*p<0.05, **p<0.01, ***p<0.001)

4.3.7. Ablation of UBE2T inhibited metastasis of HCC cells

Lastly, apart from tumorigenicity, the effect of UBE2T on metastasis was also examined. *In vivo* orthotopic HCC xenograft model was employed to inoculate luciferase-tagged shUBE2T(60) and NTC cells derived from MHCC-97L into the left liver lobe of nude mice. Suppression of UBE2T significantly diminished the tumor formation ability of MHCC-97L cells (**Figure 4.8A**). Tremendous reduction in liver weight was observed in shUBE2T(60) cells (**Figure 4.8B**). To assess the effect of UBE2T knockdown on metastasis, the luciferase signal in lungs was measured. In line with the diminished tumorigenicity, significant reduction in luciferase signal was detected in shUBE2T(60), indicating that metastasis was significantly inhibited by the knockdown of UBE2T (**Figure 4.8C**).

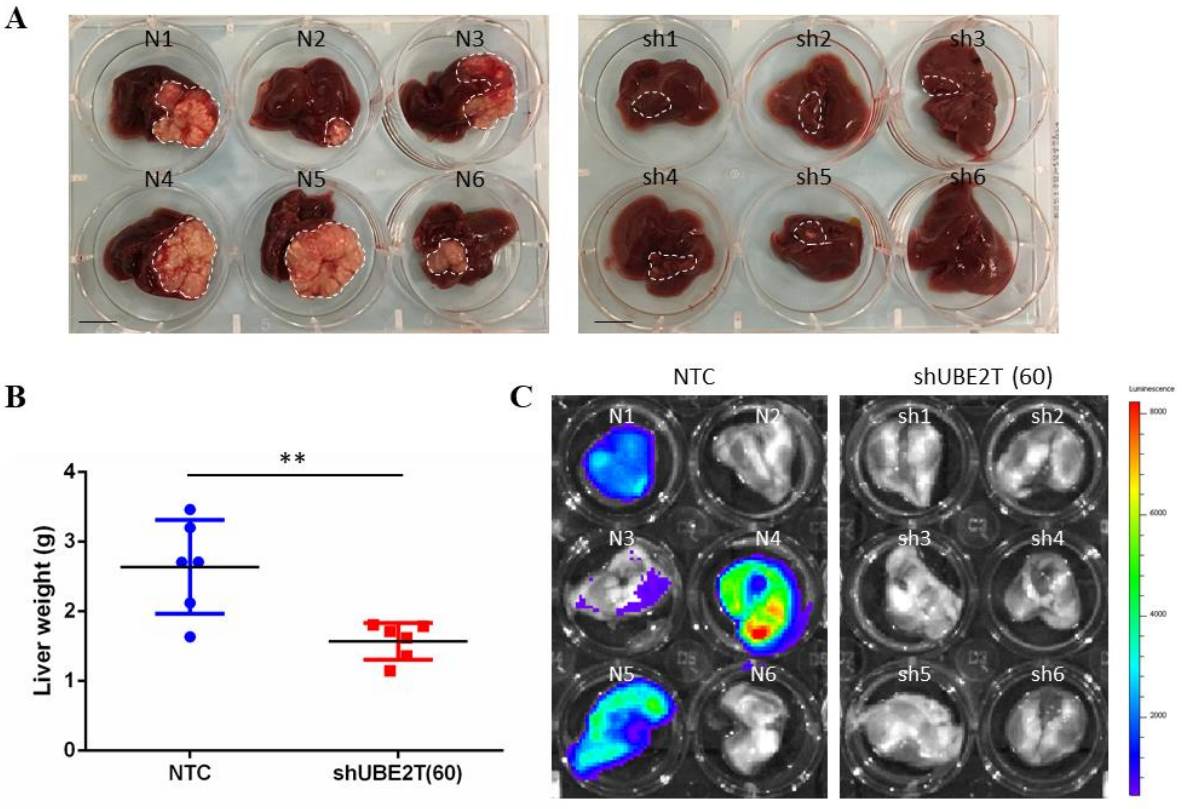

Figure 4.8. Knockdown of UBE2T inhibited metastasis of HCC cells. (A) Tumor formation was significantly reduced upon UBE2T knockdown in orthotopic xenograft model. (Scale bar: 1 cm) (B) UBE2T knockdown resulted in smaller liver weight compared to the control group, indicating the reduce in tumor formation. (C) Luciferase signal in lungs was measured to assess the metastasis. Significant decrease in luciferase signal in lungs showed the inhibition of UBE2T knockdown on metastasis. (**$p<0.01$, *t* test).

4.4. Discussion

The mechanism behind the contribution of CSCs to poor prognosis has been discussed in detail in Chapter 1.2. Briefly, CSCs, which are also termed tumor-initiating cells, are considered as the origin of cancers and the biggest contributor to drive tumorigenesis because of its pluripotency and high tumorigenicity. CSCs have been linked to EMT to support acquisition of mesenchymal features to give rise to metastasis. Besides, CSCs have efficient DNA repair system, leading to resistance to radio- and chemotherapy. Overexpression of UBE2T has been discovered in many cancers and is associated with poor clinical outcomes in the patients. However, only limited studies investigate the mechanism of UBE2T in tumorigenesis. The role of UBE2T in regulating CSCs has not been discussed in any reports yet. In this chapter, the functional role of UBE2T in regulating liver CSCs has been analyzed through a series of functional assays specific for CSCs.

The effect of UBE2T on self-renewability of HCC cells was first examined by tumor spheroid formation assay. As discussed in Section 1.2.3, spheroid formation assay is one of the widely used assays to identify and isolate CSCs. In spheroid formation assay, only the cells harboring self-renewal property can grow in the serum-free anchorage-independent culture medium. CSCs are enriched in the floating spheroids formed, which display enhanced CSC marker expression [150], [151]. Our study showed direct evidence that the expression level of UBE2T is associated with the abundance of CSCs in HCC, affecting the spheroid formation ability of the cancer cells.

Next, we assessed the expression of CSC markers in HCC cells after manipulation of UBE2T expression level. The expressions of CD47 and CD90 were investigated in our study. CD47 has been reported as CSC marker in various cancers such as lung cancer and HCC, and is associated

with poor prognosis of the cancer patients [152]–[155]. In our previous study, we reported the overexpression of CD47 in HCC and demonstrated it correlation with CSC properties [154]. Clinical trials of immunotherapy utilizing CD47-targeting antibody are ongoing (NCT02216409, NCT02367196). CD90 has also emerged as CSC marker in various cancers[156]–[159]. Multiple studies have reported the promotion of CD90 on migration and invasion of cancer cells [156], [157], [160]. Knockdown of UBE2T significantly reduced the expression of CD47 and CD90 of HCC cells while the overexpression of UBE2T enhanced the expression of the two markers. This indicates the direct effect of UBE2T on the liver CSC populations and gives a clue for the promotion of UBE2T on tumor invasiveness because of the link of CD90 and tumor migration.

Due to the critical role of UBE2T in FA DNA repair pathway and the correlation of drug resistance to CSCs, the drug sensitivity of HCC cells was assessed upon UBE2T knockdown and overexpression. Doxorubicin gives rise to apoptosis by inducing DNA damages through DNA intercalation and generation of free radicals [161]. Doxorubicin is commonly used in conventional chemotherapy and is frequently coupled with TACE for treatment of mediate-stage HCC. Cancers with FA deficiency are more sensitive to doxorubicin treatment because of the impaired DNA damage response [162]. However, so far there is no reports examining the direct correlation of UBE2T and drug resistance. Our study demonstrates the involvement of UBE2T in enhancement of chemoresistance.

As mentioned above, CSCs are associated with EMT to promote tumor migration and invasion. In nasopharyngeal carcinoma, UBE2T promotes metastasis by activation of AKT/GSK3β/β-catenin pathway [132]. Reduced UBE2T expression in prostate cancer and gastric cancer exhibits

decreased mesenchymal and elevated epithelial features and impairs cancer cell migration and invasion [127], [129]. Downregulation of UBE2T inhibits the cell migration of osteosarcoma vis PI3K/Akt signaling pathway [131]. Taken together, these studies provide convincing evidence for the critical role of UBE2T in metastasis.

Apart from *in vitro* functional assays, *in vivo* tumorigenicity assay was performed to investigate the effect of UBE2T on tumorigenicity as well as stem cell frequency. The stem cell frequency was estimated by Extreme Limiting Dilution Analysis [134]. Limiting dilution assay is widely used for determination of CSC frequency [151], [163]. The contribution of UBE2T in tumorigenicity has been reported in various cancers. In prostate cancer, the upregulation of UBE2T results in increase in size and number of the tumors formed [129]. Downregulation of UBE2T suppresses the tumor formation in gastric cancer [127]. Our study is in line with the previous findings. Knockdown of UBE2T impaired tumorigenicity while overexpression of UBE2T promoted tumor formation. Furthermore, to the best of our knowledge, this is the first report demonstrating the effect of UBE2T on CSC frequency by estimation of stem cell frequency via Extreme Limiting Dilution Analysis.

Orthotopic xenograft model was also performed to study the role of UBE2T on tumorigenicity and metastasis *in vivo*. Orthotopic xenograft model presents two substantial advantages over the conventional subcutaneous xenograft implantation. The first advantage is that orthotopic xenograft model allows tumor growth in relevant organ site to mimic the actual tumor microenvironment in human [164]. The second advantage is that the study of metastasis is available in orthotopic xenograft model [165]. In our study, we demonstrated that knockdown of UBE2T remarkably

impairs the tumor formation in livers and significantly diminished the metastasis to lungs. UBE2T has been reported to promote metastasis via tail vein injection in nasopharyngeal carcinoma [132]. However, the tail vein injection model may not reflect the actual metastatic situation because of the absence of primary tumor, which limits the study on tumor progression from primary tumor to metastasis [166]. Our study provides compelling evidence for the role of UBE2T on metastasis in HCC.

In summary, in this chapter, the effect of UBE2T on various CSC properties were demonstrated. UBE2T showed direct regulation on the CSC populations by promoting self-renewability and CSC marker expression. Extreme limited dilution analysis reveals the upregulation of CSC frequency and tumorigenicity caused by UBE2T overexpression as well. It is widely accepted that CSCs enhance metastasis and development of chemoresistance. Our studies showed that UBE2T promoted tumor invasiveness and chemoresistance to doxorubicin, demonstrating its role on regulation of the CSC features.

Chapter 5

Molecular Mechanism of How UBE2T Regulates Liver CSCs

5.1. Introduction

In Chapter 4, we have investigated the functional role of UBE2T in regulating cancer stemness in HCC. By altering UBE2T expression in HCC cells, CSC properties, including self-renewability, expression of CSC marker, chemoresistance, tumorigenicity, tumor invasiveness and metastasis, of HCC cells have been significantly affected. However, the underlying mechanism for the UBE2T-mediated regulation on liver cancer stemness remains mysterious.

The enhancing effect of UBE2T on cell proliferation has been widely reported in many cancers [125]–[127], [129], [131], [132]. Nevertheless, to the best of my knowledge, only a few studies have revealed the underlying mechanism for the role of UBE2T on tumorigenesis. In 2016, overexpression of UBE2T was found in nasopharyngeal carcinoma and was responsible for the upregulation of cell invasion and proliferation [132]. In view of the significant enhancement in cell proliferation caused by the UBE2T upregulation, UBE2T overexpression was linked to the Akt/GSK3β/β-catenin signaling, which acts as key regulator in cell proliferation, survival and metastasis. [132]. In the same year, the mechanism for the regulation of UBE2T in cell proliferation was investigated in osteosarcoma [131]. Consistently, knockdown of UBE2T inactivated the PI3K/Akt signaling by reducing the phosphorylation of PI3K and Akt [131]. PI3K/Akt signaling is one of the important signaling cascades that maintain pluripotency and CSCs [82], [167]. The association of UBE2T to the PI3K/Akt signaling shed some light on the undefined mechanism for the promotion of cancer stemness by UBE2T. Nevertheless, the molecular mechanism of how UBE2T regulates tumor behavior remains largely unknown.

UBE2T mediates monoubiquitination of FANCL and FANCI in FA DNA damage repair pathway.

At the same time, UBE2T was found to regulate protein expression of BRCA1 and p53 via ubiquitination [124], [125]. Based on the finding of these studies, UBE2T exerts its physiological and functional roles through protein-protein interaction. In order to understand the molecular mechanism of how UBE2T regulates CSC properties and tumor behavior, it is crucial to identify its direct interacting partner.

In short, although UBE2T was previously found to be associated with PI3K/Akt signaling and is responsible for the degradation of tumor suppressor p53, the underlying mechanism is not fully understood, especially in the respect of regulation of CSCs. In this chapter, we aimed to dissect the mechanism for the regulation of UBE2T on CSC properties by identifying a direct protein interacting partner of UBE2T. In addition, the downstream signaling pathway involved in UBE2T mediated CSC function was also elucidated.

5.2. Experimental Scheme

In this chapter, the potential protein partner of UBE2T was identified by tandem affinity purification coupled with mass spectrometry (TAP/MS). The interaction was validated by Co-IP and the effect of UBE2T on the protein partner was examined. The experimental outline is summarized in the following diagram. The methods used in this chapter are mentioned in Chapter 2: Materials and Methods in further detail.

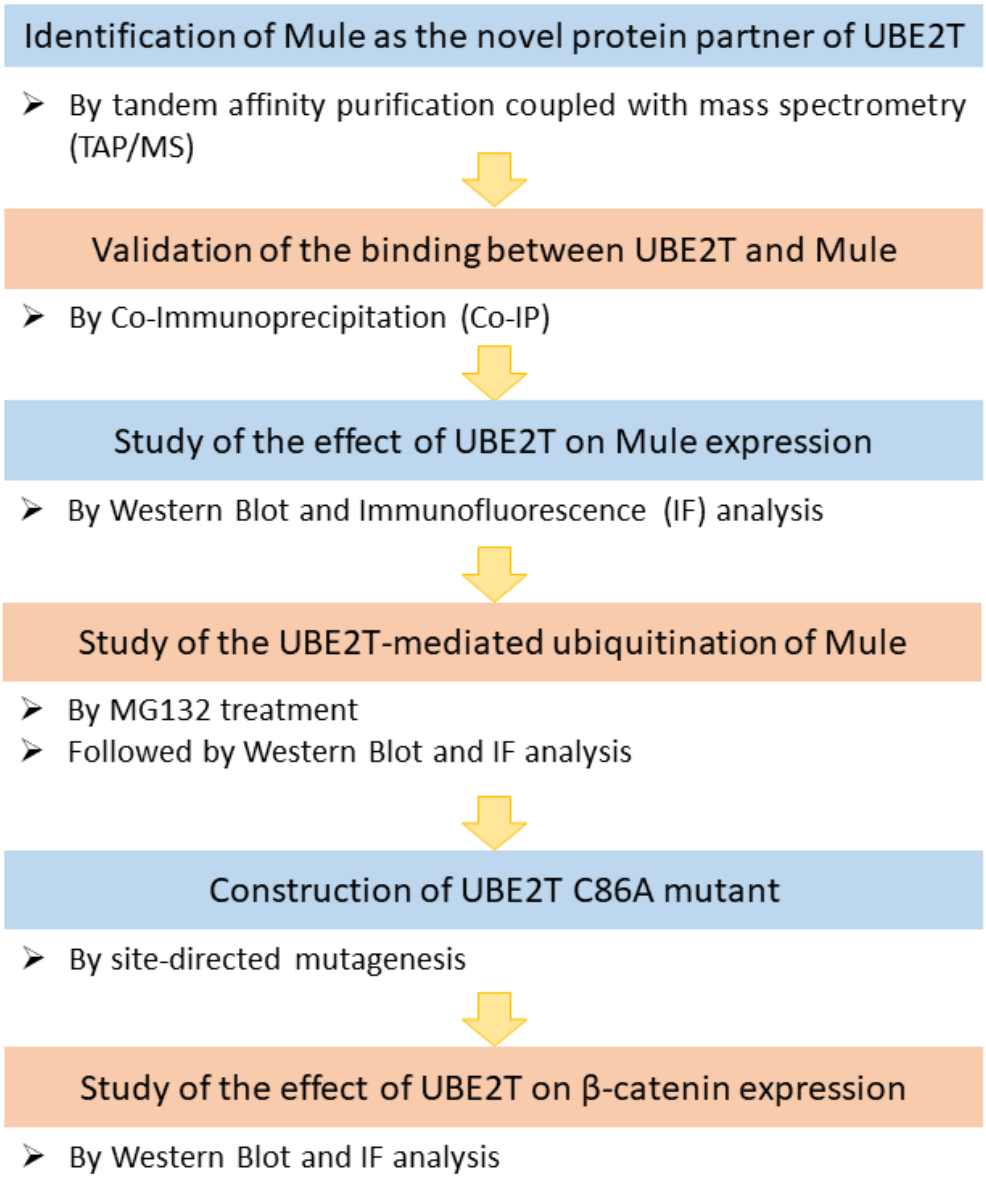

Figure 5.1. Experimental scheme of identification of novel protein partner of UBE2T.

5.3. Results

5.3.1. Establishment of SFB-UBE2T clone for TAP/MS analysis

TAP/MS analysis was employed to identify novel binding target of UBE2T for regulation of cancer stemness in HCC (**Figure 5.2**). In order to facilitate the purification, UBE2T ORF was fused with SFB tag to generate SFB-UBE2T construct. Briefly, the vector for expression of SFB-UBE2T was generated using Gateway system. The SFB-UBE2T construct was transfected into 293T cells and the stable single clone expressing the highest protein level of SFB-UBE2T was selected for the subsequent expansion. Western Blot analysis shows that all the stable single clones had similar expression level of the endogenous UBE2T while stable single clone #4 displayed the highest protein level of SFB-UBE2T whose protein size is approximately 40 kDa (**Figure 5.3**). After expansion, the 293T cells of clone #4 was harvested. Tandem affiniity purification was performed and the eluate containing the SFB-UBE2T and its protein partners was subjected to mass spectromety analysis at Taplin Mass Spectrometry Facility in Harvard Medical School.

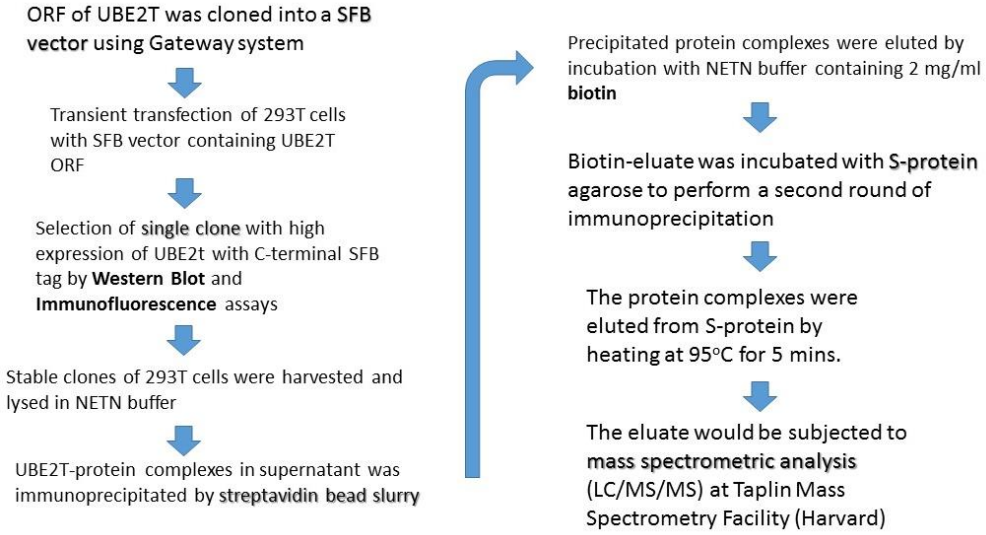

Figure 5.2. Flow chart of TAP/MS for identification of potential protein partners of UBE2T. In order to identify the potential protein partners of UBE2T, SFB-UBE2T construct was generated

by Gateway system. After selection of stable single clone expressing the highest level of SFB-UBE2T in 293T cells, the SFB-UBE2T was harvested and purified by tandem affinity purification. The purified proteins were subjected to mass spectrometry analysis at Taplin Mass Spectrometry Facility in Harvard Medical School for identification.

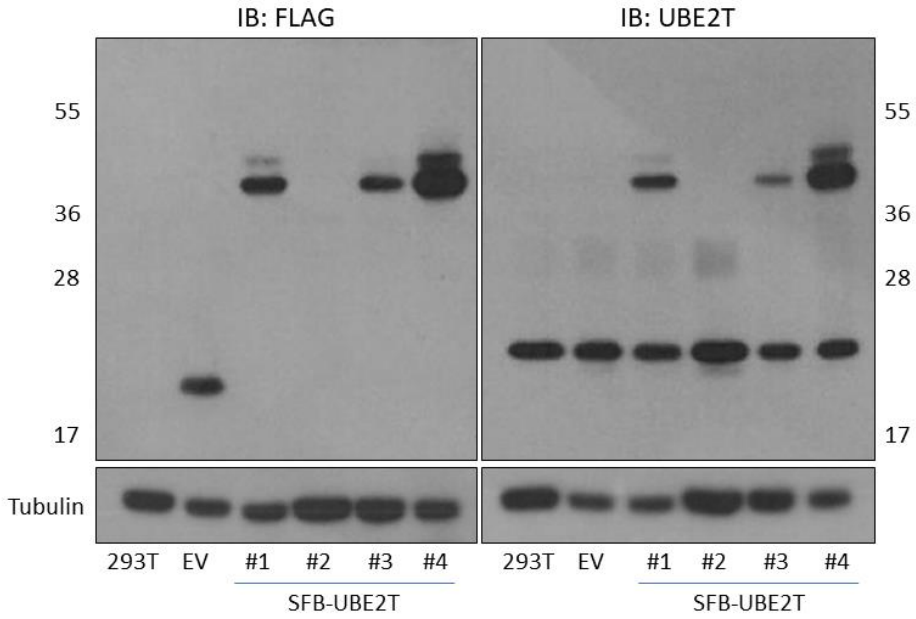

Figure 5.3. Selection of stable single clone expressing the highest protein level of SFB-UBE2T. Western Blot analysis was performed to select the stable single clone expressing the highest protein level of SFB-UBE2T for the subsequent expansion and purification. The expression was compared by detecting the FLAG (left) and the UBE2T (right). Stable single clone #4 showed the highest protein level of SFB-UBE2T was selected and subjected to TAP/MS.

5.3.2. Identification of Mule as the novel E3 binding partner of UBE2T

The mass spectrometry analysis revealed a list of potential binding target of UBE2T. Some of the potential partner candidates of UBE2T were shortlisted in **Table 5.1** according to their functions. Since E2 ubiquitin conjugating enzyme can bind to a range of E3 ligases for ubiquitination of substrate, it is believed that UBE2T may bind to E3 ligases for its function on regulating cancer stemness. Therefore, we focused on E3 ligases in the list of mass spectrometry results. Interestingly, Mcl-1 ubiquitin ligase E3 (Mule) is the only E3 ligase shown up in the list.

Mule is an enormous protein size of about 480 kDa, with 3 unique peptide sequences that have been recognized in the mass spectrometry analysis (**Figure 5.4**).

The direct interaction between UBE2T and Mule was validated by Co-IP. SFB-UBE2T was transfected into 293T cells and Huh7 cells and the SFB-UBE2T was pulled down by streptavidin. Mule was pulled down together with the SFB-UBE2T in both the 293T and Huh7 cells (**Figure 5.5A&B**). The above data demonstrated the binding between the exogenous SFB-UBE2T and the endogenous Mule. The UBE2T/Mule interaction was further investigated by Co-IP of the endogenous proteins in HCC cell line. The endogenous UBE2T and Mule were immunoprecipitated with anti-UBE2T and anti-Mule antibody respectively in MHCC-97L. Mule was pulled down in the immunoprecipitation of UBE2T while UBE2T was pulled down in the immunoprecipitation of Mule (**Figure 5.5C**). The reciprocal co-immunoprecipitation provides compelling evidence for the UBE2T/Mule interaction.

Unique	Total	Gene	MW (kDa)	Function
16	17	PARP1	113.01	Regulator of DNA repair and apoptosis
9	9	FASN	273.25	Fatty acid synthesis
9	14	OTUB1	31.26	Deubiquitinating enzyme
8	10	MAPK1	41.36	MAPK family member
8	8	USP7	128.22	Deubiquitinating enzyme
7	7	USP15	112.35	Deubiquitinating enzyme
7	7	USP11	109.75	Deubiquitinating enzyme
5	6	MAPK14	41.27	MAPK family member
3	4	MAPK3	43.11	MAPK family member
3	3	HUWE1	481.59	E3 ligase
2	2	CDK4	33.71	Cell cycle checkpoint protein
2	2	UBE2L3	17.85	E2 enzyme

Table 5.1. List of interacting partner candidates of UBE2T. TAP/MS analysis produced a list of interacting partner candidates of UBE2T. After literature review on functions of the

candidates, potential interacting partners of UBE2T were summarized in table. (Unique = number of unique peptides detected; Total = total number of peptides detected; MW = molecular weight)

Unique	Total	Gene Symbol	MWT(kDa)	AVG
3	3	HUWE1	481.59	2.7812

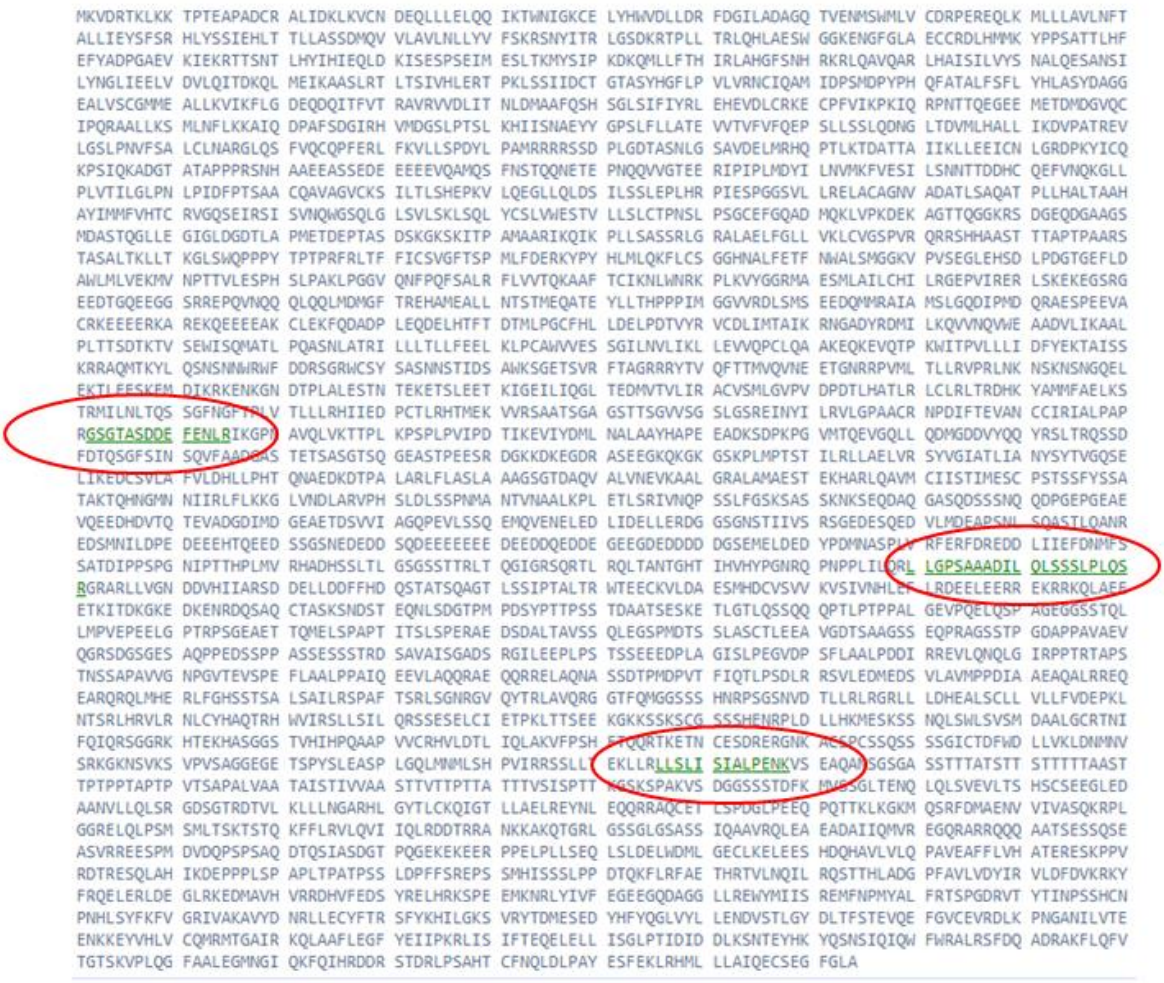

Figure 5.4. Mule was identified as the sole E3 ligase upon mass spectrometry analysis. After mass spectrometry analysis, E3 ligases were screened in the list of potential protein partners of UBE2T because of the high affinity of E2 enzyme for the E3 ligase and their biological role in ubiquitination. Mule was identified as the sole E3 ligase which may potentially bind to UBE2T in the mass spectrometry results. 3 unique peptide sequences of Mule (circled in red) were identified upon mass spectrometry analysis.

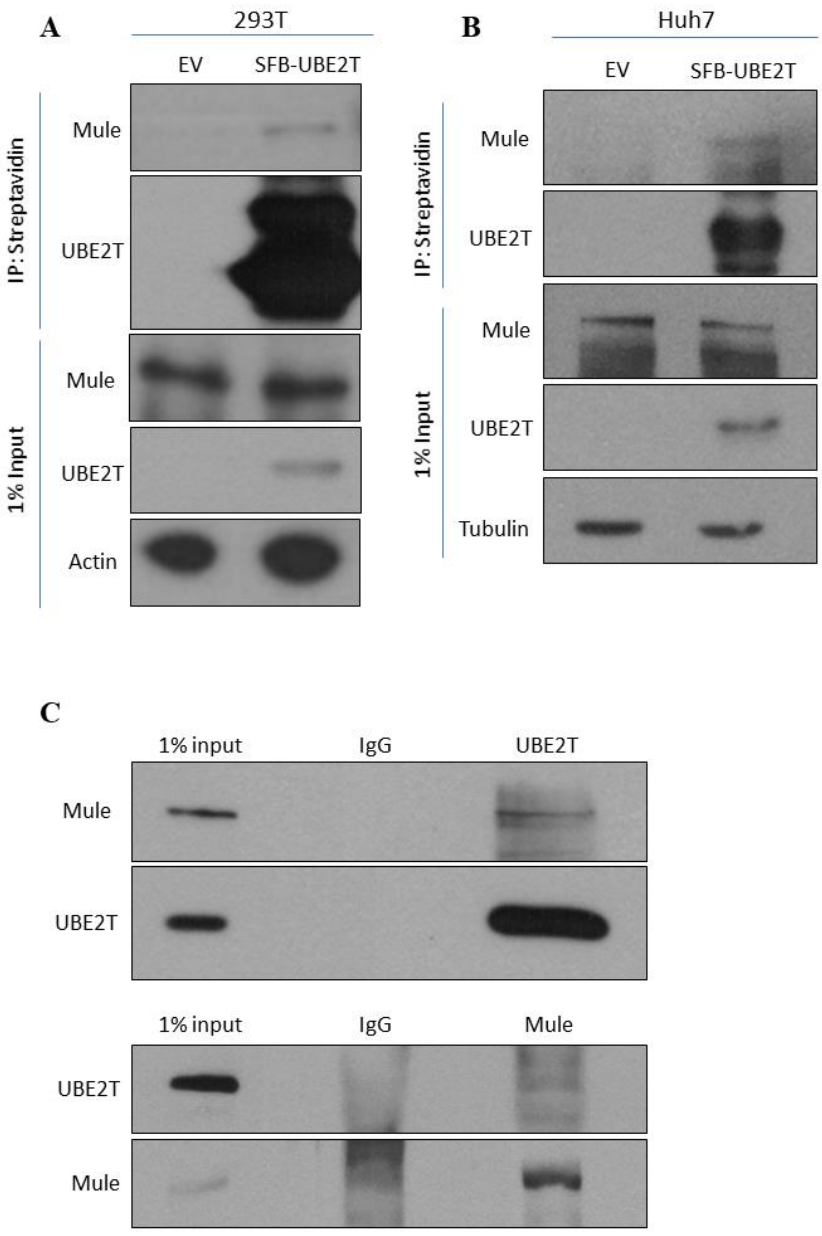

Figure 5.5. Direct interaction of UBE2T and Mule was demonstrated by Co-IP. The interaction between SFB-UBE2T and Mule was demonstrated by Co-IP in (A) 293T and (B) Huh7. Mule was detected after the pull-down of SFB-UBE2T. (C) Reciprocal Co-IP demonstrated the direction interaction between endogenous UBE2T and Mule in MHCC-97L cells.

5.3.3. UBE2T suppressed Mule expression in HCC cell lines

After demonstrating the direct interaction between UBE2T and Mule, their relationship was

investigated. Since E2 and E3 enzymes bind together to transfer activated ubiquitin from the E2 ubiquitin conjugating enzyme to substrate for ubiquitination, it is expected that the expression of Mule would be altered when UBE2T expression is modified in HCC cells. Consistent to the role of UBE2T as E2 enzyme , we found that the protein level of E3 enzyme Mule was elevated in the UBE2T knockdown PLC/PRF/5 and MHCC97L cells (**Figure 5.6A&B**). On the contrary, overexpression of UBE2T in Huh7 led to the downregulation of Mule expression (**Figure 5.6C**). The reciprocal expression patterns of UBE2T and Mule reveals the suppressive effect of UBE2T on Mule expression.

It is thought that UBE2T may suppress the expression of Mule via proteasomal degradation. Therefore, the UBE2T overexpressing Huh7 cells were subjected to MG132 treatment to inhibit the proteasomal degradation in the cells. Western Blot analysis showed that the MG132 treatment has reversed the reduction in Mule expression in the UBE2T overexpressing cells (**Figure 5.7**). At the same time, IF assay was performed to examine the expression and localization of UBE2T and Mule (**Figure 5.8**). It was found that Myc-DDK-UBE2T was mainly located in nucleus and cytoplasm while Mule was mainly located in the cytoplasm. The overexpression of UBE2T significantly reduced the expression of Mule in Huh7 cells. The MG132 treatment remarkably restored the Mule expression, confirming that UBE2T promoted proteasomal degradation of Mule.

To further demonstrate the direct role of UBE2T on the Mule degradation, UBE2T C86A mutant clone was generated. The cysteine residue C86 located at the active site of UBE2T was substituted with alanine so the E2 activity of Myc-DDK tagged UBE2T was abolished (**Figure 5.9**). The UBE2T OE gave Myc-DDK-tagged wild-type UBE2T and its monoubiquitin-conjugated form at

protein size of about 35 kDa and 45 kDa respectively. However, UBE2T C86A gave only the Myc-DDK-tagged UBE2T mutant protein without monoubiquitination at protein size of about 35 kDa.

The protein levels of Mule in the wild-type UBE2T and UBE2T mutant overexpressing Huh7 cells were compared by Western Blot analysis (**Figure 5.10A**). It was found that Mule was downregulated upon the overexpression of the wild-type UBE2T. The protein expression of Mule was at a comparable level in the control and the UBE2T mutant expressing Huh7 cells. This indicated that the proteasomal degradation of Mule is mediated by the E2 activity of UBE2T. The finding was further supported by the IF assay (**Figure 5.10B**). In the control, most of the cells expressed Mule in the cytoplasm with absence of expression of FLAG (DDK). The wild-type UBE2T overexpressing cells displayed reduction in the Mule expression, which was significantly restored by the UBE2T C86A mutation. The above data demonstrates that UBE2T directly mediates the proteasomal degradation of Mule.

Next, we investigate whether UBE2T promotes the degradation of Mule by ubiquitination. After transfecting the Huh7 cells with HA tagged ubiquitin together with control vector, UBE2T ORF or UBE2T C86A mutant, the cells were subjected to MG132 treatment to stop the proteasomal degradation. Therefore, the ubiquitinated proteins accumulated in the cells to enrich the abundance of the ubiquitinated Mule. Mule was immunoprecipitated with anti-Mule antibody for subsequent analysis of the expression of ubiquitinated Mule which was detected by anti-HA body. It was found that ubiquitinated Mule was significantly enhanced in the wild-type UBE2T overexpressing cells (**Figure 5.11**). The C86A mutation suppressed the ubiquitination of Mule to a comparable level as that in the control. This indicates that the E2 activity of UBE2T has a critical role in the

ubiquitination of Mule.

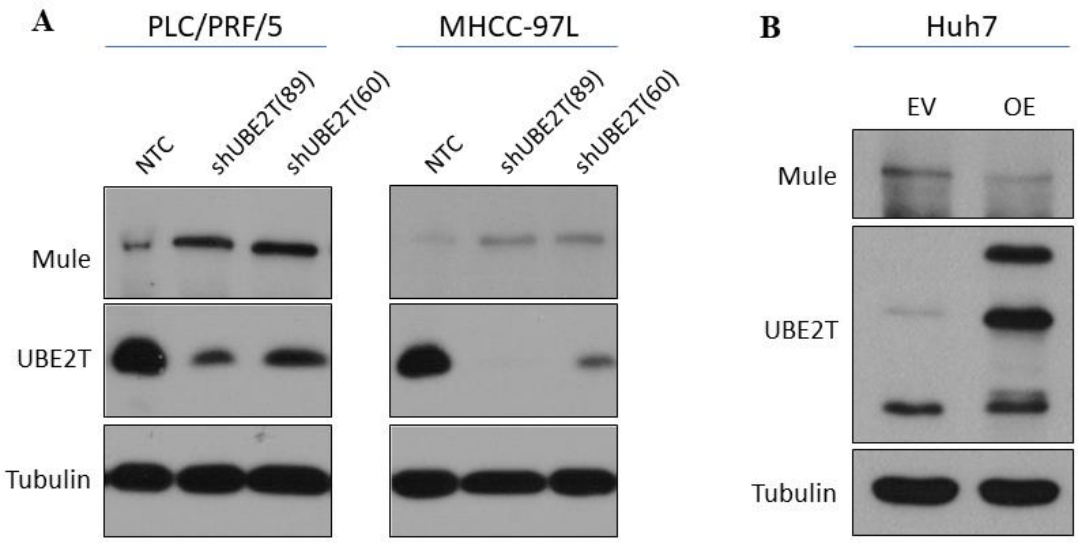

Figure 5.6. Western Blot analysis revealed the suppressive effect of UBE2T on Mule expression. Mule protein levels were upregulated upon UBE2T knockdown in (A) PLC/PRF/5 and (B) MHCC-97L. (C) UBE2T overexpression resulted in downregulation of Mule in Huh7.

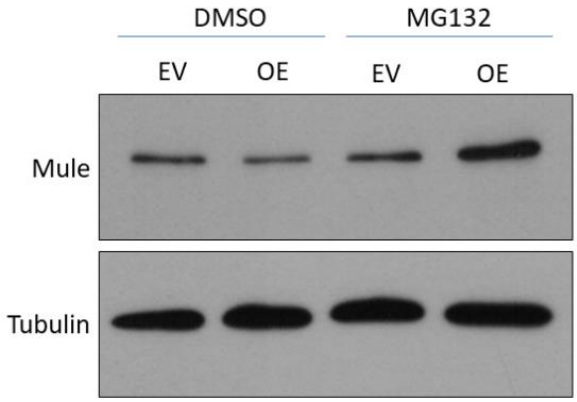

Figure 5.7. Proteasome inhibitor MG132 rescued the downregulation of Mule caused by UBE2T overexpression. UBE2T overexpressing Huh7 cells were subjected to MG132 treatment. Western Blot analysis showed that the proteasome inhibitor MG132 rescued the downregulation of Mule in the UBE2T overexpressing cells.

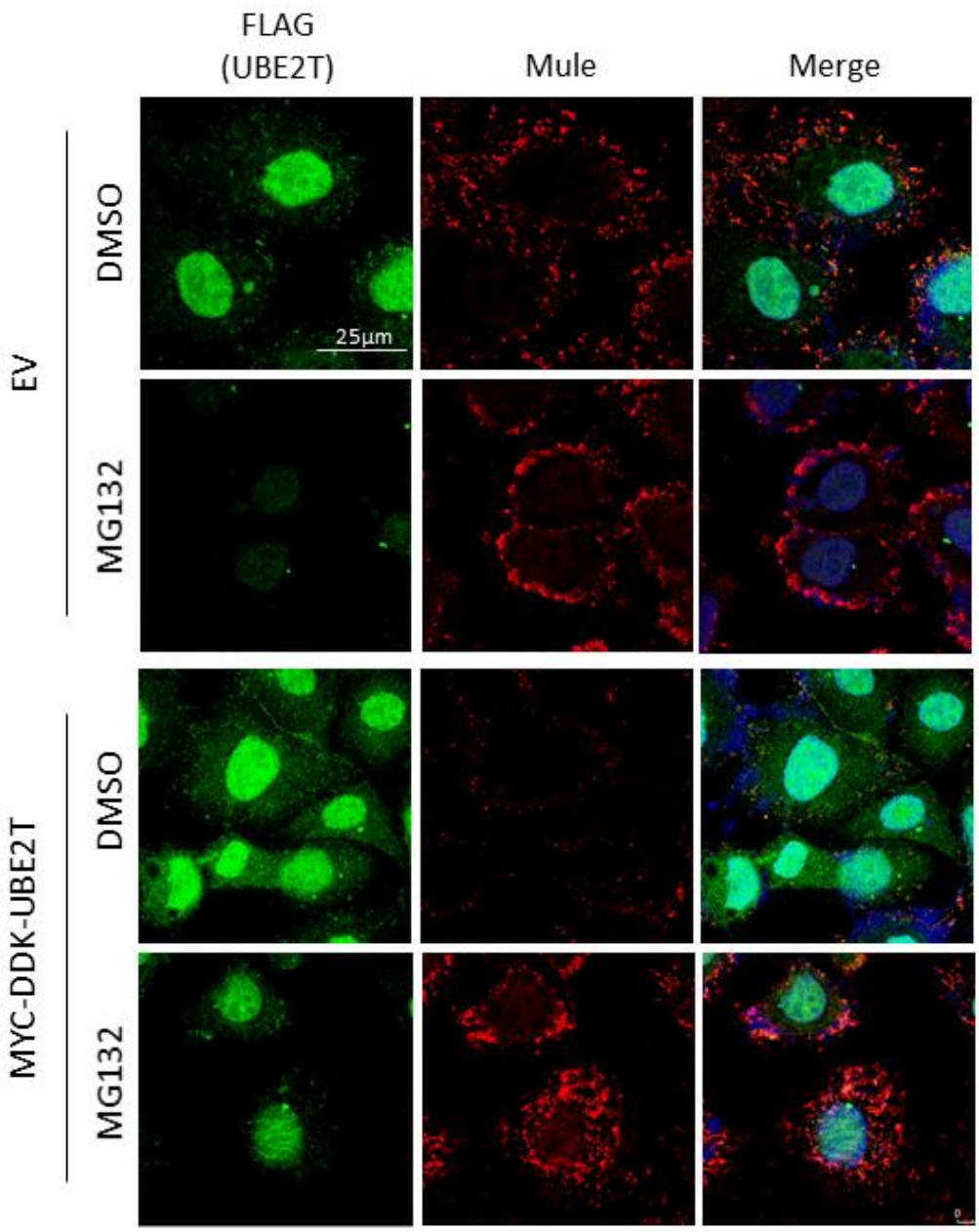

Figure 5.8. UBE2T regulated the expression of Mule via proteasomal degradation. IF analysis showed reduced Mule expression in the UBE2T overexpressing cells. The MG132 treatment enhanced the abundance of Mule in both the cytoplasm and nucleus, indicating that UBE2T regulates Mule by proteasomal degradation. (Scale bar: 25 µm)

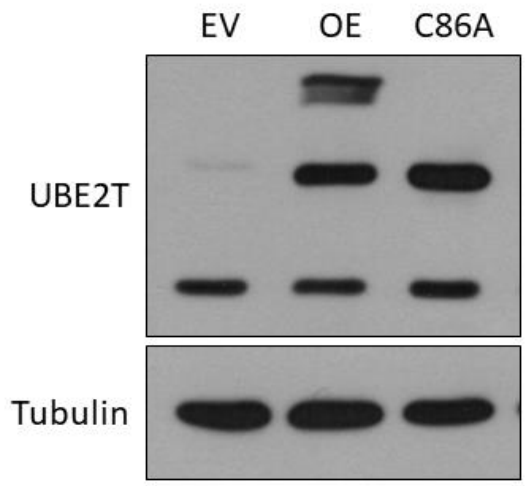

Figure 5.9. Establishment of UBE2T C86A mutant clone. In order to investigate whether UBE2T regulates the degradation of Mule by the E2 activity, cysteine residue C86 located at the active site of UBE2T was substituted by alanine by site-directed mutagenesis in the Myc-DDK-UBE2T construct to impair the ability of UBE2T to accept the ubiquitin from E1. Therefore, the C86A mutated Myc-DDK-UBE2T was unable to be monoubiquitinated.

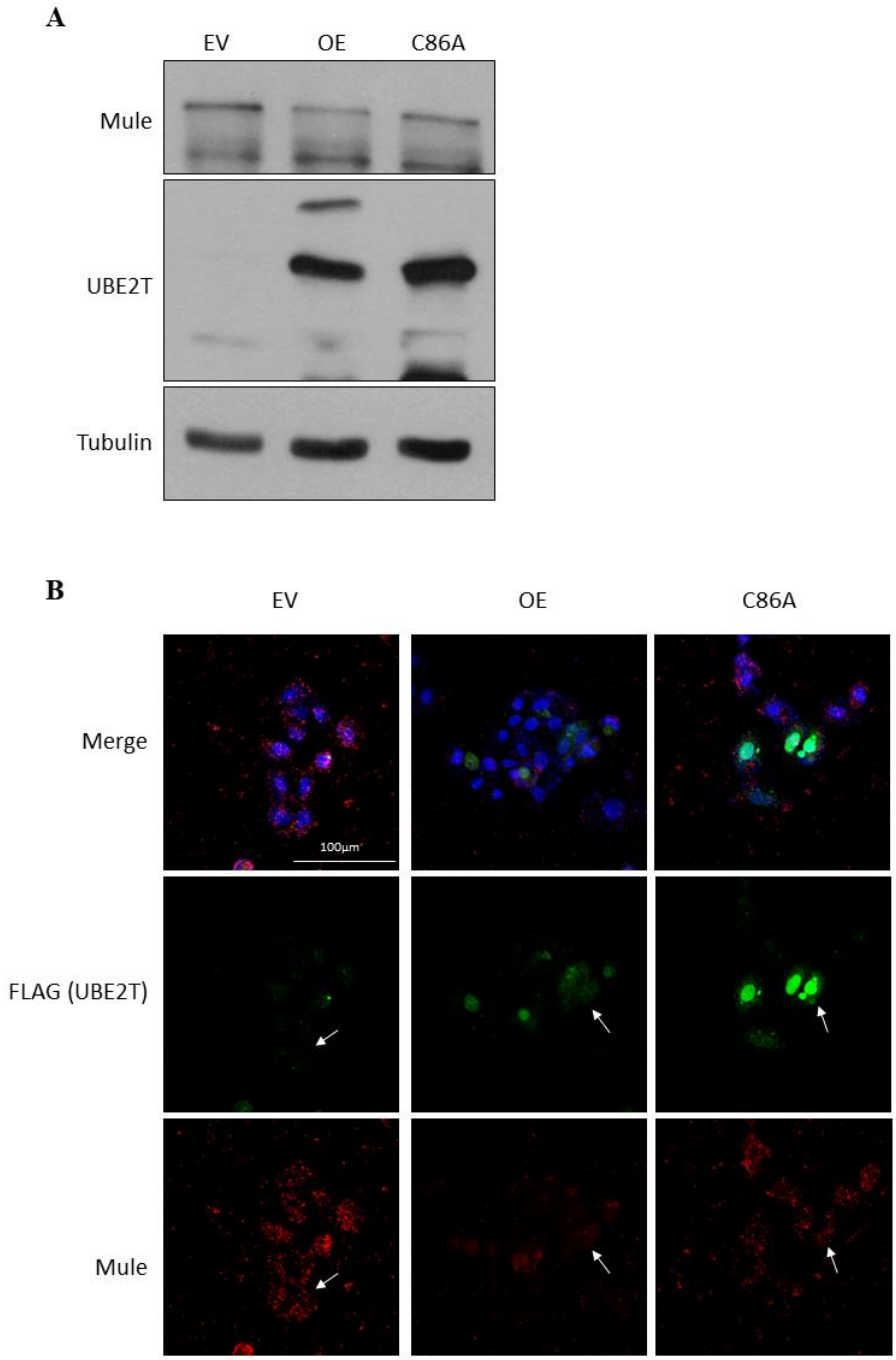

Figure 5.10. UBE2T C86A mutant reversed the reduction in Mule expression caused by UBE2T overexpression. (A) Impaired E2 activity of UBE2T reduced the degradation of Mule. (B) The C86A mutation rescued the suppression on Mule expression in the UBE2T overexpressing Huh7 cells in IF staining. (Scale bar: 100 μm)

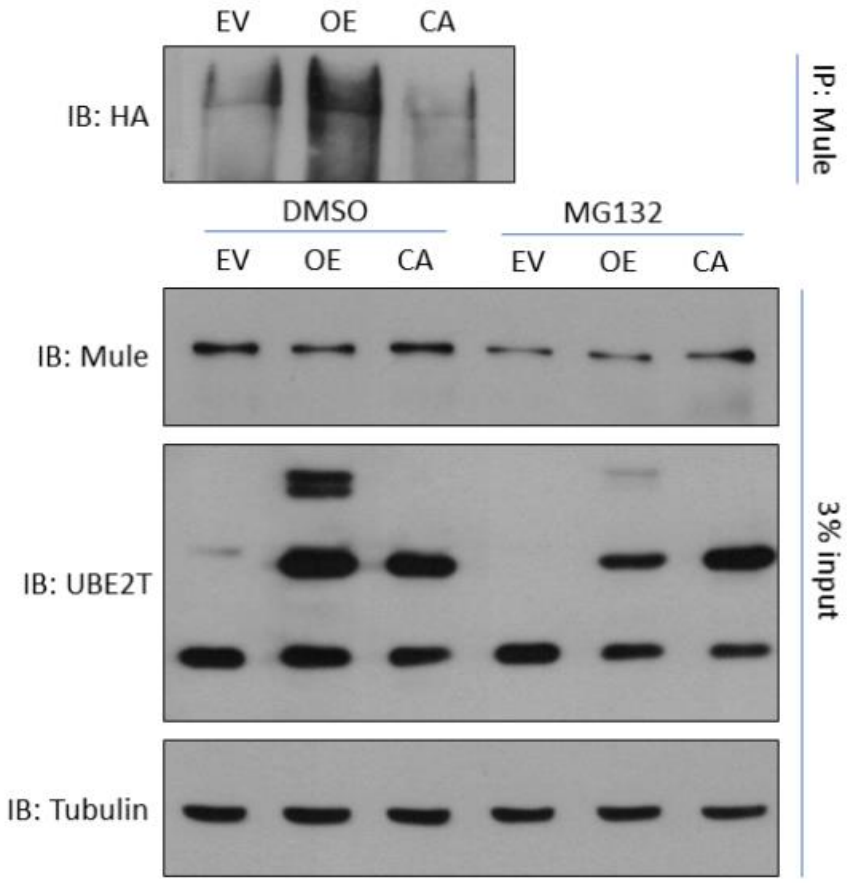

Figure 5.11. UBE2T promoted degradation of Mule by ubiquitination. HA-ubiquitin together with wild-type Myc-DDK-UBE2T, the C86A mutant or the control vector were co-transfected into Huh7 cells. After treatment of 20 μM MG132 for 7 hours, Mule was pulled down for investigation of the effect of UBE2T on the abundance of ubiquitinated Mule. Overexpression of wild-type UBE2T promoted the ubiquitination of Mule while the C86A mutation suppressed the ubiquitination significantly.

5.3.4. UBE2T regulated β-catenin via proteasomal degradation of Mule

Mule has been previously reported to bind and degrade β-catenin [168]. The Mule-mediated degradation of β-catenin was validated by knockdown of Mule in MHCC-97L. The knockdown of Mule resulted in remarkable elevation in β-catenin expression, showing that Mule suppressed the β-catenin in HCC cells (**Figure 5.12**).

The effect of UBE2T on β-catenin was first examined by Western Blot analysis. UBE2T knockdown gave rise to downregulation of β-catenin together with the upregulation of Mule in PLC/PRF/5 and MHCC-97L (**Figure 5.13A&B**). In concordance, the overexpression of UBE2T in Huh7 enhanced the β-catenin while inhibiting the expression of Mule (**Figure 5.13C**). UBE2T C86A mutation suppressed the increase in β-catenin expression in the UBE2T overexpressing cells. This suggests that the elevated β-catenin expression is probably resulted from the UBE2T mediated degradation of Mule since the impaired E2 activity caused by the UBE2T mutation can diminish the ubiquitination of Mule, giving rise to the accumulation of the E3 ligase.

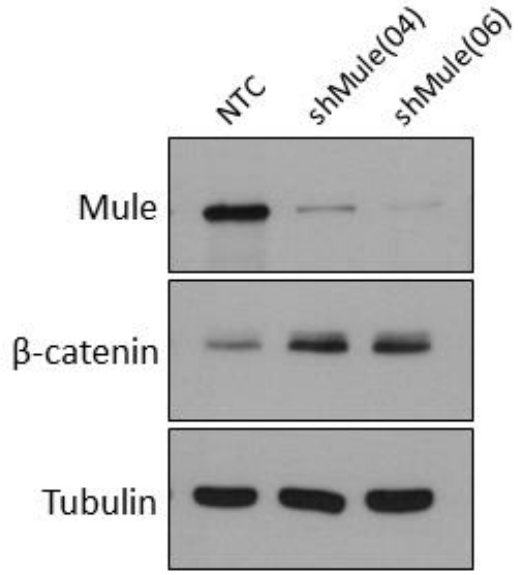

Figure 5.12. Mule mediates degradation of β-catenin. Knockdown of Mule was performed in MHCC-97L, which showed the highest Mule protein level among the HCC cell lines. Knockdown of Mule led to upregulation of β-catenin expression in HCC cells.

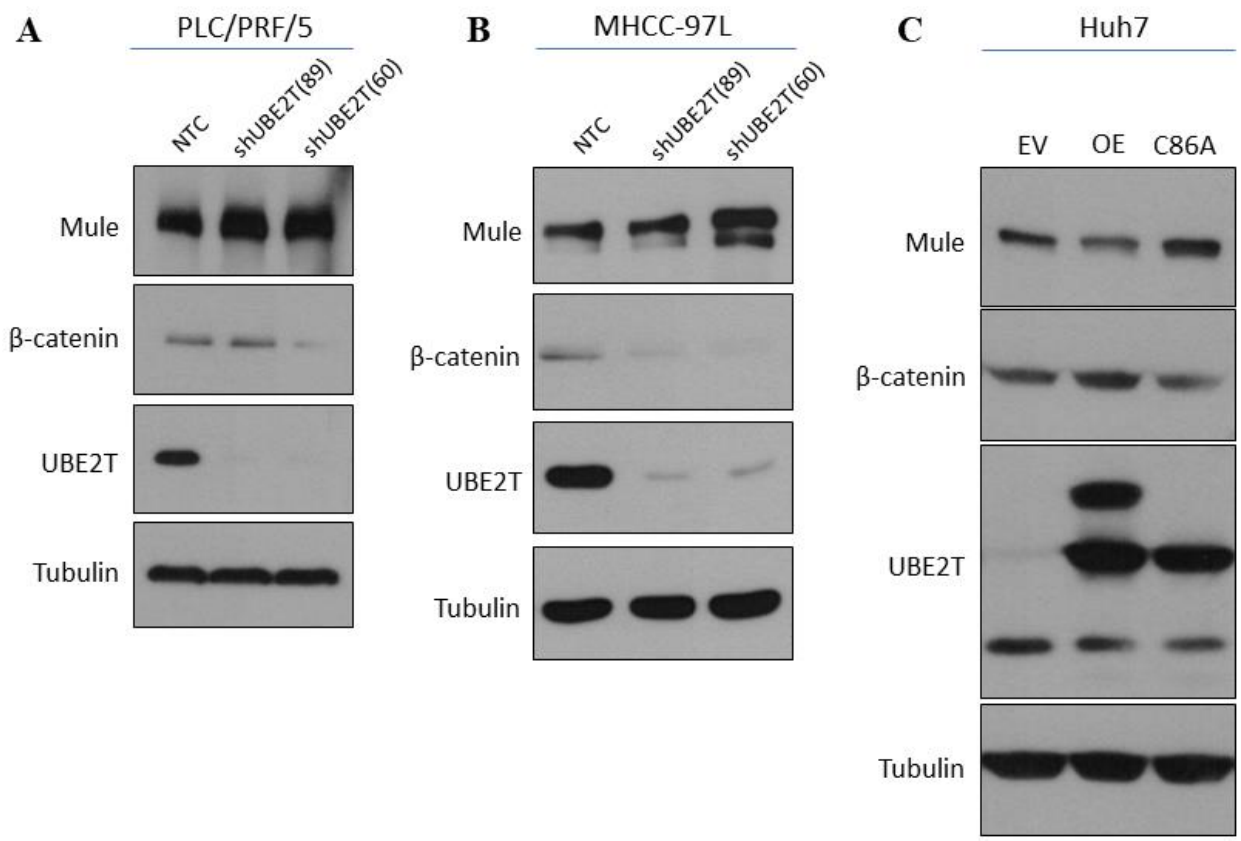

Figure 5.13. UBE2T promoted β-catenin expression by suppressing Mule. Knockdown of UBE2T in (A) PLC/PRF/5 and (B) MHCC-97L resulted in upregulation of Mule and suppression on β-catenin. (C) Overexpression of wild-type UBE2T enhanced the β-catenin expression possibly via degradation of Mule. The C86A mutation of UBE2T rescued the suppression on Mule and led to downregulation in β-catenin expression.

5.3.5. Ablation of UBE2T affected the subcellular localization of β-catenin

The β-catenin expression was further investigated in IF assay. UBE2T knockdown PLC/PRF/5 and MHCC-97L cells were subjected to IF staining for the study of β-catenin expression and localization (**Figure 5.14**). In the control PLC/PRF/5 cells, most of the β-catenin was expressed in cytoplasm while a small portion was concentrated in nucleus. The knockdown of UBE2T significantly reduced the abundance of β-catenin in the cytoplasm. Instead cytoplasm and nucleus, majority of the β-catenin was located at the cellular membrane in the UBE2T knockdown

PLC/PRF/5 cells. The finding in the MHCC-97L was in concordance. Most of the β-catenin was expressed at cellular membrane in the control cells and approximately half of the cells showed concentrated expression of β-catenin in nucleus, where the active β-catenin drives transcription of Wnt/β-catenin signaling target genes. The UBE2T knockdown led to a remarkable reduction of the nuclear β-catenin. β-catenin was barely observable in the nucleus of the knockdown cells. The expression of β-catenin at the cellular membrane of the UBE2T knockdown cells was diminished as well. The proportion of cells displaying β-catenin at the cellular membrane dropped to around a half in the UBE2T knockdown MHCC-97L.

The β-catenin expression upon UBE2T overexpression has also been studied (**Figure 5.15A**). The control cells of Huh7 showed moderate expression level of β-catenin, which was mainly expressed at cellular membrane. The overexpression of wild-type UBE2T significantly increased the expression of β-catenin in all the cellular compartments including the nucleus, cytoplasm and cellular membrane. Increased β-catenin expression could be clearly observed in the nucleus. However, β-catenin has been notably decreased when the E2 activity of UBE2T was impaired by C86A mutation. Nuclear expression of β-catenin has been greatly reduced in the UBE2T C86A mutant expressing cells. Most of the β-catenin expression was limited at the cellular membrane. The expression of β-catenin has been quantified in **Figure 5.15B**. The total β-catenin expression in the control Huh7 cells was approximately 40% while that in the wild-type UBE2T overexpressing cells has jumped to around 90%. The total β-catenin has been reduced to around 50% in the UBE2T C86A mutant. Regarding the distribution of β-catenin, both the control cells and the UBE2T C86A mutant expressing cells showed very low expression level of β-catenin in the nucleus while the wild-type UBE2T overexpression resulted in approximately 40% of cells

displaying nuclear expression of β-catenin. To summarize, the finding in IF is in line with that in Western Blot results. UBE2T promotes β-catenin expression which can be diminished by impairing the E2 activity of UBE2T via C86A mutation.

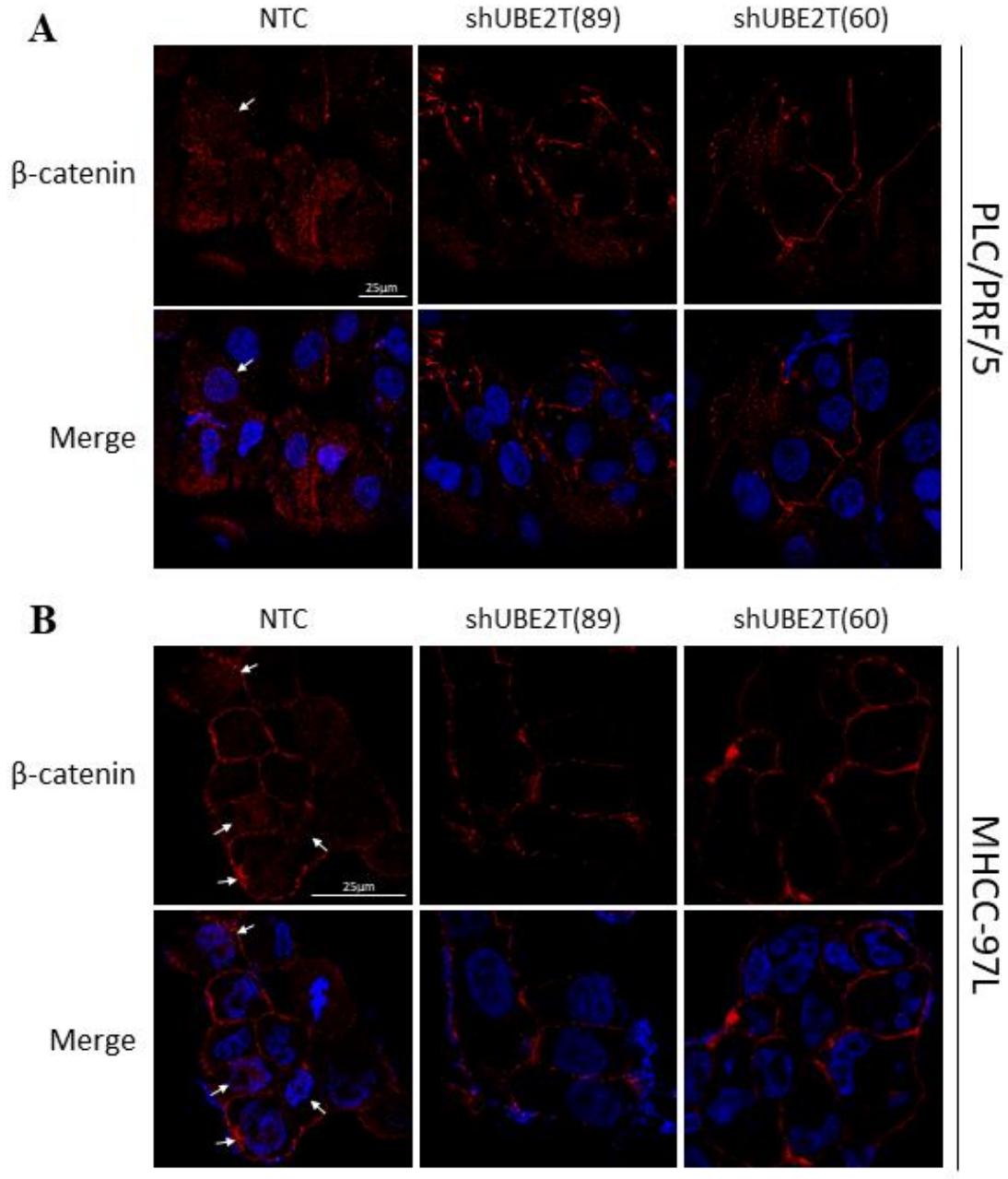

Figure 5.14. β-catenin expression was significantly diminished in UBE2T knockdown cells. IF staining of β-catenin showed significant reduction in total expression and nuclear expression

(indicated by arrows) of β-catenin in UBE2T knockdown (A) PLC/PRF/5 and (B) MHCC-97L cells.

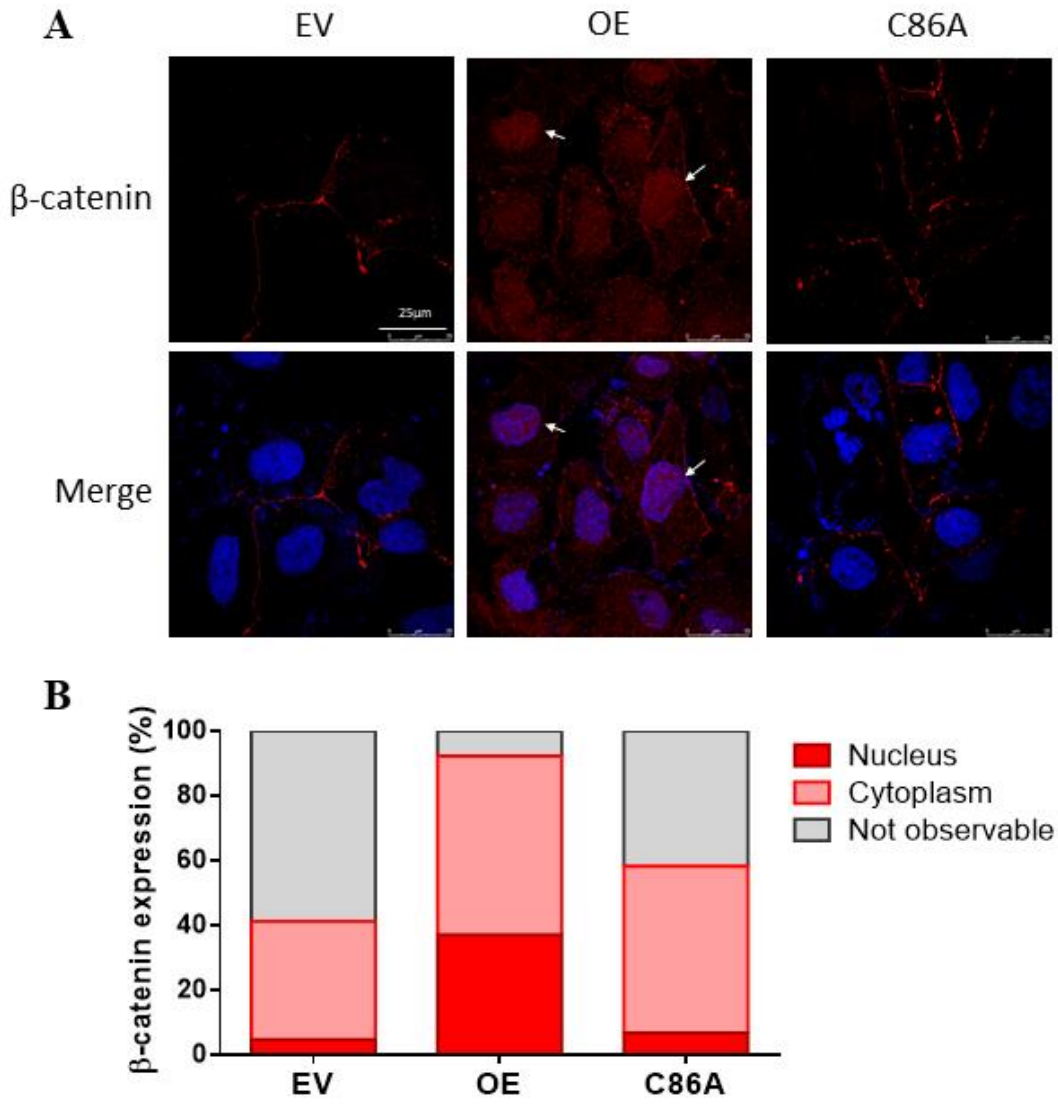

Figure 5.15. UBE2T overexpression remarkably increased the β-catenin expression especially in the nucleus of Huh7. (A) Overexpression of wild-type UBE2T showed remarkable upregulation of β-catenin in nucleus and cytoplasm of Huh7. (B) The β-catenin expression in the nucleus and cytoplasm of Huh7 cells was quantified.

5.4. Discussion

In this chapter, in the aim of investigating the underlying mechanism for the regulation of UBE2T on cancer stemness that has not yet been reported before, TAP/MS analysis was employed to identify the novel binding target of UBE2T. Tandem affinity purification was performed for the purification of UBE2T and its protein partners because of the high specificity and efficiency to allow great reduction in the non-specific proteins eluted together with the UBE2T. False positive results can thus be eliminated. UBE2T was labelled with SFB tag to facilitate the purification utilizing the affinity for streptavidin and S protein. The eluate obtained was subjected to mass spectrometry analysis performed by Taplin Mass Spectrometry Facility in the Harvard Medical School for identification of the potential protein partners of UBE2T.

It is supposed that UBE2T regulate cancer stemness by promoting degradation of tumor suppressor through ubiquitination in the help of an unknow E3 ligase. Since UBE2T is a E2 ubiquitin conjugating enzyme, it has a high affinity for E3 ligase for ubiquitination of substrate. We looked for any E3 ligase as the potential protein partner of UBE2T in the results obtained from the mass spectrometry. Intriguingly, Mcl-1 Ubiquitin Ligase E3 (Mule) was identified as the sole E3 ligase in the results.

Mule is a large E3 ligase of protein size of 480 kDa. It is first discovered in 2005 for its mediation on degradation of tumor suppressor p53 [169]. At the same time, Mule was identified to catalyze polyubiquitination of anti-apoptotic protein Mcl-1 to promote DNA damage-induced apoptosis [170]. Therefore, the role of Mule in tumorigenesis remains controversial. Mule was reported to be highly expressed in lung cancer and associated with poor prognosis of patients by promoting

tumor proliferation through p53 degradation [171]. Mule enhances cell migration and invasion by enhancing ubiquitination of TIAM1, an important regulator of cell adhesion, at cell-cell junction [172]. It also promotes degradation of tumor suppressor BRCA1 in breast cancer cells [173]. Meanwhile, Mule is widely reported to reduce stability of c-Myc for tumor suppression. It suppresses tumor motility and tumorigenicity of prostate cancer in c-Myc-dependent manner [174]. It is also well recognized as the tumor suppressor in colorectal cancer via inhibition on Wnt/β-catenin signaling, giving rise to the suppression on c-Myc [168], [175], [176]. De Groot et al [177] revealed that Mule inhibits Wnt signaling via negative feedback loop. In HCC, Mule is identified to inactivate Akt signaling and mediate tumor suppression by ubiquitination of oncogenic PREX2 [178]. It is also reported to suppresses EMT in HCC and is associated with better survival of the patients [179]. Mule functions as a tumor suppressor in HCC while UBE2T is oncogenic and highly expressed in HCC tumors. Considering that UBE2T may drive protein degradation by ubiquitination, UBE2T/Mule interaction may lead to degradation of the tumor suppressor Mule to promote tumorigenesis. UBE2T has been previously reported to degrade the E3 ligase BRCA1 in breast cancer [124]. This may provide hint on the potential UBE2T-mediated degradation of Mule, which is also an E3 ligase.

Besides, Mule plays a critical role in stem cell regulation. In hematopoietic stem cells, the loss of Mule leads to upregulation of N-Myc and stem cell exhaustion [180]. Mule controls murine intestinal stem cell proliferation by modulating the Wnt signaling pathway [176]. It promotes the proliferating hippocampal stem cells to return to quiescence state by preventing the accumulation of cyclin Ds through destabilization of Ascl1 [181]. Dysregulation of Mule will cause poor embryo development in humans as well [182]. In view of the importance of Mule in stem cell maintenance,

UBE2T/Mule interaction may be substantial in regulating cancer stemness, which greatly fits our hypothesis that UBE2T plays a critical role in maintaining CSC properties in HCC.

In this chapter, we discovered that UBE2T inhibits Mule expression by promoting proteasomal degradation of Mule via ubiquitination. The protein level of Mule is negatively correlated with UBE2T expression and the treatment of MG132 can reverse the reduction in Mule upon UBE2T overexpression. MG132 is a commonly used proteasome inhibitor. Recognition of ubiquitin chains, especially the K48-polyubiquitin chains, by the UBP of 26S proteasome stimulates proteolysis of the ubiquitinated substrate [183]. Using MG132 to enrich the ubiquitinated proteins, we observed enhanced ubiquitinated Mule in the UBE2T overexpressing cells. This indicates that UBE2T mediates the degradation of Mule through ubiquitin-proteasome pathway.

Besides, UBE2T C86A mutation was performed to study the direct effect of UBE2T, especially its E2 activity, on the degradation of Mule. The cysteine residue C86 located at the active site for the acceptance of ubiquitin from E1 was substituted with alanine to impair the E2 activity of UBE2T. Previous studies have shown that C86A mutation diminishes the monoubiquitination of UBE2T [118], [124]. In our study, the UBE2T C86A mutation reduced the ubiquitination of Mule, suggesting that UBE2T is the E2 enzyme responsible for the ubiquitination and degradation of Mule. UBE2T interacts with Mule for the ubiquitination of Mule instead of promoting the degradation of Mule by other E2 enzymes.

In this chapter, we discovered the E3 ligase Mule as the novel degradation target of UBE2T. UBE2T binds to Mule to transfer ubiquitin chain to Mule for degradation. However, the link between the UBE2T-mediated degradation of Mule and the regulation of cancer stemness in HCC

remains unclear.

Mule is critical in regulation of Wnt/β-catenin signaling pathway by inhibiting Dvl, β-catenin and c-Myc [184]. In response to activation of Wnt signaling, Mule promotes K63-linked polyubiquitination of Dvl to suppress multimerization of Dvl [177]. The impair in function of Dvl leads to phosphorylation and subsequent degradation of β-catenin. In addition, Mule directly mediates the degradation of β-catenin in colorectal cancer [168]. Overexpression of Mule reduces mRNA level of c-Myc in prostate cancer [174]. The suppression on multiple effectors of Wnt/β-catenin signaling indicates that Mule plays an important role in the negative feedback loop of the active Wnt/β-catenin signaling in cancers.

Wnt signaling pathway is well-recognized for its key role in embryonic development and regulation of self-renewability. It is categorized based on the involvement of β-catenin. The non-canonical Wnt signaling cascades are independent of β-catenin and are involved in maintenance of stem cells and regulation of cell polarity; the canonical Wnt signaling cascade is dependent on β-catenin and is involved in self-renewal of stem cells and cell proliferation [185]. It is widely accepted that Wnt/β-catenin signaling promotes CSC proliferation [186]. Upon the activation of the Wnt/β-catenin signaling receptors Fz and LRP6, Dvl is recruited to the activated receptor for the subsequent recruitment of Axin. Axin is one of the main components of destruction complex, which is responsible for the phosphorylation and degradation of β-catenin. The translocation of Axin inhibits the phosphorylation ability of the destruction complex on β-catenin, leading to the accumulation of β-catenin in the cytoplasm. The cytoplasmic β-catenin can translocate into the nucleus, where it binds to the transcription factors of TCF/LEF family to drive expression of the

Wnt/β-catenin signaling target genes to promote cell proliferation and CSC properties. C-Myc and cyclin D1, the Wnt/β-catenin signaling target genes, have been reported to maintain self-renewal and EMT transition in CSCs [187], [188]. Activation of Wnt/β-catenin signaling can enrich the EpCAM-positive CSC population in HCC [51], [189].

The ubiquitination of β-catenin by Mule has been previously demonstrated in the study of Dominguez-Brauer [168]. Because of the key role of β-catenin in CSCs, it triggered our interest in the effect of UBE2T and the UBE2T-mediated Mule degradation on the β-catenin. Therefore, we examined the expression of β-catenin in the HCC cells with altered UBE2T protein levels. Decrease in Mule and increase in β-catenin protein expression were found in the UBE2T overexpressing cells. The lack of UBE2T E2 activity suppressed β-catenin while enhancing the expression of Mule. This shows that UBE2T promotes the expression of β-catenin by proteasomal degradation of Mule. Meanwhile, the subcellular localization of β-catenin was studied. Although β-catenin is mainly located at cellular membrane without the activation of Wnt/β-catenin signaling pathway because of its association with E-cadherin, cytoplasmic and nuclear localization was still observable in the control PLC/PRF/5 and MHCC-97L cells. The knockdown of UBE2T significantly reduced the β-catenin in not only the cellular membrane but also the cytoplasmic and nuclear pool, where β-catenin drives the transcription of many oncogenes by the association with the TCF/LEF transcription factors. In consistent with the finding in the UBE2T knockdown cells, remarkable elevation in total β-catenin expression was found in the UBE2T overexpressing cells. Nuclear localization of β-catenin was also significantly enhanced upon UBE2T overexpression. The active transcription of Wnt/β-catenin signaling target genes caused by the enhanced nuclear expression of β-catenin can in turn promote CSC proliferation [185].

In summary, we have identified Mule as the novel degradation target of UBE2T. The UBE2T-mediated ubiquitination of Mule leads to the intracellular accumulation of β-catenin, especially in the nucleus. The nuclear localization of β-catenin drives transcription of many CSC-related genes to promote CSC properties of the HCC cells.

Chapter 6

Conclusion and Future Perspective

6.1. Conclusion

HCC is prevalent and is the second leading cause of cancer death worldwide [1]. Poor prognosis of patients is attributed to frequent tumor relapse and development of drug resistance. CSC model has been raised to explain tumor heterogeneity, which limits the efficacy of chemotherapy and molecular targeted therapy by genotypic complexities. In brief, tumor heterogeneity is supported by tumor hierarchy. CSCs are distinct subsets of cancer cells with stem cell-like properties including abilities of self-renewal, differentiation and tumorigenesis. In addition, upregulation of stemness-related genes such as Sox2 and Nanog has been observed in many cancers [47], [48]. CSCs are considered as metastatic precursors and are positively associated with EMT, which is important to development of metastasis. Efficient DNA damage repair system in CSCs contributes to resistance to radio-/chemotherapy. In view of the substantial role that CSCs play in tumorigenesis, it is critical to have a better understanding in the regulatory mechanism of CSCs in HCC.

In our study, we first focused on the genes with significant upregulation in regenerating liver in partial hepatectomy mouse model. This hypothesis is based on the fact that normal stem cells and CSCs share high molecular similarity so exploring the genetic profile of normal stem cells was considered a great starting point to identify substantial molecule/signaling pathway involved in regulation of liver CSCs [190]. In the early regenerating liver to which stem cells are mobilized for active liver regeneration, UBE2T within DDR pathway was found to be the most significant upregulated. Besides, UBE2T expression was increased in EpCAM-enriched liver CSC populations. The association of UBE2T upregulation with stem cell/CSC enrichment suggests the pivotal role of UBE2T in regulation of CSCs.

Firstly, we found that UBE2T mRNA and protein levels were found to be overexpressed and correlated with aggressive tumor phenotypes and poorer patient's survival. We have demonstrated the regulatory role of UBE2T in CSCs by lentiviral based knockdown and ectopic overexpression approaches. Modulation of UBE2T expression level exhibited direct effect on CSC properties, as indicated by tumor spheroid formation ability and expression of CSC markers. Other CSC related properties including drug resistance and cell migration and invasion abilities were also regulated by UBE2T. Altered UBE2T level affected *in vivo* tumorigenicity of HCC cells, and lung metastasis *in vivo* in orthotopic HCC xenograft model. Our study uncovered the important role of UBE2T in regulation of liver cancer stemness. However, only limited study has investigated the underlying mechanism to date.

In order to identify downstream target of UBE2T for CSC regulation, TAP/MS was performed. E3 ligase Mule, which is a tumor suppressor in HCC, was identified and its interaction with UBE2T was validated by reciprocal Co-IP. Intriguingly, UBE2T was found to suppress expression of Mule in Western Blot and IF analyses. Proteasome inhibitor MG132 treatment indicated that UBE2T regulated Mule expression by proteasomal degradation. Ubiquitination assay further supported that UBE2T reduced the expression of Mule by promoting ubiquitination of the E3 ligase. At the same time, site-directed mutagenesis on cysteine residue C86 at active site of UBE2T demonstrated that UBE2T-mediated downregulation of Mule was directly regulated by E2 activity of UBE2T.

Mule was reported to suppress tumorigenesis by targeting β-catenin for ubiquitination and

degradation [168]. It is well established that Wnt/β-catenin signaling plays an important role in regulation of CSCs [51], [185], [186]. It is reasoned to believe that UBE2T promotes liver cancer stemness by degrading Mule and hence enhance β-catenin expression. In our study, we demonstrated that overexpression of UBE2T was associated with downregulation of Mule and upregulation of β-catenin in protein level. IF analysis also revealed that UBE2T overexpression significantly increased accumulation of β-catenin in nucleus where cytoplasmic β-catenin translocate to drive transcriptional activation of Wnt/β-catenin signaling downstream targets for promotion of CSC properties.

Taken together, our study uncovered UBE2T/Mule/β-catenin signaling cascade in regulation of liver CSCs (**Figure 6.1**). Our finding contributes to better understanding of underlying mechanism for CSC regulation. We have also revealed a new therapeutic target for treatment of HCC. However, there are some limitations of this study and further experiments are needed to further support the role of UBE2Ton regulation of liver CSCs.

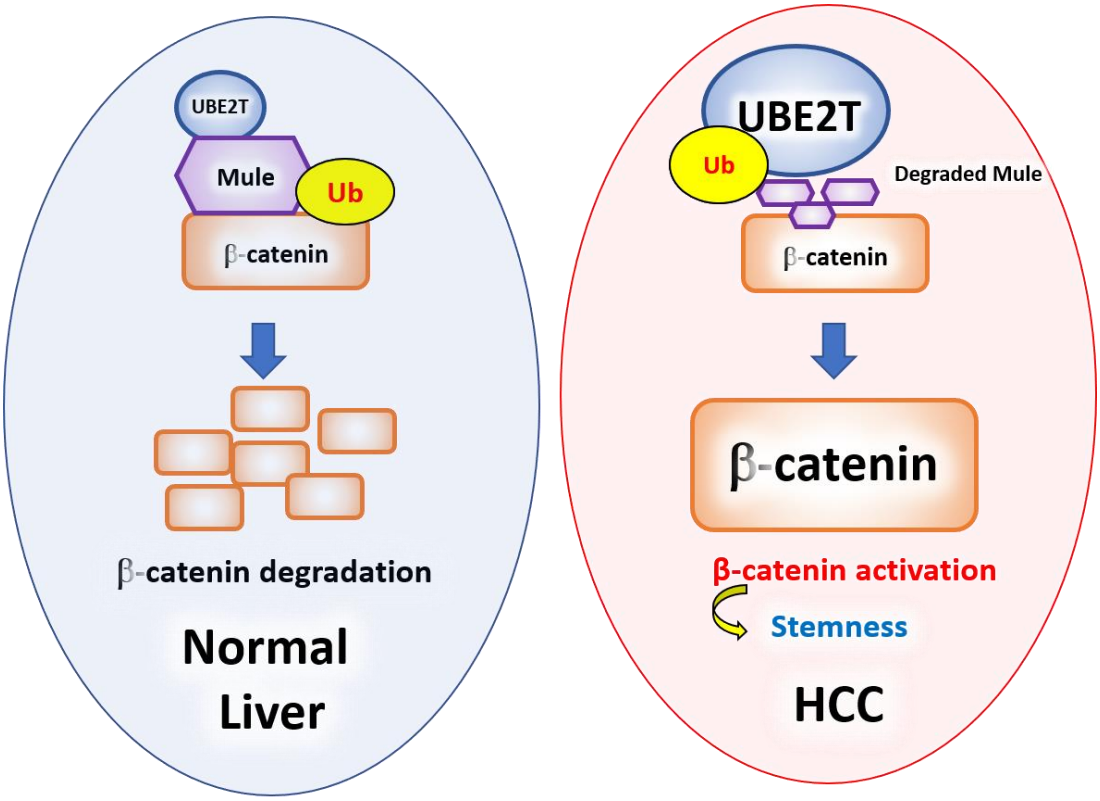

Figure 6.1. UBE2T/Mule/β-catenin signaling cascade was discovered in our study. Our study reported the overexpression of UBE2T in HCC promotes cancer stemness by causing proteasomal degradation of tumor suppressor Mule to increase accumulation of β-catenin in HCC cells especially inside nucleus. The β-catenin accumulation leads to transcriptional activation of Wnt/β-catenin signaling target genes to increase liver CSC properties.

6.2. Future Perspective

Firstly, we are going to demonstrate that the UBE2T-mediated degradation of Mule is caused by K48-linked ubiquitination. Protein substrates are destined for a wide variety of cellular process dependent of the ubiquitination at different lysine residues on ubiquitin. Ubiquitin conjugation is divided into monoubiquitination and polyubiquitination. Monoubiquitination is related to intracellular localization and trafficking while polyubiquitination is related to protein signaling and clearance [191]. Specific lysine residues (K6, K11, K27, K29, K33, K48 and K63) or methionine residue (M1) on ubiquitin is covalently linked to protein substrate. K63-linked polyubiquitin chain is associated with proteasome-independent roles such as DNA repair and endocytosis [192]. Polyubiquitination on K48 is mostly related to proteasomal degradation [193]. In order to validate the UBE2T-mediated suppression of Mule is caused by proteasomal degradation, the abundance of K48-specific ubiquitinated Mule upon UBE2T overexpression would be examined.

Secondly, we are going to inhibit expression of β-catenin by knockdown approach to rescue the enhanced cancer stemness caused by UBE2T overexpression. We hypothesized that UBE2T regulates CSC properties by promoting β-catenin accumulation via degradation of Mule. β-catenin would be suppressed by knockdown approach to investigate whether the increased CSC properties could be removed in the UBE2T overexpressing HCC cells. Likewise, similar experiment will be performed in UBE2T knockdown HCC cells with introduction of dominant-active form of β-catenin.

Thirdly, we are going to examine whether UBE2T overexpression and its mediation of Mule

degradation together with β-catenin accumulation are clinically relevant in HCC clinical samples. We will correlate the expression of UBE2T, Mule and β-catenin in a cohort of HCC samples by IHC analysis. We will also examine the co-expression of UBE2T, Mule and β-catenin in HCC clinical samples to validate the UBE2T/Mule/β-catenin axis.

Fourthly, we would also study whether UBE2T overexpression and β-catenin is mutually inclusive or exclusive in HCC. β-catenin activating mutations are frequently detected in HCC and drive tumorigenesis [194]–[196]. Whether the increase in CSC properties in HCC is solely contributed by UBE2T overexpression or contributed by both the UBE2T overexpression and β-catenin activation remains unknown. Therefore, we are going to compare the percentage of β-catenin mutation in HCC clinical samples with high and low UBE2T expression levels. If HCC cases with high UBE2T expression levels show lower percentage of β-catenin, the UBE2T overexpression and β-catenin activation are mutually exclusive in HCC.

Last but not least, we are going to explore the upstream mechanism for significant UBE2T overexpression in HCC. The gene of UBE2T is located at chromosome 1q32.1 Copy number gain in chromosome 1q is frequently detected in HCC and gains of 1q32 was found in 35% of HCC cases [197]. We doubted whether the significantly overexpression of UBE2T in HCC was due to the amplification in copy number of UBE2T. The correlation of copy number and mRNA level of UBE2T was studied (**Figure 6.2**). Nevertheless, the copy number of UBE2T is not related to the transcriptional expression of UBE2T. The significant upregulation of UBE2T is not caused by the amplification in gene copy number. Next, we examined enhancer marker distribution in HCC cell line HepG2 to assess the possibility of existence of super-enhancer that causes upregulation in

UBE2T transcription. H3K27ac was found at the promoter region of UBE2T (**Figure 6.3**). H3K27ac refers to the acetylation of histone H3 at lysine residue K27. H3K27ac facilitates binding of transcription factors to enhance gene transcription and is commonly used for identification of active enhancers. Therefore, we would further investigate the upstream mechanism to identify possible active enhancer that contributes to UBE2T overexpression in HCC.

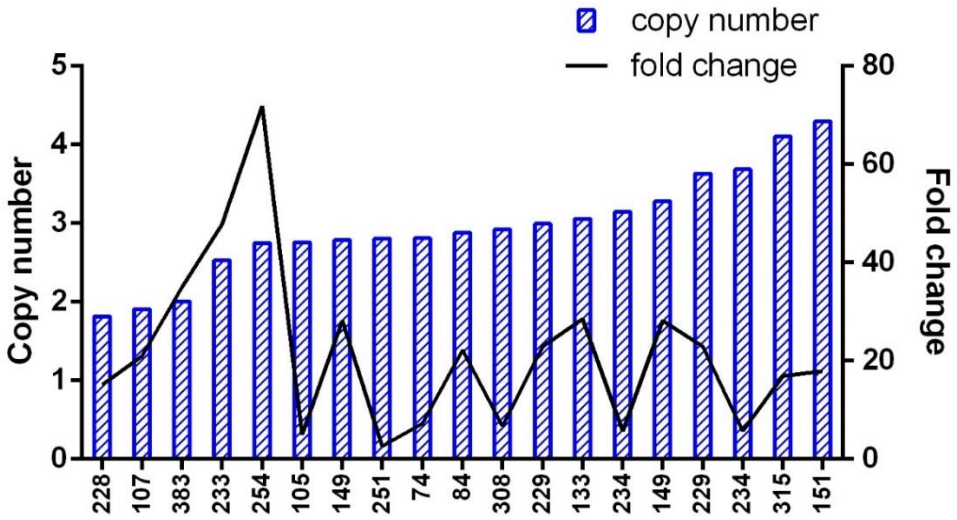

Figure 6.2. Copy number of UBE2T is not related to mRNA level of UBE2T. Correlation of UBE2T copy number and its mRNA level was studied. Copy number of UBE2T is not related to the mRNA level of UBE2T.

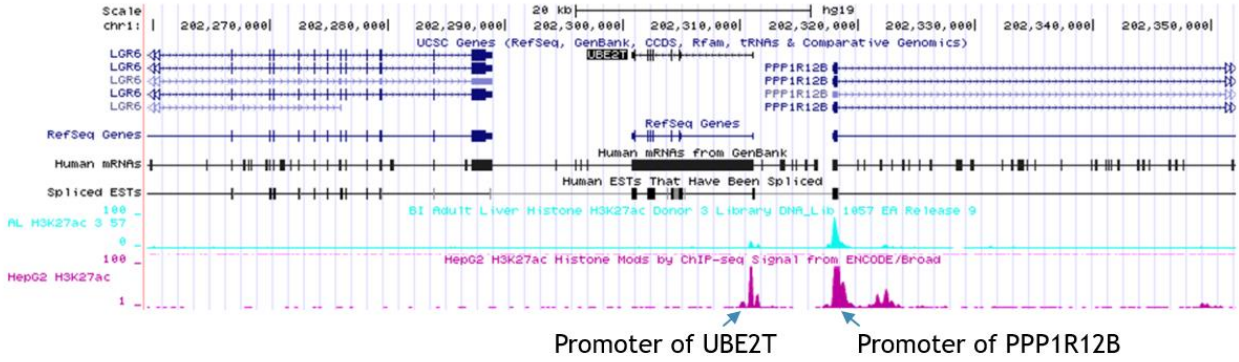

Figure 6.3. H3K27ac was found at promoter region of UBE2T. Enhancer mark distribution was examined in HepG2. H3K27ac was found at promoter region of UBE2T.

List of References

[1] L. A. Torre, F. Bray, R. L. Siegel, J. Ferlay, J. Lortet-Tieulent, and A. Jemal, 'Global cancer statistics, 2012', *CA: A Cancer Journal for Clinicians*, vol. 65, no. 2, pp. 87–108, 2015.

[2] K. J. Lafaro, A. N. Demirjian, and T. M. Pawlik, 'Epidemiology of Hepatocellular Carcinoma', *Surgical Oncology Clinics of North America*, vol. 24, no. 1, pp. 1–17, Jan. 2015.

[3] R. Hefaiedh, R. Ennaifer, H. Romdhane, H. Ben Nejma, N. Arfa, N. Belhadj, L. Gharbi, and T. Khalfallah, 'Gender difference in patients with hepatocellular carcinoma', *Tunis Med*, vol. 91, no. 8–9, pp. 505–508, Sep. 2013.

[4] V. W. Keng, D. A. Largaespada, and A. Villanueva, 'Why men are at higher risk for hepatocellular carcinoma?', *J Hepatol*, vol. 57, no. 2, pp. 453–454, Aug. 2012.

[5] Y. Li, H. Li, J. M. Spitsbergen, and Z. Gong, 'Males develop faster and more severe hepatocellular carcinoma than females in krasV12 transgenic zebrafish', *Sci Rep*, vol. 7, Jan. 2017.

[6] A. Petruzziello, 'Epidemiology of Hepatitis B Virus (HBV) and Hepatitis C Virus (HCV) Related Hepatocellular Carcinoma', *Open Virol J*, vol. 12, pp. 26–32, Feb. 2018.

[7] N. P. Malek, S. Schmidt, P. Huber, M. P. Manns, and T. F. Greten, 'The Diagnosis and Treatment of Hepatocellular Carcinoma', *Dtsch Arztebl Int*, vol. 111, no. 7, pp. 101–106, Feb. 2014.

[8] Y. Liu and F. Wu, 'Global Burden of Aflatoxin-Induced Hepatocellular Carcinoma: A Risk Assessment', *Environ Health Perspect*, vol. 118, no. 6, pp. 818–824, Jun. 2010.

[9] C. Qu, T. Chen, F. Fan, Q. Zhan, Y. Wang, J. Lu, L. Lu, *et al.*, 'Efficacy of Neonatal HBV Vaccination on Liver Cancer and Other Liver Diseases over 30-Year Follow-up of the Qidong Hepatitis B Intervention Study: A Cluster Randomized Controlled Trial', *PLoS Med*, vol. 11, no. 12, Dec. 2014.

[10] H. B. El–Serag and K. L. Rudolph, 'Hepatocellular Carcinoma: Epidemiology and Molecular Carcinogenesis', *Gastroenterology*, vol. 132, no. 7, pp. 2557–2576, Jun. 2007.

[11] F. Kanwal, J.R. Kramer, S. Mapakshi, Y. Natarajan, M. Chayanupatkul, P.A. Richardson, L. Li, *et al.*, 'Risk of Hepatocellular Cancer in Patients With Non-Alcoholic Fatty Liver Disease', *Gastroenterology*, vol. 155, no. 6, pp. 1828-1837.e2, Dec. 2018.

[12] M. S. Grandhi, A. K. Kim, S. M. Ronnekleiv-Kelly, I. R. Kamel, M. A. Ghasebeh, and T. M.

Pawlik, ‘Hepatocellular carcinoma: From diagnosis to treatment’, *Surgical Oncology*, vol. 25, no. 2, pp. 74–85, Jun. 2016.

[13] T. Clark, S. Maximin, J. Meier, S. Pokharel, and P. Bhargava, ‘Hepatocellular Carcinoma: Review of Epidemiology, Screening, Imaging Diagnosis, Response Assessment, and Treatment’, *Current Problems in Diagnostic Radiology*, vol. 44, no. 6, pp. 479–486, Nov. 2015.

[14] J. M. Llovet, J. Fuster, and J. Bruix, ‘Intention-to-treat analysis of surgical treatment for early hepatocellular carcinoma: Resection versus transplantation’, *Hepatology*, vol. 30, no. 6, pp. 1434–1440, 1999.

[15] M. Schwartz, S. Roayaie, and M. Konstadoulakis, ‘Strategies for the management of hepatocellular carcinoma’, *Nature Reviews Clinical Oncology*, vol. 4, no. 7, pp. 424–432, Jul. 2007.

[16] S. G. Delis and C. Dervenis, ‘Selection criteria for liver resection in patients with hepatocellular carcinoma and chronic liver disease’, *World J Gastroenterol*, vol. 14, no. 22, pp. 3452–3460, Jun. 2008.

[17] N. Kemeny, ‘Presurgical Chemotherapy in Patients Being Considered for Liver Resection’, *The Oncologist*, vol. 12, no. 7, pp. 825–839, Jan. 2007.

[18] N. Akamatsu and Y. Sugawara, ‘Primary biliary cirrhosis and liver transplantation’, *Intractable Rare Dis Res*, vol. 1, no. 2, pp. 66–80, May 2012.

[19] V. Mazzaferro, E. Regalia, R. Doci, S. Andreola, A. Pulvirenti, F. Bozzetti, F. Montalto, M. Ammatuna, A. Morabito, and L. Gennari, ‘Liver transplantation for the treatment of small hepatocellular carcinomas in patients with cirrhosis’, *N. Engl. J. Med.*, vol. 334, no. 11, pp. 693–699, Mar. 1996.

[20] C. C. Jadlowiec and T. Taner, ‘Liver transplantation: Current status and challenges’, *World J Gastroenterol*, vol. 22, no. 18, pp. 4438–4445, May 2016.

[21] M. C. Jansen, R. van Hillegersberg, R. A. F. M. Chamuleau, O. M. van Delden, D. J. Gouma, and T. M. van Gulik, ‘Outcome of regional and local ablative therapies for hepatocellular carcinoma: a collective review’, *European Journal of Surgical Oncology (EJSO)*, vol. 31, no. 4, pp. 331–347, May 2005.

[22] J. M. Llovet, M. Sala, and J. Bruix, ‘Nonsurgical treatment of hepatocellular carcinoma’, *Liver Transplantation*, vol. 6, no. 6B, pp. s11–s15, 2000.

[23] R. Lencioni, ‘Loco-regional treatment of hepatocellular carcinoma’, *Hepatology*, vol. 52, no. 2, pp. 762–773, 2010.

[24] A. Shen, H. Zhang, C. Tang, Y. Chen, Y. Wang, C. Zhang, and Z. Wu, ‘A systematic review of radiofrequency ablation versus percutaneous ethanol injection for small hepatocellular carcinoma up to 3 cm’, *Journal of Gastroenterology and Hepatology*, vol. 28, no. 5, pp. 793–800, 2013.

[25] M. Tsurusaki and T. Murakami, ‘Surgical and Locoregional Therapy of HCC: TACE’, *Liver Cancer*, vol. 4, no. 3, p. 165, Sep. 2015.

[26] J. Lei, J. Zhong, Ye. Luo, L. Yan, J. Zhu, W. Wang, B. Li, T. Wen, and J. Yang, ‘Response to transarterial chemoembolization may serve as selection criteria for hepatocellular carcinoma liver transplantation’, *Oncotarget*, vol. 8, no. 53, pp. 91328–91342, Aug. 2017.

[27] J. M. Llovet, M. I. Real, X. Montaña, R. Planas, S. Coll, J. Aponte, C. Ayuso, *et al.*, ‘Arterial embolisation or chemoembolisation versus symptomatic treatment in patients with unresectable hepatocellular carcinoma: a randomised controlled trial’, *The Lancet*, vol. 359, no. 9319, pp. 1734–1739, May 2002.

[28] S. M. Wilhelm, C. Carter, L. Tang, D. Wilkie, A. McNabola, H. Rong, C. Chen, *et al.*, ‘BAY 43-9006 exhibits broad spectrum oral antitumor activity and targets the RAF/MEK/ERK pathway and receptor tyrosine kinases involved in tumor progression and angiogenesis’, *Cancer Res.*, vol. 64, no. 19, pp. 7099–7109, Oct. 2004.

[29] M. Le Grazie, M. R. Biagini, M. Tarocchi, S. Polvani, and A. Galli, ‘Chemotherapy for hepatocellular carcinoma: The present and the future’, *World J Hepatol*, vol. 9, no. 21, pp. 907–920, Jul. 2017.

[30] Y. Zhu, B. Zheng, H. Wang, and L. Chen, ‘New knowledge of the mechanisms of sorafenib resistance in liver cancer’, *Acta Pharmacol Sin*, vol. 38, no. 5, pp. 614–622, May 2017.

[31] J. M. Llovet, S. Ricci, V. Mazzaferro, P. Hilgard, E. Gane, J. Blanc, A.C. de Oliveira, *et al.*, ‘Sorafenib in Advanced Hepatocellular Carcinoma’, *New England Journal of Medicine*, vol. 359, no. 4, pp. 378–390, Jul. 2008.

[32] T. Lee, C. Lin, C. Chen, T. Wang, G. Lo, C. Chang, and Y. Chao, ‘Combination of transcatheter arterial chemoembolization and interrupted dosing sorafenib improves patient survival in early–intermediate stage hepatocellular carcinoma’, *Medicine (Baltimore)*, vol. 96, no. 37, Sep. 2017.

[33] S. Li, F. Yang, and X. Ren, 'Immunotherapy for hepatocellular carcinoma', *DD&T*, vol. 9, no. 5, pp. 363–371, 2015.

[34] I. N. Crispe, 'The Liver as a Lymphoid Organ', *Annu. Rev. Immunol.*, vol. 27, no. 1, pp. 147–163, Mar. 2009.

[35] J. Prieto, I. Melero, and B. Sangro, 'Immunological landscape and immunotherapy of hepatocellular carcinoma', *Nature Reviews Gastroenterology & Hepatology*, vol. 12, no. 12, pp. 681–700, Dec. 2015.

[36] F. Xu, T. Jin, Y. Zhu, and C. Dai, 'Immune checkpoint therapy in liver cancer', *J Exp Clin Cancer Res*, vol. 37, May 2018.

[37] G. Willimsky, K. Schmidt, C. Loddenkemper, J. Gellermann, and T. Blankenstein, 'Virus-induced hepatocellular carcinomas cause antigen-specific local tolerance', *J Clin Invest*, vol. 123, no. 3, pp. 1032–1043, Mar. 2013.

[38] K. Li, Y. Lan, J. Wang, and L. Liu, 'Chimeric antigen receptor–engineered T cells for liver cancers, progress and obstacles', *Tumour Biol.*, vol. 39, no. 3, p. 1010428317692229, Mar. 2017.

[39] A. B. El-Khoueiry, B. Sangro, T. Yau, T. S. Crocenzi, M. Kudo, C. Hsu, T. Kim, *et al.*, 'Nivolumab in patients with advanced hepatocellular carcinoma (CheckMate 040): an open-label, non-comparative, phase 1/2 dose escalation and expansion trial', *The Lancet*, vol. 389, no. 10088, pp. 2492–2502, Jun. 2017.

[40] M. Kudo, 'Immune Checkpoint Blockade in Hepatocellular Carcinoma: 2017 Update', *Liver Cancer*, vol. 6, no. 1, pp. 1–12, Nov. 2016.

[41] B. Sangro, C. Gomez-Martin, M. de la Mata, M. Iñarrairaegui, E. Garralda, P. Barrera, J.I. Riezu-Boj, *et al.*, 'A clinical trial of CTLA-4 blockade with tremelimumab in patients with hepatocellular carcinoma and chronic hepatitis C', *J. Hepatol.*, vol. 59, no. 1, pp. 81–88, Jul. 2013.

[42] I. Dagogo-Jack and A. T. Shaw, 'Tumour heterogeneity and resistance to cancer therapies', *Nature Reviews Clinical Oncology*, vol. 15, no. 2, pp. 81–94, Feb. 2018.

[43] M. Greaves and C. C. Maley, 'Clonal Evolution in Cancer', *Nature*, vol. 481, no. 7381, pp. 306–313, Jan. 2012.

[44] R. A. Gatenby and R. J. Gillies, 'A microenvironmental model of carcinogenesis', *Nature Reviews Cancer*, vol. 8, no. 1, pp. 56–61, Jan. 2008.

[45] P. Zhu and Z. Fan, ‘Cancer stem cells and tumorigenesis’, *Biophysics Reports*, vol. 4, no. 4, p. 178, 2018.

[46] J. M. Heddleston, Z. Li, A. B. Hjelmeland, and J. N. Rich, ‘The Hypoxic Microenvironment Maintains Glioblastoma Stem Cells and Promotes Reprogramming towards a Cancer Stem Cell Phenotype’, *Cell Cycle*, vol. 8, no. 20, pp. 3274–3284, Oct. 2009.

[47] G. Maurizi, N. Verma, A. Gadi, A. Mansukhani, and C. Basilico, ‘Sox2 is required for tumor development and cancer cell proliferation in osteosarcoma’, *Oncogene*, vol. 37, no. 33, p. 4626, Aug. 2018.

[48] C. R. Jeter, T. Yang, J. Wang, H.-P. Chao, and D. G. Tang, ‘NANOG in cancer stem cells and tumor development: An update and outstanding questions’, *Stem Cells*, vol. 33, no. 8, pp. 2381–2390, Aug. 2015.

[49] Y. Xiao, X. Yang, Y. Miao, X. He, M. Wang, and W. Sha, ‘Inhibition of cell proliferation and tumor growth of colorectal cancer by inhibitors of Wnt and Notch signaling pathways’, *Oncol Lett*, vol. 12, no. 5, pp. 3695–3700, Nov. 2016.

[50] T. Zhan, N. Rindtorff, and M. Boutros, ‘Wnt signaling in cancer’, *Oncogene*, vol. 36, no. 11, pp. 1461–1473, Mar. 2017.

[51] T. Yamashita, A. Budhu, M. Forgues, and X. W. Wang, ‘Activation of Hepatic Stem Cell Marker EpCAM by Wnt–β-Catenin Signaling in Hepatocellular Carcinoma’, *Cancer Res*, vol. 67, no. 22, pp. 10831–10839, Nov. 2007.

[52] H. Guo, Y. Lu, J. Wang, X. Liu, E.T. Keller, Q. Liu, Q. Zhou, and J. Zhang., ‘Targeting the Notch signaling pathway in cancer therapeutics’, *Thorac Cancer*, vol. 5, no. 6, pp. 473–486, Nov. 2014.

[53] M. Shimokawa, Y. Ohta, S. Nishikori, M. Matano, A. Takano, M. Fujii, S. Date, S. Sugimoto, T. Kanai, and T. Sato, ‘Visualization and targeting of LGR5+ human colon cancer stem cells’, *Nature*, vol. 545, no. 7653, pp. 187–192, 11 2017.

[54] L. Mourao, G. Jacquemin, M. Huyghe, W.J. Nawrocki, N. Menssouri, N. Servant, and S. Fre, ‘Lineage tracing of Notch1-expressing cells in intestinal tumours reveals a distinct population of cancer stem cells’, *Scientific Reports*, vol. 9, no. 1, p. 888, Jan. 2019.

[55] D. H. Kim, T. Xing, Z. Yang, R. Dudek, Q. Lu, and Y.-H. Chen, ‘Epithelial Mesenchymal Transition in Embryonic Development, Tissue Repair and Cancer: A Comprehensive Overview’, *J Clin Med*, vol. 7, no. 1, Dec. 2017.

[56] S. A. Mani *et al.*, 'The epithelial-mesenchymal transition generates cells with properties of stem cells', *Cell*, vol. 133, no. 4, pp. 704–715, May 2008.

[57] P. Zhou *et al.*, 'The epithelial to mesenchymal transition (EMT) and cancer stem cells: implication for treatment resistance in pancreatic cancer', *Mol. Cancer*, vol. 16, no. 1, p. 52, 28 2017.

[58] T. Migita, A. Ueda, T. Ohishi, M. Hatano, H. Seimiya, S. Horiguchi, F. Koga, and F. Shibasaki., 'Epithelial–mesenchymal transition promotes SOX2 and NANOG expression in bladder cancer', *Laboratory Investigation*, vol. 97, no. 5, pp. 567–576, May 2017.

[59] H. Gao, C. Teng, W. Huang, J. Peng, and C. Wang, 'SOX2 Promotes the Epithelial to Mesenchymal Transition of Esophageal Squamous Cells by Modulating Slug Expression through the Activation of STAT3/HIF-α Signaling', *Int J Mol Sci*, vol. 16, no. 9, pp. 21643–21657, Sep. 2015.

[60] S. Liu, Y. Cong, D. Wang, Y. Sun, L. Deng, Y. Liu, R. Martin-Trevino, *et al.*, 'Breast Cancer Stem Cells Transition between Epithelial and Mesenchymal States Reflective of their Normal Counterparts', *Stem Cell Reports*, vol. 2, no. 1, pp. 78–91, Dec. 2013.

[61] Y. Jing, Z. Han, S. Zhang, Y. Liu, and L. Wei, 'Epithelial-Mesenchymal Transition in tumor microenvironment', *Cell Biosci*, vol. 1, p. 29, Aug. 2011.

[62] D. Hanahan and R. A. Weinberg, 'Hallmarks of Cancer: The Next Generation', *Cell*, vol. 144, no. 5, pp. 646–674, Mar. 2011.

[63] K. Liu, M. Hao, Y. Ouyang, J. Zheng, and D. Chen, 'CD133+ cancer stem cells promoted by VEGF accelerate the recurrence of hepatocellular carcinoma', *Scientific Reports*, vol. 7, p. 41499, Jan. 2017.

[64] C. Calabrese, H. Poppleton, M. Kocak, T.L. Hogg, C. Fuller, B. Hamner, E.Y. Oh, *et al.*, 'A Perivascular Niche for Brain Tumor Stem Cells', *Cancer Cell*, vol. 11, no. 1, pp. 69–82, Jan. 2007.

[65] T. Gridley, 'Notch signaling in the vasculature', *Curr Top Dev Biol*, vol. 92, pp. 277–309, 2010.

[66] Y. Zhao, Q. Bao, A. Renner, P. Camaj, M. Eichhorn, I. Ischenko, M. Angele, A. Kleespies, K. Jauch, and C. Bruns, 'Cancer stem cells and angiogenesis', *Int. J. Dev. Biol.*, vol. 55, no. 4–5, pp. 477–482, Jun. 2011.

[67] Q. Ge, H. Zhang, J. Hou, L. Wan, W. Cheng, X. Wang, D. Dong, *et al.*, 'VEGF secreted by

mesenchymal stem cells mediates the differentiation of endothelial progenitor cells into endothelial cells via paracrine mechanisms', *Mol Med Rep*, vol. 17, no. 1, pp. 1667–1675, Jan. 2018.

[68] M. Izumiya, A. Kabashima, H. Higuchi, T. Igarashi, G. Sakai, H. Iizuka, S. Nakamura, *et al.*, 'Chemoresistance Is Associated with Cancer Stem Cell-like Properties and Epithelial-to-Mesenchymal Transition in Pancreatic Cancer Cells', *Anticancer Res*, vol. 32, no. 9, pp. 3847–3853, Jan. 2012.

[69] X. S. Qi, F. Pajonk, S. McCloskey, D.A. Low, P. Kupelian, M. Steinberg, and K. Sheng, 'Radioresistance of the breast tumor is highly correlated to its level of cancer stem cell and its clinical implication for breast irradiation', *Radiother Oncol*, vol. 124, no. 3, pp. 455–461, 2017.

[70] M. Diehn, R.W. Cho, N.A. Lobo, T. Kalisky, M.J. Dorie, A.N. Kulp, D. Qian, *et al.*, 'Association of Reactive Oxygen Species Levels and Radioresistance in Cancer Stem Cells', *Nature*, vol. 458, no. 7239, pp. 780–783, Apr. 2009.

[71] K. Rycaj and D. G. Tang, 'CANCER STEM CELLS AND RADIORESISTANCE', *Int J Radiat Biol*, vol. 90, no. 8, pp. 615–621, Aug. 2014.

[72] W. Chen, J. Dong, J. Haiech, M. C. Kilhoffer, and M. Zeniou, 'Cancer Stem Cell Quiescence and Plasticity as Major Challenges in Cancer Therapy', *Stem Cells Int*, vol. 2016, 2016.

[73] Z. Li, 'CD133: a stem cell biomarker and beyond', *Exp Hematol Oncol*, vol. 2, p. 17, Jul. 2013.

[74] S. Kazama, J. Kishikawa, T. Kiyomatsu, K. Kawai, H. Nozawa, S. Ishihara, and T. Watanabe, 'Expression of the stem cell marker CD133 is related to tumor development in colorectal carcinogenesis', *Asian Journal of Surgery*, vol. 41, no. 3, pp. 274–278, May 2018.

[75] C. Wang, J. Xie, J. Guo, H. C. Manning, J. C. Gore, and N. Guo, 'Evaluation of CD44 and CD133 as cancer stem cell markers for colorectal cancer', *Oncology Reports*, vol. 28, no. 4, pp. 1301–1308, Oct. 2012.

[76] P. M. Glumac and A. M. LeBeau, 'The role of CD133 in cancer: a concise review', *Clin Transl Med*, vol. 7, Jul. 2018.

[77] W. T. Kim and C. J. Ryu, 'Cancer stem cell surface markers on normal stem cells', *BMB Rep*, vol. 50, no. 6, pp. 285–298, Jun. 2017.

[78] S. Moossavi, 'Heterogeneity of the Level of Activity of Lgr5+ Intestinal Stem Cells', *Int J*

Mol Cell Med, vol. 3, no. 4, pp. 216–224, 2014.

[79] M. Maugeri-Saccà, M. Bartucci, and R. D. Maria, 'DNA Damage Repair Pathways in Cancer Stem Cells', *Mol Cancer Ther*, vol. 11, no. 8, pp. 1627–1636, Aug. 2012.

[80] S. Bao, Q. Wu, R. E. McLendon, Y. Hao, Q. Shi, A. B. Hjelmeland, M.W. Dewhirst, D.D. Bigner, and J.N. Rich., 'Glioma stem cells promote radioresistance by preferential activation of the DNA damage response', *Nature*, vol. 444, no. 7120, p. 756, Dec. 2006.

[81] H. O. King, T. Brend, H. L. Payne, A. Wright, T. A. Ward, K. Patel, T. Egnuni, *et al.*, 'RAD51 Is a Selective DNA Repair Target to Radiosensitize Glioma Stem Cells', *Stem Cell Reports*, vol. 8, no. 1, pp. 125–139, Jan. 2017.

[82] D. Hambardzumyan, O. J. Becher, M. K. Rosenblum, P. P. Pandolfi, K. Manova-Todorova, and E. C. Holland, 'PI3K pathway regulates survival of cancer stem cells residing in the perivascular niche following radiation in medulloblastoma in vivo', *Genes Dev.*, vol. 22, no. 4, pp. 436–448, Feb. 2008.

[83] A. Karimaian, M. Majidinia, H. Bannazadeh Baghi, and B. Yousefi, 'The crosstalk between Wnt/β-catenin signaling pathway with DNA damage response and oxidative stress: Implications in cancer therapy', *DNA Repair*, vol. 51, pp. 14–19, Mar. 2017.

[84] J. H. Van Drie, 'Protein folding, protein homeostasis, and cancer', *Chin J Cancer*, vol. 30, no. 2, pp. 124–137, Feb. 2011.

[85] T. K. Chaudhuri and S. Paul, 'Protein-misfolding diseases and chaperone-based therapeutic approaches', *The FEBS Journal*, vol. 273, no. 7, pp. 1331–1349, Apr. 2006.

[86] L. H. Gallo, J. Ko, and D. J. Donoghue, 'The importance of regulatory ubiquitination in cancer and metastasis', *Cell Cycle*, vol. 16, no. 7, pp. 634–648, Feb. 2017.

[87] J. K. Morrow, H.-K. Lin, S. C. Sun, and S. Zhang, 'Targeting ubiquitination for cancer therapies', *Future Med Chem*, vol. 7, no. 17, pp. 2333–2350, Nov. 2015.

[88] J. Cheng, Y.H. Fan, X. Xu, H. Zhang, J. Dou, Y. Tang, X. Zhong, *et al.*, 'A small-molecule inhibitor of UBE2N induces neuroblastoma cell death via activation of p53 and JNK pathways', *Cell Death & Disease*, vol. 5, no. 2, p. e1079, Feb. 2014.

[89] A. Dikshit, Y.J. Jin, S. Degan, J. Hwang, M.W. Foster, C. Li, and J.Y. Zhang, 'UBE2N promotes melanoma growth via MEK/FRA1/SOX10 signaling', *Cancer Res*, p. canres.1040.2018, Jan. 2018.

[90] Z. Hao, H. Zhang, and J. Cowell, 'Ubiquitin-conjugating enzyme UBE2C: molecular

biology, role in tumorigenesis, and potential as a biomarker', *Tumor Biol.*, vol. 33, no. 3, pp. 723–730, Jun. 2012.

[91] J. Wang, Y. Huang, Z. Guan, J. Zhang, H. Su, W. Zhang, C. Yue, M. Yan, S. Guan, and Q. Liu, 'E3-ligase Skp2 predicts poor prognosis and maintains cancer stem cell pool in nasopharyngeal carcinoma', *Oncotarget*, vol. 5, no. 14, pp. 5591–5601, Jun. 2014.

[92] L. Zhao, J. Huang, H. Zhang, Y. Wang, L.E. Matesic, M. Takahata, H. Awad, D. Chen, and L. Xing, 'Tumor Necrosis Factor Inhibits Mesenchymal Stem Cell Differentiation into Osteoblasts Via the Ubiquitin E3 Ligase Wwp1', *Stem Cells*, vol. 29, no. 10, pp. 1601–1610, Oct. 2011.

[93] M. Tsuchiya, Y. Nakajima, N. Hirata, T. Morishita, H. Kishimoto, Y. Kanda, and K. Kimura, 'Ubiquitin ligase CHIP suppresses cancer stem cell properties in a population of breast cancer cells', *Biochemical and Biophysical Research Communications*, vol. 452, no. 4, pp. 928–932, Oct. 2014.

[94] S. Takeishi and K. I. Nakayama, 'Role of Fbxw7 in the maintenance of normal stem cells and cancer-initiating cells', *Br J Cancer*, vol. 111, no. 6, pp. 1054–1059, Sep. 2014.

[95] E. Levy-Lahad and E. Friedman, 'Cancer risks among BRCA1 and BRCA2 mutation carriers', *Br J Cancer*, vol. 96, no. 1, pp. 11–15, Jan. 2007.

[96] N. E. Buckley and P. B. Mullan, 'BRCA1 – Conductor of the Breast Stem Cell Orchestra: The Role of BRCA1 in Mammary Gland Development and Identification of Cell of Origin of BRCA1 Mutant Breast Cancer', *Stem Cell Rev and Rep*, vol. 8, no. 3, pp. 982–993, Sep. 2012.

[97] K. S. Harris and B. A. Kerr, 'Prostate Cancer Stem Cell Markers Drive Progression, Therapeutic Resistance, and Bone Metastasis', *Stem Cells Int*, vol. 2017, 2017.

[98] T. Ishiwata, Y. Matsuda, H. Yoshimura, N. Sasaki, S. Ishiwata, N. Ishikawa, K. Takubo, T. Arai, and J. Aida, 'Pancreatic cancer stem cells: features and detection methods', *Pathol. Oncol. Res.*, vol. 24, no. 4, pp. 797–805, Oct. 2018.

[99] G. Hardavella, R. George, and T. Sethi, 'Lung cancer stem cells—characteristics, phenotype', *Transl Lung Cancer Res*, vol. 5, no. 3, pp. 272–279, Jun. 2016.

[100] L. Qiu, H. Li, S. Fu, X. Chen, and L. Lu, 'Surface markers of liver cancer stem cells and innovative targeted-therapy strategies for HCC', *Oncol Lett*, vol. 15, no. 2, pp. 2039–2048, Feb. 2018.

[101] J. D. Lathia, S. C. Mack, E. E. Mulkearns-Hubert, C. L. L. Valentim, and J. N. Rich, 'Cancer stem cells in glioblastoma', *Genes Dev*, vol. 29, no. 12, pp. 1203–1217, Jun. 2015.

[102] Y. Hatano, S. Fukuda, K. Hisamatsu, A. Hirata, A. Hara, and H. Tomita, 'Multifaceted Interpretation of Colon Cancer Stem Cells', *Int J Mol Sci*, vol. 18, no. 7, Jul. 2017.

[103] W. C. Sin and C. L. Lim, 'Breast cancer stem cells—from origins to targeted therapy', *Stem Cell Investig*, vol. 4, Nov. 2017.

[104] S. Hashimoto, H. Anai, and K. Hanada, 'Mechanisms of interstrand DNA crosslink repair and human disorders', *Genes Environ*, vol. 38, May 2016.

[105] W. Wang, 'A major switch for the Fanconi anemia DNA damage–response pathway', *Nature Structural & Molecular Biology*, vol. 15, no. 11, pp. 1128–1130, Nov. 2008.

[106] A. M. Kolinjivadi, V. Sannino, A. de Antoni, H. Técher, G. Baldi, and V. Costanzo, 'Moonlighting at replication forks - a new life for homologous recombination proteins BRCA1, BRCA2 and RAD51', *FEBS Lett.*, vol. 591, no. 8, pp. 1083–1100, 2017.

[107] R. Ceccaldi *et al.*, 'Bone marrow failure in Fanconi anemia is triggered by an exacerbated p53/p21 DNA damage response that impairs hematopoietic stem and progenitor cells', *Cell Stem Cell*, vol. 11, no. 1, pp. 36–49, Jul. 2012.

[108] P. S. Rosenberg, M. H. Greene, and B. P. Alter, 'Cancer incidence in persons with Fanconi anemia', *Blood*, vol. 101, no. 3, pp. 822–826, Feb. 2003.

[109] B. P. Alter, 'Fanconi anemia and the development of leukemia', *Best Pract Res Clin Haematol*, vol. 27, no. 0, pp. 214–221, 2014.

[110] C. Stoepker, N. Ameziane, P. Lelij, I.E. Kooi, A.B. Oostra, M.A. Rooimans, S. Mil, *et al.*, 'Defects in the Fanconi Anemia Pathway and Chromatid Cohesion in Head and Neck Cancer', *Cancer Res*, vol. 75, no. 17, pp. 3543–3553, Sep. 2015.

[111] L.E. Romick-Rosendale, E.E. Hoskins, L. Vinnedge, G.D. Foglesong, M.G. Brusadelli, S.S. Potter, K. Komurov, *et al.*, 'Defects in the Fanconi Anemia Pathway in Head and Neck Cancer Cells Stimulate Tumor Cell Invasion through DNA-PK and Rac1 Signaling', *Clin Cancer Res*, vol. 22, no. 8, pp. 2062–2073, Apr. 2016.

[112] P. van der Groep, M. Hoelzel, H. Buerger, H. Joenje, J. P. de Winter, and P. J. van Diest, 'Loss of expression of FANCD2 protein in sporadic and hereditary breast cancer', *Breast Cancer Res Treat*, vol. 107, no. 1, pp. 41–47, Jan. 2008.

[113] E. Barroso, R. L. Milne, L.P. Fernández, P. Zamora, J. I. Arias, J. Benítez, and G. Ribas,

‘FANCD2 associated with sporadic breast cancer risk’, *Carcinogenesis*, vol. 27, no. 9, pp. 1930–1937, Sep. 2006.

[114] X. Zhang, X. Lu, S. Akhter, M.-M. Georgescu, and R. J. Legerski, ‘FANCI is a negative regulator of Akt activation’, *Cell Cycle*, vol. 15, no. 8, pp. 1134–1143, 2016.

[115] D. P. Silver and D. M. Livingston, ‘Mechanisms of BRCA1 Tumor Suppression’, *Cancer Discov*, vol. 2, no. 8, pp. 679–684, Aug. 2012.

[116] T. Shahid, J. Soroka, E. Kong, L. Malivert, M.J. McIlwraith, T. Pape, S.C. West, and X. Zhang, ‘Structure and Mechanism of Action of the BRCA2 Breast Cancer Tumor Suppressor’, *Nat Struct Mol Biol*, vol. 21, no. 11, pp. 962–968, Nov. 2014.

[117] K. T. Dao, M.D. Rotelli, C. L. Petersen, S. Kaech, W. D. Nelson, J. E. Yates, A. Newell, S. B. Olson, B. J. Druker, and G. C. Bagby, ‘FANCL ubiquitinates β-catenin and enhances its nuclear function’, *Blood*, vol. 120, no. 2, pp. 323–334, Jul. 2012.

[118] Y. J. Machida, Y. Machida, Y. Chen, A. M. Gurtan, G. M. Kupfer, A. D. D’Andrea, and A. Dutta, ‘UBE2T Is the E2 in the Fanconi Anemia Pathway and Undergoes Negative Autoregulation’, *Molecular Cell*, vol. 23, no. 4, pp. 589–596, Aug. 2006.

[119] K. A. Rickman, F. P. Lach, A. Abhyankar, F. X. Donovan, E. M. Sanborn, J. A. Kennedy, C. Sougnez, *et al.*, ‘Deficiency of UBE2T, the E2 ubiquitin ligase necessary for FANCD2 and FANCI ubiquitination, causes FA-T subtype of Fanconi anemia’, *Cell Rep*, vol. 12, no. 1, pp. 35–41, Jul. 2015.

[120] A. Hira, K. Yoshida, K. Sato, Y. Okuno, Y. Shiraishi, K. Chiba, H. Tanaka, *et al.*, ‘Mutations in the gene encoding the E2 conjugating enzyme UBE2T cause Fanconi anemia’, *Am. J. Hum. Genet.*, vol. 96, no. 6, pp. 1001–1007, Jun. 2015.

[121] G. Nalepa and D. W. Clapp, ‘Fanconi anaemia and cancer: an intricate relationship’, *Nature Reviews Cancer*, vol. 18, no. 3, pp. 168–185, Mar. 2018.

[122] J. Hao, A. Xu, X. Xie, J. Hao, T. Tian, S. Gao, X. Xiao, and D. He, ‘Elevated expression of UBE2T in lung cancer tumors and cell lines’, *Tumour Biol.*, vol. 29, no. 3, pp. 195–203, 2008.

[123] J. Perez-Peña, V. Corrales-Sánchez, E. Amir, A. Pandiella, and A. Ocana, ‘Ubiquitin-conjugating enzyme E2T (UBE2T) and denticleless protein homolog (DTL) are linked to poor outcome in breast and lung cancers’, *Sci Rep*, vol. 7, no. 1, p. 17530, Dec. 2017.

[124] T. Ueki, J. Park, T. Nishidate, K. Kijima, K. Hirata, Y. Nakamura, and T. Katagiri,

‘Ubiquitination and Downregulation of BRCA1 by Ubiquitin-Conjugating Enzyme E2T Overexpression in Human Breast Cancer Cells’, *Cancer Res*, vol. 69, no. 22, pp. 8752–8760, Nov. 2009.

[125] L. Liu, M. Yang, Q. Peng, M. Li, Y. Zhang, Y. Guo, Y. Chen, and S. Bao., ‘UBE2T promotes hepatocellular carcinoma cell growth via ubiquitination of p53’, *Biochem. Biophys. Res. Commun.*, vol. 493, no. 1, pp. 20–27, 04 2017.

[126] Y. Q. Gong, D. Peng, X. H. Ning, X. Y. Yang, X. S. Li, L. Q. Zhou, and Y. L. Guo, ‘UBE2T silencing suppresses proliferation and induces cell cycle arrest and apoptosis in bladder cancer cells’, *Oncol Lett*, vol. 12, no. 6, pp. 4485–4492, Dec. 2016.

[127] C. Luo, Y. Yao, Z. Yu, H. Zhou, L. Guo, J. Zhang, H. Cao, G. Zhang, Y. Li, and Z. Jiao, ‘UBE2T knockdown inhibits gastric cancer progression’, *Oncotarget*, vol. 8, no. 20, pp. 32639–32654, May 2017.

[128] H. Yu, P. Xiang, Q. Pan, Y. Huang, N. Xie, and W. Zhu, ‘Ubiquitin-Conjugating Enzyme E2T is an Independent Prognostic Factor and Promotes Gastric Cancer Progression’, *Tumor Biol.*, vol. 37, no. 9, pp. 11723–11732, Sep. 2016.

[129] M. Wen, Y. Kwon, Y. Wang, J.-H. Mao, and G. Wei, ‘Elevated expression of UBE2T exhibits oncogenic properties in human prostate cancer’, *Oncotarget*, vol. 6, no. 28, pp. 25226–25239, Sep. 2015.

[130] W. Zhang, Y. Zhang, Z. Yang, X. Liu, P. Yang, J. Wang, K. Hu, X. He, X. Zhang, and H. Jing, ‘High expression of UBE2T predicts poor prognosis and survival in multiple myeloma’, *Cancer Gene Ther.*, Jan. 2019.

[131] Y. Wang, H. Leng, H. Chen, L. Wang, N. Jiang, X. Huo, and B. Yu, ‘Knockdown of UBE2T Inhibits Osteosarcoma Cell Proliferation, Migration, and Invasion by Suppressing the PI3K/Akt Signaling Pathway’, *Oncol. Res.*, vol. 24, no. 5, pp. 361–369, 2016.

[132] W. Hu, L. Xiao, C. Cao, S. Hua, and D. Wu, ‘UBE2T promotes nasopharyngeal carcinoma cell proliferation, invasion, and metastasis by activating the AKT/GSK3β/β-catenin pathway’, *Oncotarget*, vol. 7, no. 12, pp. 15161–15172, Mar. 2016.

[133] M. Mladinich, D. Ruan, and C. H. Chan, ‘Tackling Cancer Stem Cells via Inhibition of EMT Transcription Factors’, *Stem Cells Int*, vol. 2016, p. 5285892, 2016.

[134] Y. Hu and G. K. Smyth, ‘ELDA: extreme limiting dilution analysis for comparing depleted and enriched populations in stem cell and other assays’, *J. Immunol. Methods*, vol. 347, no.

1–2, pp. 70–78, Aug. 2009.

[135] K. Eun, S. W. Ham, and H. Kim, ‘Cancer stem cell heterogeneity: origin and new perspectives on CSC targeting’, *BMB Rep*, vol. 50, no. 3, pp. 117–125, Mar. 2017.

[136] M. Shackleton, ‘Normal stem cells and cancer stem cells: similar and different’, *Seminars in Cancer Biology*, vol. 20, no. 2, pp. 85–92, Apr. 2010.

[137] K. J. Andersen, A. R. Knudsen, A. Kannerup, H. Sasanuma, J. R. Nyengaard, S. Hamilton-Dutoit, E.J. Erlandsen, B. Jørgensen, and F.V. Mortensen, ‘The natural history of liver regeneration in rats: Description of an animal model for liver regeneration studies’, *International Journal of Surgery*, vol. 11, no. 9, pp. 903–908, Nov. 2013.

[138] A. W. Duncan, C. Dorrell, and M. Grompe, ‘Stem Cells and Liver Regeneration’, *Gastroenterology*, vol. 137, no. 2, pp. 466–481, Aug. 2009.

[139] S. H. Oh, H. M. Hatch, and B. E. Petersen, ‘Hepatic oval “stem” cell in liver regeneration’, *Seminars in Cell & Developmental Biology*, vol. 13, no. 6, pp. 405–409, Dec. 2002.

[140] S. Wabitsch, C. Benzing, F. Krenzien, K. Splith, P.K. Haber, A. Arnold, M. Nösser, *et al.*, ‘Human Stem Cells Promote Liver Regeneration After Partial Hepatectomy in BALB/C Nude Mice’, *J. Surg. Res.*, vol. 239, pp. 191–200, Jul. 2019.

[141] S. J. Forbes and P. N. Newsome, ‘Liver regeneration — mechanisms and models to clinical application’, *Nature Reviews Gastroenterology & Hepatology*, vol. 13, no. 8, pp. 473–485, Aug. 2016.

[142] R. Zhai, Y. Wang, L. Qi, G.M. Williams, B. Gao, G. Song, J.F. Burdick, and Z. Sun, ‘Pharmacological Mobilization of Endogenous Bone Marrow Stem Cells Promotes Liver Regeneration after Extensive Liver Resection in Rats’, *Scientific Reports*, vol. 8, no. 1, p. 3587, Feb. 2018.

[143] C. X. Deng, ‘BRCA1: cell cycle checkpoint, genetic instability, DNA damage response and cancer evolution’, *Nucleic Acids Res*, vol. 34, no. 5, pp. 1416–1426, 2006.

[144] T. K. MacLachlan and W. El-Deiry, *Functional Interactions Between BRCA1 and the Cell Cycle*. Landes Bioscience, 2013.

[145] S. Ma, K. Chan, L. Hu, T.K. Lee, J. Y. Wo, I.O. Ng, B. Zheng, and X. Guan., ‘Identification and Characterization of Tumorigenic Liver Cancer Stem/Progenitor Cells’, *Gastroenterology*, vol. 132, no. 7, pp. 2542–2556, Jun. 2007.

[146] M. Tanaka and A. Miyajima, ‘Liver regeneration and fibrosis after inflammation’,

Inflammation and Regeneration, vol. 36, no. 1, p. 19, Oct. 2016.

[147] M. K. Behnke, M. Reimers, and R. A. Fisher, 'Stem cell and hepatocyte proliferation in hepatitis C cirrhosis and hepatocellular carcinoma: transplant implications', *Ann Hepatol*, vol. 13, no. 1, pp. 45–53, Feb. 2013.

[148] K. N. Lowes, B. A. Brennan, G. C. Yeoh, and J. K. Olynyk, 'Oval Cell Numbers in Human Chronic Liver Diseases Are Directly Related to Disease Severity', *Am J Pathol*, vol. 154, no. 2, pp. 537–541, Feb. 1999.

[149] Q. H. Zhang, M. Ye, X. Y. Wu, S. X. Ren, M. Zhao, C. J. Zhao, G. Fu, et al, 'Cloning and functional analysis of cDNAs with open reading frames for 300 previously undefined genes expressed in CD34+ hematopoietic stem/progenitor cells', *Genome Res.*, vol. 10, no. 10, pp. 1546–1560, Oct. 2000.

[150] T. Ishiguro, H. Ohata, A. Sato, K. Yamawaki, T. Enomoto, and K. Okamoto, 'Tumor-derived spheroids: Relevance to cancer stem cells and clinical applications', *Cancer Sci*, vol. 108, no. 3, pp. 283–289, Mar. 2017.

[151] S. Shaheen, M. Ahmed, F. Lorenzi, and A. S. Nateri, 'Spheroid-Formation (Colonosphere) Assay for in Vitro Assessment and Expansion of Stem Cells in Colon Cancer', *Stem Cell Rev*, vol. 12, pp. 492–499, 2016.

[152] S. Jaiswal, C. Jamieson, W.W. Pang, C.Y. Park, M. P. Chao, R. Majeti, D. Traver, N. van Rooijen, and I.L. Weissman., 'CD47 is up-regulated on circulating hematopoietic stem cells and leukemia cells to avoid phagocytosis', *Cell*, vol. 138, no. 2, pp. 271–285, Jul. 2009.

[153] J. Wang, S. Huang, L. Zhang, Z. Liu, R. Liang, S. Jiang, Y. Jiang, *et al.*, 'Combined prognostic value of the cancer stem cell markers CD47 and CD133 in esophageal squamous cell carcinoma', *Cancer Med*, vol. 8, no. 3, pp. 1315–1325, Mar. 2019.

[154] T. K. Lee, V. C. Cheung, P. Lu, E. Lau, S. Ma, K.H. Tang, M. Tong, J. Lo, and I.O. Ng, 'Blockade of CD47-mediated cathepsin S/protease-activated receptor 2 signaling provides a therapeutic target for hepatocellular carcinoma', *Hepatology*, vol. 60, no. 1, pp. 179–191, Jul. 2014.

[155] L. Liu, L. Zhang, L. Yang, H. Li, R. Li, J. Yu, L. Yang, *et al.*, 'Anti-CD47 Antibody As a Targeted Therapeutic Agent for Human Lung Cancer and Cancer Stem Cells', *Front Immunol*, vol. 8, Apr. 2017.

[156] T. Avril, A. Etcheverry, R. Pineau, J. Obacz, G. Jegou, F. Jouan, P. Le Reste, *et al.*, 'CD90

Expression Controls Migration and Predicts Dasatinib Response in Glioblastoma', *Clin. Cancer Res.*, vol. 23, no. 23, pp. 7360–7374, Dec. 2017.

[157] K. Zhang, S. Che, Z. Su, S. Zheng, H. Zhang, S. Yang, W. Li, and J. Liu., 'CD90 promotes cell migration, viability and sphere-forming ability of hepatocellular carcinoma cells', *Int J Mol Med*, vol. 41, no. 2, pp. 946–954, Feb. 2018.

[158] M. V. Shaikh, M. Kala, and M. Nivsarkar, 'CD90 a potential cancer stem cell marker and a therapeutic target', *Cancer Biomark*, vol. 16, no. 3, pp. 301–307, 2016.

[159] X. Yan, H. Luo, X. Zhou, B. Zhu, *et al.*, 'Identification of CD90 as a marker for lung cancer stem cells in A549 and H446 cell lines', *Oncology Reports*, vol. 30, no. 6, pp. 2733–2740, Dec. 2013.

[160] R. Yang, L. Y. An, Q.F. Miao, F.M. Li, Y. Han, H. X. Wang, D. P. Liu, R. Chen, and S. Q. Tang., 'Effective elimination of liver cancer stem-like cells by CD90 antibody targeted thermosensitive magnetoliposomes', *Oncotarget*, vol. 7, no. 24, pp. 35894–35916, Apr. 2016.

[161] C. F. Thorn, C. Oshiro, S. Marsh, T. Hernandez-Boussard, H. McLeod, T. E. Klein, and R. B. Altman, 'Doxorubicin pathways: pharmacodynamics and adverse effects', *Pharmacogenet Genomics*, vol. 21, no. 7, pp. 440–446, Jul. 2011.

[162] J. Niraj, A. Färkkilä, and A. D. D'Andrea, 'The Fanconi Anemia Pathway in Cancer', *Annu Rev Cancer Biol*, vol. 3, pp. 457–478, Mar. 2019.

[163] H. B. Sieburg, R. H. Cho, and C. E. Müller-Sieburg, 'Limiting dilution analysis for estimating the frequency of hematopoietic stem cells: Uncertainty and significance', *Experimental Hematology*, vol. 30, no. 12, pp. 1436–1443, Dec. 2002.

[164] A. S. Huynh, D. F. Abrahams, M. S. Torres, M. K. Baldwin, R. J. Gillies, and D. L. Morse, 'Development of an Orthotopic Human Pancreatic Cancer Xenograft Model Using Ultrasound Guided Injection of Cells', *PLoS One*, vol. 6, no. 5, May 2011.

[165] T. Murakami, Y. Zhang, X. Wang, Y. Hiroshima, H. Kasashima, M. Yashiro, K. Hirakawa, *et al.*, 'Orthotopic Implantation of Intact Tumor Tissue Leads to Metastasis of OCUM-2MD3 Human Gastric Cancer in Nude Mice Visualized in Real Time by Intravital Fluorescence Imaging', *Anticancer Res*, vol. 36, no. 5, pp. 2125–2130, Jan. 2016.

[166] O.M. Rashid, M. Nagahashi, S. Ramachandran, C.I. Dumur, J.C. Schaum, A. Yamada, T. Aoyagi, S. Milstien, S. Spiegel, and K. Takabe., 'Is tail vein injection a relevant breast

cancer lung metastasis model?', *J Thorac Dis*, vol. 5, no. 4, pp. 385–392, Aug. 2013.

[167] J. Yu and W. Cui, 'Proliferation, survival and metabolism: the role of PI3K/AKT/mTOR signalling in pluripotency and cell fate determination', *Development*, vol. 143, no. 17, pp. 3050–3060, Sep. 2016.

[168] C. Dominguez-Brauer, R. Khatun, A. J. Elia, K.L. Thu, P. Ramachandran, S. P. Baniasadi, Z. Hao, *et al.*, 'E3 ubiquitin ligase Mule targets β-catenin under conditions of hyperactive Wnt signaling', *Proc. Natl. Acad. Sci. U.S.A.*, vol. 114, no. 7, pp. E1148–E1157, 14 2017.

[169] D. Chen, N. Kon, M. Li, W. Zhang, J. Qin, and W. Gu, 'ARF-BP1/Mule Is a Critical Mediator of the ARF Tumor Suppressor', *Cell*, vol. 121, no. 7, pp. 1071–1083, Jul. 2005.

[170] Q. Zhong, W. Gao, F. Du, and X. Wang, 'Mule/ARF-BP1, a BH3-Only E3 Ubiquitin Ligase, Catalyzes the Polyubiquitination of Mcl-1 and Regulates Apoptosis', *Cell*, vol. 121, no. 7, pp. 1085–1095, Jul. 2005.

[171] D. Yang, D. Cheng, Q. Tu, H. Yang, B. Sun, L. Yan, H. Dai, *et al.*, 'HUWE1 controls the development of non-small cell lung cancer through down-regulation of p53', *Theranostics*, vol. 8, no. 13, pp. 3517–3529, 2018.

[172] L. Vaughan, C. Tan, A. Chapman, D. Nonaka, N. A. Mack, D. Smith, R. Booton, A. Hurlstone, and A. Malliri, 'HUWE1 Ubiquitylates and Degrades the RAC Activator TIAM1 Promoting Cell-Cell Adhesion Disassembly, Migration, and Invasion', *Cell Rep*, vol. 10, no. 1, pp. 88–102, Dec. 2014.

[173] X. Wang, G. Lu, L. Li, J. Yi, K. Yan, Y. Wang, B. Zhu, *et al.*, 'HUWE1 interacts with BRCA1 and promotes its degradation in the ubiquitin–proteasome pathway', *Biochemical and Biophysical Research Communications*, vol. 444, no. 3, pp. 290–295, Feb. 2014.

[174] H. Qu, H. Liu, Y. Jin, Z. Cui, and G. Han, 'HUWE1 upregulation has tumor suppressive effect in human prostate cancer cell lines through c-Myc', *Biomedicine & Pharmacotherapy*, vol. 106, pp. 309–315, Oct. 2018.

[175] K. B. Myant, P. Cammareri, M. C. Hodder, J. Wills, A. V. Kriegsheim, B. Győrffy, M. Rashid, *et al.*, 'HUWE1 is a critical colonic tumour suppressor gene that prevents MYC signalling, DNA damage accumulation and tumour initiation', *EMBO Mol Med*, vol. 9, no. 2, pp. 181–197, Feb. 2017.

[176] C. Dominguez-Brauer, Z. Hao, A. J. Elia, J. M. Fortin, R. Nechanitzky, P. M. Brauer, Y. Sheng, *et al.*, 'Mule Regulates the Intestinal Stem Cell Niche via the Wnt Pathway and

Targets EphB3 for Proteasomal and Lysosomal Degradation', *Cell Stem Cell*, vol. 19, no. 2, pp. 205–216, Aug. 2016.

[177] R. de Groot, R. S. Ganji, O. Bernatik, B. Lloyd-Lewis, K. Seipel, K. Šedová, Z. Zdráhal, *et al.*, 'Huwe1-mediated ubiquitylation of dishevelled defines a negative feedback loop in the Wnt signaling pathway', *Sci Signal*, vol. 7, no. 317, p. ra26, Mar. 2014.

[178] C. Li, C. Yen, Y. Chen, K. Lee, C. Fang, X. Zhang, C. Lai, S. Huang, H. Lin, and Y. A. Chen, 'Characterization of the GNMT-HectH9-PREX2 tripartite relationship in the pathogenesis of hepatocellular carcinoma', *Int. J. Cancer*, vol. 140, no. 10, pp. 2284–2297, 15 2017.

[179] T. Kodama, J. Y. Newberg, M. Kodama, R. Rangel, K. Yoshihara, J. C. Tien, P. H. Parsons, *et al.*, 'Transposon mutagenesis identifies genes and cellular processes driving epithelial-mesenchymal transition in hepatocellular carcinoma', *Proc Natl Acad Sci U S A*, vol. 113, no. 24, pp. E3384–E3393, Jun. 2016.

[180] B. King, F. Boccalatte, K. Moran-Crusio, E. Wolf, J. Wang, C. Kayembe, C. Lazaris, *et al.*, 'The ubiquitin ligase HUWE1 regulates hematopoietic stem cell maintenance and lymphoid commitment', *Nat Immunol*, vol. 17, no. 11, pp. 1312–1321, Nov. 2016.

[181] N. Urbán, D. van den Berg, A. Forget, J. Andersen, J. A. Demmers, C. Hunt, O. Ayrault, and F. Guillemot, 'Return to quiescence of murine neural stem cells by degradation of a pro-activation protein', *Science*, vol. 353, no. 6296, pp. 292–295, Jul. 2016.

[182] L. J. Chen, W. M. Xu, M. Yang, K. Wang, Y. Chen, X. J. Huang, and Q. H. Ma., 'HUWE1 plays important role in mouse preimplantation embryo development and the dysregulation is associated with poor embryo development in humans', *Sci Rep*, vol. 6, Nov. 2016.

[183] G. L. Grice and J. A. Nathan, 'The recognition of ubiquitinated proteins by the proteasome', *Cell Mol Life Sci*, vol. 73, pp. 3497–3506, 2016.

[184] S. H. Kao, H. T. Wu, and K. J. Wu, 'Ubiquitination by HUWE1 in tumorigenesis and beyond', *J. Biomed. Sci.*, vol. 25, no. 1, p. 67, Sep. 2018.

[185] M. Katoh, 'Canonical and non-canonical WNT signaling in cancer stem cells and their niches: Cellular heterogeneity, omics reprogramming, targeted therapy and tumor plasticity (Review)', *Int J Oncol*, vol. 51, no. 5, pp. 1357–1369, Sep. 2017.

[186] J. D. Holland, A. Klaus, A. N. Garratt, and W. Birchmeier, 'Wnt signaling in stem and cancer stem cells', *Current Opinion in Cell Biology*, vol. 25, no. 2, pp. 254–264, Apr. 2013.

[187] H. L. Zhang, P. Wang, M. Z. Lu, S. D. Zhang, and L. Zheng, 'c-Myc maintains the

self-renewal and chemoresistance properties of colon cancer stem cells', *Oncology Letters*, vol. 17, no. 5, pp. 4487–4493, May 2019.

[188] J. Jiao, L. Huang, F. Ye, M. Shi, X. Cheng, X. Wang, D. Hu, X. Xie, and W. Lu, 'Cyclin D1 affects epithelial-mesenchymal transition in epithelial ovarian cancer stem cell-like cells', *Onco Targets Ther*, vol. 6, pp. 667–677, 2013.

[189] H. Pandit, Y. Li, X. Li, W. Zhang, S. Li, and R. C. G. Martin, 'Enrichment of cancer stem cells via β-catenin contributing to the tumorigenesis of hepatocellular carcinoma', *BMC Cancer*, vol. 18, Aug. 2018.

[190] J. U. Marquardt and S. S. Thorgeirsson, 'Stem Cells in Hepatocarcinogenesis: Evidence from Genomic Data', *Semin Liver Dis*, vol. 30, no. 1, pp. 26–34, Feb. 2010.

[191] Z. A. Ronai, 'Monoubiquitination in proteasomal degradation', *PNAS*, vol. 113, no. 32, pp. 8894–8896, Aug. 2016.

[192] K. L. Lim and G. G. Y. Lim, 'K63-linked ubiquitination and neurodegeneration', *Neurobiology of Disease*, vol. 43, no. 1, pp. 9–16, Jul. 2011.

[193] F. Ohtake, H. Tsuchiya, Y. Saeki, and K. Tanaka, 'K63 ubiquitylation triggers proteasomal degradation by seeding branched ubiquitin chains', *Proc Natl Acad Sci U S A*, vol. 115, no. 7, pp. E1401–E1408, Feb. 2018.

[194] H. Huang, H. Fujii, A. Sankila, B. M. Mahler-Araujo, M. Matsuda, G. Cathomas, and H. Ohgaki. 'β-Catenin Mutations Are Frequent in Human Hepatocellular Carcinomas Associated with Hepatitis C Virus Infection', *Am J Pathol*, vol. 155, no. 6, pp. 1795–1801, Dec. 1999.

[195] P. Legoix, O. Bluteau, J. Bayer, C. Perret, C. Balabaud, J. Belghiti, D. Franco, G. Thomas, P. Laurent-Puig, and J. Zucman-Rossi., 'Beta-catenin mutations in hepatocellular carcinoma correlate with a low rate of loss of heterozygosity', *Oncogene*, vol. 18, no. 27, p. 4044, Jul. 1999.

[196] C. M. Wong, S. T. Fan, and I. O. Ng, 'beta-Catenin mutation and overexpression in hepatocellular carcinoma: clinicopathologic and prognostic significance', *Cancer*, vol. 92, no. 1, pp. 136–145, Jul. 2001.

[197] L. Chen, T. H. M. Chan, and X. Guan, 'Chromosome 1q21 amplification and oncogenes in hepatocellular carcinoma', *Acta Pharmacol Sin*, vol. 31, no. 9, pp. 1165–1171, Sep. 2010.

Conference Presentations

1. **Ho NP**, Lee TK. UBE2T: a molecular regulator for cancer stemness in hepatocellular carcinoma. The Liver Week 2018, The Korean Association for the Study of Liver, Incheon Korea, 2018. (***Travel award***)
2. **Ho NP**, Lee TK. UBE2T: a molecular regulator for cancer stemness in hepatocellular carcinoma. The AACR Annual Meeting 2018, Chicago USA, 2018.
3. **Ho NP**, Lee TK. UBE2T: a molecular regulator for cancer stemness in hepatocellular carcinoma. The Sunney & Irene Chan Lecture in Chemical Biology 2017, Hong Kong, 2017.
4. **Ho NP**, Cheng BY, Ng IO, Lee TK. IRAK1 augments cancer stemness and drug resistance via the AP-1/AKR1B10 signaling cascade in hepatocellular carcinoma. The 76th Annual Meeting of Japanese Cancer Association, Yokohama Japan, 2017.
5. **Ho NP**, Cheng BY, Ng IO, Lee TK. IRAK1 augments cancer stemness and drug resistance via the AP-1/AKR1B10 signaling cascade in hepatocellular carcinoma. The Liver Week 2017, The Korean Association for the Study of Liver, Incheon Korea, 2017.

Awards

1. Travel award of The Liver Week 2017, The Korean Association for the Study of Liver, South Korea (2017)
2. Travel award of the 76th Annual Meeting of Japanese Cancer Association, Japan (2017)
3. Travel award of The Liver Week 2018, The Korean Association for the Study of Liver, South Korea (2018)

Grant Support

This project is supported by Hong Kong Research Grant Council General Research Fund (15104618).